Report

Oxidation of methane in seawater

Laboratory experiments and the use of models

Authors:

Odd G. Brakstad, Tor Nordam, Ida B. Øverjordet, Kjersti Almås, Marianne U. Rønsberg, Marianne A. Molid, Marianne Aas and Sigrid Hakvåg

Report No:

OC2022 A-114 – Unrestricted

Clients:

Offshore Norway; Equinor Energy AS; AkerBP ASA; Lundin Energy Norge AS; Wintershall Dea Norge AS

SINTEF Ocean AS
Postadresse:
Postboks 4762 Torgarden
7465 Trondheim

Sentralbord: 46415000

Foretaksregister:
NO 937 357 370 MVA

Report

Oxidation of methane in seawater

Laboratory experiments and the use of models

KEYWORDS
Methane oxidation, biodegradation, modelling, methane monooxigenase

VERSION
1.5

DATE
2022-12-16

AUTHORS
Odd G. Brakstad, Tor Nordam, Ida B. Øverjordet, Kjersti Almås, Marianne U. Rønsberg, Marianne A. Molid, Marianne Aas and Sigrid Hakvåg

CLIENTS
Offshore Norway; Equinor Energy AS; AkerBP ASA; Lundin Energy Norge AS; Wintershall Dea Norge AS

REFERENCE

PROJECT NO
302006186

NUMBER OF PAGES/APPENDICES
65/3

SUMMARY
Oxidation of methane was determined in this project by two methods: Stable isotope analyses ($^{13}CH_4$) and by the use of tritium-labelled methane (^{3}H-CH_4). The intentions of the project were to obtain methane oxidation rates for the marine water column, which may be of relevance for the Norwegian Continental Shelf. Experimental, sampling, and analytical methods were established for both methods. Relatively few experiments were of a quality considered to be acceptable. The oxidation data determined by the two methods resulted in half-lives of 21.6 ± 6.2 days at 5°C incubation temperature with the stable isotope method, and 5.6 ± 0.7 and 4.6 ± 2.5 days with the tritium method at 5 to 8.5°C incubation temperature, respectively. Based on the comparison to data for field studies, it seemed that the data obtained by the tritium methods represented an overestimation of methane oxidation rates, while the stable isotope data were more in agreement with field data. The oxidation data were used in model simulations to determine atmospheric releases of methane from seeps at different seep depths.

PREPARED BY
Odd Gunnar Brakstad

SIGNATURE (FOR BRAKSTAD)
Sigrid Hakvåg (Dec 16, 2022 15:04 GMT+1)

CHECKED BY
Konstantinos Kotzakoulakis

SIGNATURE
Konstantinos Kotzakoulakis (Dec 16, 2022 16:19 GMT+1)

APROVED BY
Mimmi Throne-Holst

SIGNATURE
Mimmi Throne-Holst (Dec 16, 2022 16:33 GMT+1)

COMPANY WITH MANAGEMENT SYSTEM CERTIFIED BY DNV
ISO 9001 • ISO 14001
ISO 45001

REPORT NO.
OC2022 A-114

ISBN
978-82-7174-450-2

CLASSIFICATION
Unrestricted

CLASSIFIFICATION THIS PAGE
Unrestricted

Document History

VERSION	DATE	VERSIONS DESCRIPTION
1.0	2022-07-08	Draft version 1 for comments from the partners
1.1	2022-08-10	Draft version 2 with models described
1.2	2022-09-01	Final Draft after comments from partners
1.3	2022-09-28	Final version after minor corrections to draft from partners
1.4	2022-10-04	Final version. Minor corrections
1.5	2022-12-16	Final version. Classification changed to 'unrestricted'

Table of content

APPENDICES

Executive summary

Microbial oxidation of methane is a simple process, since a C_1-compound (CH_4) is transformed to another C_1-compound (CO_2). In seawater (SW), the process is usually performed in the presence of oxygen (aerobic oxidation) and performed by methanotrophic microbes. Methane oxidation rates are determined by first-order rates, in which the rate constant (k1) is related to the substrate concentration, and with the oxidation half-life to be directly determined from the rate constant. Several studies have shown highly variable methane oxidation rates in SW, with half-lives ranging from a few days to several years in the marine water column.

Based on findings from a desktop study, it was decided to perform methane oxidation studies in natural SW by two methods: Stable isotope ($^{13}CH_4$) analyses and the use of tritium-labelled methane (^{3}H-CH_4). The stable isotope method was performed in collaboration with the National Laboratory of Age Determination at the Natural Museum at NTNU on an Isotope-ratio mass spectrometer (IRMS). The analyses with tritium-labelled methane were performed in a laboratory dedicated for this kind of work at NTNU Sealab, and by a scientist approved for work with radioactive materials.

All the experiments were performed in natural seawater collected from 80 m depth in the Trondheimsfjord outside the harbour of Trondheim (close to the island of Munkholmen). The SW was directly supplied to SINTEF's laboratories through a pipeline system. Pure $^{13}CH_4$ gas was used as stable isotope, while tritium-labelled methane (^{3}H-CH_4) provided on break-seal ampoules were applied in a solvent (hexane) and stored as stock solutions on crimp-sealed vials. In most experiments SW was pre-adapted in methane gas (normal high-quality (HiQ) $^{12}CH_4$) before spiked with stable isotope or tritium-labelled methane. In most experiments, the methane concentrations were quantified by GC-FID analyses.

The typical experimental and analytical procedures were as follows:

For stable isotope experiments, crimp-sealed serum flasks were spiked with stable isotope ($^{13}CH_4$), incubated at 4-5 °C, and sampled by creating a nitrogen headspace and acidifying the dissolved inorganic carbon (DIC) to CO_2. The headspace, containing $^{13}CO_2$ formed during methane oxidation was then injected into the IRMS, and the $\delta^{13}CO_2$ ratio determined, from which $^{13}CO_2$ as fraction of the complete CO_2 was determined and corrected for this fraction in SW blanks. From the excess $^{13}CO_2$ in test samples methane oxidation was determined. In experiments with SW spiked with ^{3}H-CH_4, headspaces were created in samples and sterilized controls, and the liquid phases sparged with nitrogen to remove residual ^{3}H-CH_4 after oxidation, and oxidation products determined as ^{3}H-H_2O in test samples after correcting for radioactivity in sterilized samples. For both experiments with stable isotope and tritium-labeled methane, rate coefficients, half-lives concentration-dependent methane oxidation (MOX) and turnover times were determined.

The objectives of the project were to determine methane oxidation rates by the two methods in relation to incubation times, methane concentrations and SW temperature. In addition, experiments should include enough replicates to secure test robustness.

In initial experiments, methods were tested to provide low stable methane concentrations in the SW, usually at concentrations of 50 nmol/L.

Experiments with stable isotopes were performed according to reported procedures, with different incubation times (3 to 28 days), with and without pre-incubation with $^{12}CH_4$ gas, and with different volumes of spiked stable isotope ($^{13}CH_4$). During these studies it was experienced that the stable isotope concentrations were too low to achieve $\delta^{13}CO_2$ ratios significantly above the levels in natural SW not spiked with stable isotope. While initial volumes of spiked gas were 50 µL to 100-mL crimp-sealed vials, volumes needed to be raised to 250 µL before $\delta^{13}CO_2$ ratios reached significantly above the SW blank levels. At this level, and in combination with a freeze-drying technique to purify the CO_2 samples, we were able to determine $^{13}CH_4$ oxidation after 3 days of exposure. Methane oxidation was calculated to be approximately 10 nmol/L d^{-1} from rate coefficients determined with the spiked stable isotope volume of 250 µL at 5 °C, and with a half-life of 22 ± 6 days and a turnover of 31 ± 10 days. These data were within the faster range of reported methane oxidation results with stable isotopes. However, since the stable isotope experiments were performed for method development, further studies with the isotope are recommended to confirm these data with the method now established at SINTEF Ocean in collaboration the researchers at the National Laboratory of Age Determination at the Natural Museum at NTNU.

Methane oxidation studies with $^{3}H\text{-}CH_4$ were performed in crimp-sealed 100-ml flasks. Initial studies included comparison of vials for storage of the tritium stock solutions, establishment of method based on activated carbon filters to collect residual $^{3}H\text{-}CH_4$ during nitrogen-sparging, and determination of liquid volumes in the test flasks during sparging. An experiment at 5 °C with sampling after different incubation periods (4 to 27 days), showed that 4-days incubation period was sufficient for these analyses. Rate coefficients, half-lives, MOX and methane turnover were determined. However, an experiment where different concentrations of methane (50, 100 and 200 nmol/L) were pre-incubated at 5 °C and then spiked with $^{3}H\text{-}CH_4$ showed high replicate variations and low oxidation rates, and we considered these data to be of limited value. In a final experiment, we attempted to increase incubation temperature to 13 °C, but since the experiment needed to be performed in a refrigerator, the temperature achieved during incubation, was only 8.5 °C. The oxidation rates achieved, with an incubation time of 2 days, were in agreement with 4-days incubation results from the experiment with different incubation times. The oxidation rates from the two experiments with $^{3}H\text{-}CH_4$ resulted in half-lives of within 6 ± 1 days at an incubation temperature of 5°C and 5 ± 3 days at an incubation temperature of 8.5°C. Corresponding turnover was estimated within 10 days with the tritium and 6 weeks with the stable isotope method.

In total we considered three experiments to be of acceptable quality in this project, one with stable isotopes, and two with tritium-labelled methane (**table 10** in report):

Parameter	**$^{13}CH_4$ Increased $^{13}CH_4$ conc[A)]**	**$^{3}H\text{-}CH_4$ Incubation time[B)]**	**$^{3}H\text{-}CH_4$ Increased temperature[C)]**
K1	0.0338 ± 0.0077	0.1243 ± 0.0173	0.1735 ± 0.062
Half-life (days)	21.6 ±6.2	5.6 ± 0.7	4.6 ± 2.5
MOX (nmol/L d^{-1})[D)]	10.4 ±2.4	6.2 ± 0.9	8.7 ± 3.1
Turnover (days)[D)]	31.1 ± 9.9	8.2 ± 1.0	6.7 ± 3.5

[A)] Test with 250 µL $^{13}CH_4$ applied; [B)] Incubation period 4 days; [C)] Incubation period 2 days; [D)] MOX and turnover based on the methane concentrations in the experiments.

The ranges of methane oxidation half-lives related to the use of different analytical methods both from literature data (red lines) and the data obtained in our laboratory study with local SW (green lines) is shown below (**Figure 34** in report**)**. Vertical arrows show average half-lives from the laboratory experiments conducted at SINTEF Ocean.

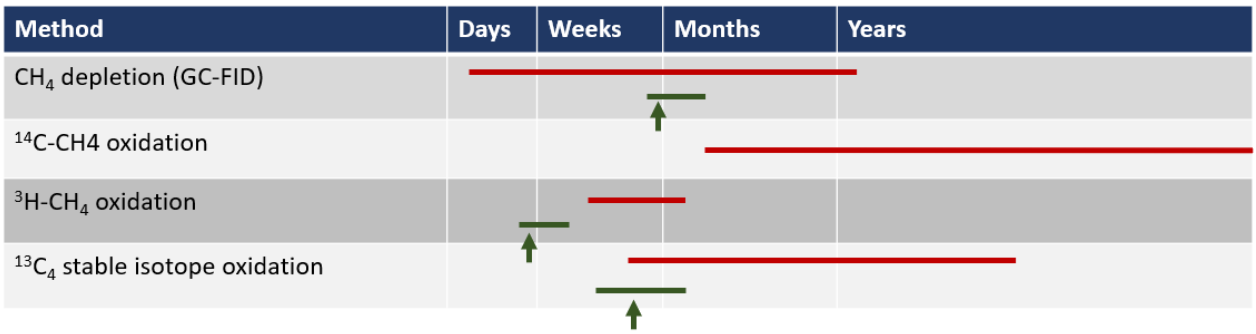

The results with the stable isotope were obtained at significantly higher methane concentrations than with the tritium-labelled material, but it seems that if additional experiments are to be performed, these may be conducted with the stable isotope method. One reason for this is that the stable isotope data were more in agreement with published methane oxidation rates from field experiments than the data from the tritium experiments, which seemed to overestimate oxidation rates. In addition, the stable isotope method, which now has been appropriately developed, is not associated with potential health risks, compared to the work with radiolabelled materials like tritium.

Model simulations were performed with methane seeps from different water depths and including the methane oxidation data provided by the laboratory experiments. When a bubble of methane is released from the sea floor, methane will dissolve from the bubble into the surrounding water while other gases that are dissolved in the water column will enter the bubble via mass transfer. Consequently, a bubble which initially contained pure methane may later contain nitrogen and oxygen, and little or no methane (Olsen et al., 2019). In shallow water, some fraction of the methane will reach the atmosphere directly with the bubbles, without being affected by methane oxidation. However, most of the methane is likely to dissolve in the water, and turbulent mixing and biodegradation will become important processes for determining if it eventually reaches the atmosphere. An illustration of the relevant processes affecting methane from sea-floor seeps, accounted for in our model is shown below (**Figure 31** in report).

Using seep releases from different water depths (50 to 360 m) and half-life from the tritium experiments (4.6 days) atmospheric emissions of dissolved methane ranged from negligible (360-210 m) to 40 % at 50 m depth. The corresponding data with the stable isotope half-life (21.6 days) resulted in 2 % to 74% atmospheric emissions with seeps from 360 m to 50 m depths.

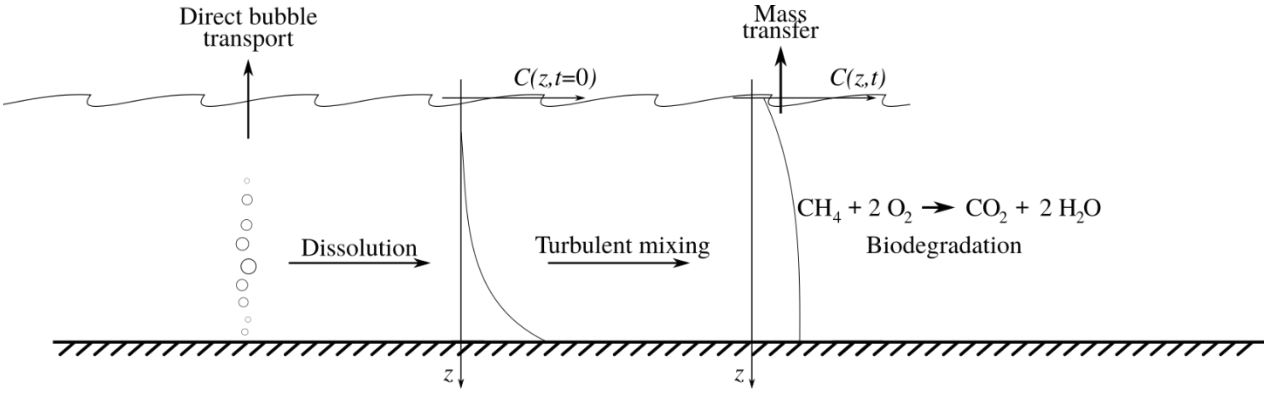

1. Background and acknowledgements

SINTEF Ocean performed a desktop study in 2020/2021 for NOROG on modelling and biodegradation of methane seeps (Nordam et al., 2021). The objective of the study was to collect data which could be used for modelling of methane emissions to atmosphere from natural seeps and de-commissioned wells leaking methane. The collected literature data on methane biodegradation rates in seawater showed significant variations, with biodegradation half-lives ranging from a few days, to several years. The collected data also showed that variations between different analytical methods used, and particularly the use of ^{14}C-labelled methane ($^{14}CH_4$) showed large ranges of methane oxidation. The wide ranges of methane oxidation rates also had significant implications for modelling the fate of methane in the water column, and subsequently for determining fluxes onto the atmosphere of this greenhouse gas (GHG).

Offshore Norway therefore asked SINTEF Ocean to perform a laboratory study to determine microbial methane oxidation in natural seawater, to obtain more consistent data which could be used for the model simulations. SINTEF Ocean suggested to perform experiments with two analytical methods, determination of oxidation by stable isotope analyses (^{13}C-CH_4), and by using tritium-labelled methane (^{3}H-CH_4).

The analyses in this project required instruments and competence not available at SINTEF Ocean. The stable isotope analyses were performed at the National Laboratory for Age Determination at NTNU, and we wish to thank Associate Professor Marie-Josée Nadeau, head of the National Laboratory for Age Determination, and Scientist Martin Seiler for their contribution, competence, and interest in the project. The tritium experiments were conducted at a laboratory dedicated for work with radioactive isotopes at NTNU Sealab, and we wish to thank Senior Engineer Arne Kjøsnes for organizing access to the laboratory, and Principal Engineer Grethe Stavik Eggen for help and guidance, particularly for HSE-related planning of these experiments.

2. Introduction

Methane is considered to be a potent greenhouse gas (GHG) with a warming influence on the climate. In the marine environment, CH_4 is generated basically from thermogenic or biogenic processes. While the sources of thermogenic formation are deep methane sources, the biogenic sources are methane formation caused by microbial degradation of organic material or CO_2 in oxygen-free methane zone of marine sediments (**Figure 1**). In cold seawater (SW) methane may also be released from destabilized gas hydrates (Naqvi et al., 2010). The formed methane may be subject to several oxidation processes in the marine sediment but may reach the overlying SW column in gas bubbles or in a dissolved form (Figure 1: Methane processes in the marine environment. Based on a similar figure by Bui (2018).**Figure 1**). In shallow SW bubbles may be transported and released to the atmosphere. However, methane released from rising or dissolved bubbles will be subject to microbial oxidation processes in the SW column (**Figure 1**).

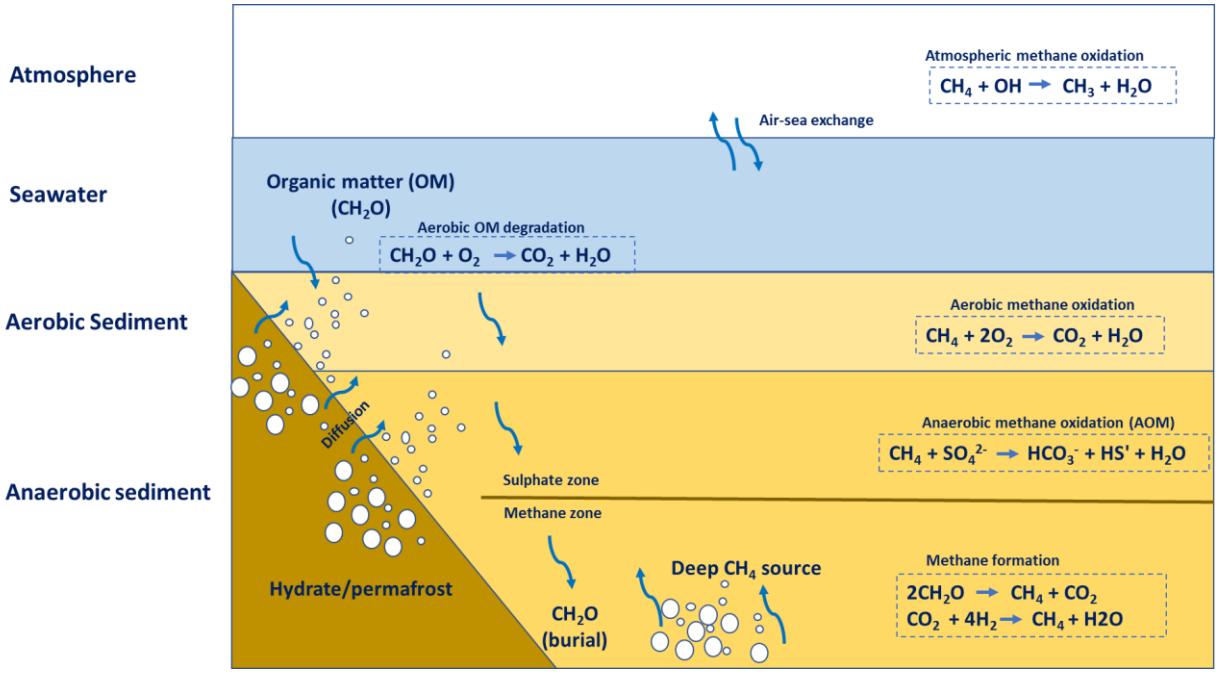

Figure 1: Methane processes in the marine environment. Based on a similar figure by Bui (2018).

Microbial oxidation of methane is a simple process, since a C_1- compound (CH_4) is transformed to another C_1-compound (CO_2). The degradation process is a one-step process, in which methane is directly transformed to carbon dioxide, without any intermediate metabolite products.

$$CH_4+2O_2 \rightarrow CO_2+2H_2O \text{ (Eq1)}$$

As Eq 1 shows, this process is aerobic, including molecular oxygen in the oxidation. The process is performed in the SW column, or in oxygenated parts of sediments (**Figure 1**). Methane oxidation is performed by so-called methanotrophic microbes, contrary to methanogenic microbes, which are responsible for anaerobic methane formation. These microbes include typical C1-utilizing bacteria within a wide range of bacterial and archaeal genera, including *Methylomarinum*, *Methylobacter*, *Methylococcus*, *Methylomicrobium*, *Methylomonas*, *Methylocaldum*, *Methylocystis*, *Methylosinus*, *Methylocella*, *Methyloacidophilum*, *Methylothermus*, *Methylocapsa*, *Methylophaga*, and *Methylosarcina* (Abdallah et al., 2014; Gutierrez and Aitken, 2014).

Although methane oxidation is often associated with oxygenated environments, this process may also occur in anaerobic environments like marine sediments and oxygen-free water. This process is known as anaerobic oxidation of methane (AOM) and may involve consortia of methane methanotrophic archaea (ANME), often in syntrophy (partnership) with other microbes organisms like sulphate-reducing bacteria (SRB) or nitrate- or nitrite-reducing bacteria (Haroon et al., 2013; Luesken et al., 2011; Nauhaus et al., 2005; Niewöhner et al., 1998). These sediment oxidation processes may work as important 'biofilter' for methane sieving up through the sediments. However, once methane is released to the water column, aerobic oxygen-dependent processes are predominant for methane oxidation. Both aerobic and anaerobic methane oxidation are catalyzed by a particulate methane monooxygenase, encoded by the *pmoA*-gene (Luesken et al., 2011; McDonald and Murrell, 1997).

Methane is often released from sediments to the marine water column as bubbles. The bubbles will rise rapidly in the water column, and in very shallow water, some fraction of the methane may be directly transported in the bubbles up to the surface and released to the atmosphere. As an example, in 50 m depth, and assuming typical conditions for the North Sea, around 10% of the methane was found to reach the atmosphere directly with bubbles, while the other 90% dissolved. In deeper water, essentially all the methane will be dissolved from the gas bubbles and become accessible for microbial oxidation, determined by the methane dissolution rates from the bubbles. Dissolved methane will then be rapidly diluted in the water column, SW stratification, particularly in summer periods, may result in methane accumulations at certain water depths. This may further result in elevated methane oxidation in the layers with the highest methane concentrations (Mau et al., 2013; Ward et al., 1989).

Methane oxidation can be determined by calculations of rates. In an oxygen-containing environment, the rates are normally determined by performing experiments with the substrate in the presence of oxygen (and securing that oxygen does not become limited during the experiment), and the substrate (i.e. methane) is incubated over time in a medium containing microbes with the ability to oxidize the substrate (aerobic biodegradation). Samples are normally collected for determination of substrate depletion during the degradation period (primary biodegradation), or by measurements of oxygen consumption or CO_2 evolution (ultimate biodegradation). These data are then compared to potential depletion in sterilized samples, to correct for abiotic degradation. Depletion curves are then formed to determine the degradation rates, i.e.

depletion of the substrate per time unit. Depending on the concentrations of bacteria in the media, and the substrate concentration, the degradation curves usually follow one of the alternatives described in **Figure 2.**

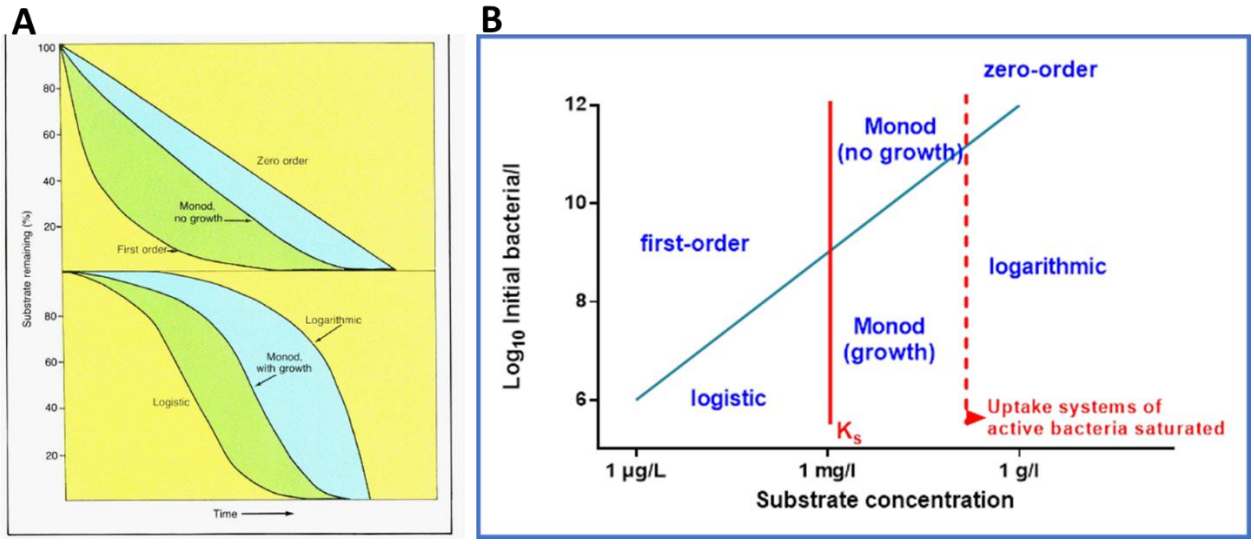

Figure 2: Different types of biodegradation curves (A) and their dependence on concentrations of substrate and bacteria (B). For further explanation, see the text (ref. Alexander, 1985).

At a combination of low substrate concentrations, the biodegradation curves follow immediate decay (first order) or sigmoid (logistic) approach. The logistic curve is caused by very low concentrations of competent bacteria (bacteria with the ability to biodegrade the substrate), so the bacterial populations must adapt to the substrate before biodegradation starts. First-order rates are followed with the combination of low substrate concentrations and enough competent bacteria to start immediate biodegradation. The Monod rates are relevant for situation with high substrate concentrations, usually in bacterial cultures supplemented with substrate. The Monod approach will, in contrast to first order and logistic degradation, require active growth of bacterial biomass during the degradation process since the substrate will be converted to biomass. Finally, at even higher substrate concentrations, the bacterial biomass becomes saturated, and biodegradation will become independent of substrate concentration (zero-order degradation).

Methane oxidation has been described to follow first-order rates, in which the rate coefficients are related to the substrate concentration in the environment (Valentine et al., 2001):

$$R_{ox} = k\,[CH_4] \text{ (Eq2)},$$

where Rox is the oxidation rate of methane, k is a rate coefficient, and $[CH_4]$ is the methane concentration. Since the first-order rates follows a typical exponential decay, the half-life (T50) may be derived directly from the first-order rate coefficient k:

$$T_{50} = \ln(2)/k \text{ (Eq3)},$$

where ln (2) = 0.693, which is the natural logarithm of 2.

The R_{ox} data can further be used to determine the turnover rate (τ), as shown later in Eq12. The turnover time describes the time it takes to empty substrate from a reservoir, e.g. the number of days needed to completely biodegrade a specified concentration of substrate at ([S]/R_{ox}).

Biodegradation rates typically follow first-order rates as long as the enzymes involved in the degradation process are saturated, i.e. when the methane concentration in the environment is lower than the capacities of the microbes to degrade the gas. When methane concentration increases, the capacities to biodegrade may be increased by increasing the concentrations of the competent microbes up to a level where essential nutrients or dissolved oxygen in the water become limited. Further increases in methane concentrations may then become substrate-independent, since the available microbial enzyme systems becomes saturated. The biodegradation rates then changes from first order to zero-order rates, i.e., the rates only depend on the rate coefficient and not the substrate concentration:

$$R_{ox} = k \text{ (Eq4)},$$

The limits for changes from first order to zero-order kinetics will vary between different environments, depending on previous exposure to a substrate, nutrient access, dissolved oxygen concentrations, etc. During the Deepwater Horizon oil spill in the Gulf of Mexico in 2010, large volumes of natural gas was released, and first-order rates were used for methane oxidation rates up to concentrations of several µmols/L of methane (Kessler et al., 2011). For propane oxidation, it was estimated that zero-order rates became evident at propane concentrations as high as 5 µmol/L (Valentine et al., 2010). Reported methane concentrations in seawater from the Norwegian Continental Shelf (NCS) showed levels 4 and 200 nmol/L (Vielstädte et al., 2017; von Deimling et al., 2011). A study of methane concentrations close to an abandoned North Sea well 22/4b, showed nearfield concentrations of 500 nmol/L to >60 µml/L in the bottom water close to the well at 60–85 m depth, levels of 40 nmol/L to 3 µmol/L in the thermocline (40–60 m depth), and from less than 5 nmol/L to 20 nmol/L above the thermocline, while far field concentrations showed median concentrations of 200 nmol/L below and 20 nmol/L above thermocline (Steinle et al., 2016; von Deimling et al., 2015). These concentrations should therefore indicate that methane oxidation rates should be estimated by first-order rates, accounting for the assumptions that the highest concentrations will be rapidly diluted in the water column. Estimated methane oxidation rates from some of these studies resulted in half-lives of 50-360 days (Steinle et al., 2016; Vielstädte et al., 2017).

In the recent desktop study performed by SINTEF Ocean, it was interesting to observe that the two variables which seemed to affect methane oxidation rates were choice of analytical methods and methane concentrations in the environment (Nordam et al., 2021). The latter was expected from concentration-dependent oxidation rates. However, seawater temperature did not have any obvious impacts, since some of the highest rates were measured in very cold Arctic seawater (Mau et al., 2013; Uhlig et al., 2018). Biodegradation is often anticipated to follow the Arrhenius curve, which describes a temperature dependency of reactions (Q_{10} approach), with suggested rate coefficients reduced by factor of 2 when temperatures are decreased by 10 °C (Bagi et al., 2013; Nordam et al., 2020).

Mainly three different analytical methods have been used for measurements of methane oxidation rates in the seawater, mainly associated with as seepage areas, analyses of methane depletion by gas chromatography, use of radiolabelled methane (^{14}C-CH_4 or ^{3}H-CH_4), or the use of stable isotope analyses (^{13}C-CH_4). Gas chromatographic methods like GC-FID have detection limits of 0.01-0.1 mg/L, corresponding to approximately 1 µmol/L, while methane concentrations in natural seawater are usually in the nmol/L range. In order to perform studies with environmentally relevant methane concentrations, radiolabelled methane is used instead in most studies to determine oxidation rates at realistic concentrations. Some comparative studies have indicated that the use of ^{3}H-labeled CH_4 results in faster oxidation rates than the

use of ^{14}C-labeled CH_4 (Mau et al., 2013; Pack et al., 2015), and several studies have been performed with tritium (^{3}H)-labelled methane oxidation studies (Valentine et al., 2010, 2001). Both isotopes determine the formation of oxidation end products, either as $^{14}CO_2$ or $^{3}H_2O$. *Ex situ* or *in situ* use of stable isotopes (^{13}C-CH_4) and analyses of ^{13}C-CO_2 oxidation products by isotope-ratio mass spectrometry (IRMS) methods have been applied in several studies (Leonte et al., 2017; Valentine et al., 2001; Weinstein et al., 2016). The differences in oxidation half-lives between the studies performed with the different methods are illustrated in **Figure 3**. However, it must be emphasized that the large variations may be the results also of other factors than the analytical methods.

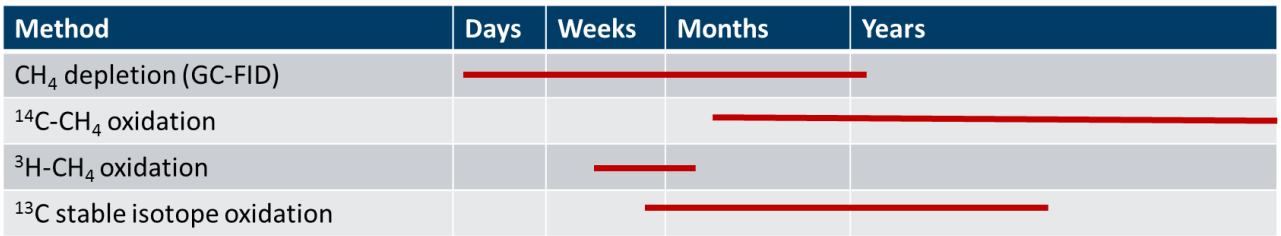

Figure 3: Ranges of methane oxidation half-lives related to the use of different analytical methods.

3. Study objectives

Based on findings in the desktop study, and in agreement with the ad-hoc group on methane emissions, it was suggested by SINTEF Ocean to focus on two analytical methods with studies of methane oxidation in natural Norwegian seawater (SW):

- Stable isotopes method with ^{13}C-CH_4
- The use of tritium-labelled methane (^{3}H-CH_4)

Stable isotope methods were suggested, since considerable methane field data exist with this method, both concerning measurement of methane related to various origins and processes, and for determinations of methane oxidation. Of importance is also that the National Laboratory of Age Determination at the Natural Museum at NTNU is located in Trondheim, and both scientific competence and analytical instrumentation (IRMS) is therefore locally available. Tritium-labelled can be used to work with low methane concentrations of environmental relevance. This method also requires a dedicated laboratory with a beta-counter and work with radioactive hazardous materials, which is available at NTNU, Institute of Biology, in the same building as SINTEF Ocean. This work had to be performed by a SINTEF Ocean scientist approved for this kind of work. Both methods are described in more details below.

Since none of these methods are currently in use at SINTEF Ocean, one main objective would be to establish methods. SINTEF Ocean has well established methods for working with methane in relation to 'high' concentrations and GC-FID analyses, but methods needed to be established for work with stable isotopes and tritium. In addition, methods needed to be established for handling of methane without contaminating the sampling, and for establishing HSE-procedures for handling of tritium. Parts of these method establishments included decisions on experimental incubation periods. When experimental and analytical methods were established, study objective included methane oxidation rates in relation to selected environmental variables:

- Methane concentrations, which was indicated as an important factor for oxidation rates in the desktop study
- SW temperature, which normally is considered as an important factor for biodegradation, although this was not identified in the desktop study
- Test robustness, which should be secured by high replicate numbers

Data obtained from the experimental work could then be used in model simulations. An objective of the model work would also be to perform a review of some selected publications for comparison of different mathematical models for growth of bacteria and oxidation of methane.

3.1 Stable isotope analyses

Stable isotope analyses were performed with different modifications of a method originally described by Leonte et al. (2017) for field samples. In principle, crimp-sealed flasks with butyl rubber septa with SW field samples were spiked with $^{13}C\text{-}CH_4$, except for blank controls in their studies, and some of the flasks poisoned with $HgCl_2$ to work as sterilized controls. The flasks were then incubated for 3 days. Samples were acidified by phosphoric acid (H_3PO_4) to convert all dissolved inorganic carbon (DIC) to CO_2, and isotopes of CO_2 ($^{12}CO_2$, $^{13}CO_2$ and $^{14}CO_2$) formed in the headspace of test vials analysed in a Delta XP Isotope Ratio Mass Spectrometer (IRMS) to determine the $\delta^{13}C$ isotopic ratio of CO_2 after being normalized against the isotope standard. Oxidation rates were then determined by calculations of $^{13}CO_2/^{12}CO_2$ ratios as described above (Eq6 and Eq7) in samples spiked with $^{13}CO_2$ isotope, and by subtracting the $^{13}CO_2/^{12}CO_2$ ratios in blanks not spiked with the isotope (Leonte et al., 2017).

The original method used for our studies (Leonte et al., 2017; Valentine et al., 2001), included a) spiking of each SW sample (160 ml) with 50 µL $^{13}CH_4$, b) acidification of 1 mL sample with 0.5 mL H_3PO_4 in 12 mL vials, and c) sampling of generated CO_2 using a Finnigan Gas Bench, delivering a total of ten aliquots of CO_2 to the IRMS. Based on this method, the procedure was stepwise developed until acceptable results were obtained, and the final method described. This stepwise method development is summarized below (**section 5.4.1** and **Table 1**) and described in more detail in **Appendix 1**. The final established method used for the stable isotope results is described below (**section 5.4.2**).

The method established for the oxidation method included flasks with test solutions ($^{13}CH_4$ in natural SW), controls solutions ($^{13}CH_4$ in sterilized SW; see **section 5.2.2**), and blank solutions without $^{13}CH_4$). The blank solutions contained either SW alone or SW with pre-incubated HiQ methane.

The method development is summarized below (**section 5.4.1** and **Table 1**) and described in more detail in **Appendix A**. The final established method used for the stable isotope results is described below (**section 5.4.2**).

3.1.1 Method development

As described in **Table 1** and in **Appendix A**, the use of the original method described by Leonte at al. (2017) and by Valentine et al. (2001) did not result in detectable IRMS signals. One reason for this may be that the analytical method for $^{13}CO_2$ quantification and determination of $\delta^{13}CO_2$ ratios in these reports included the use of a Finnegan Gas Bench (Leonte et al., 2017; Valentine et al., 2001). This system feeds the IRMS instrument with 10 mL purified CO_2 sample, thereby increasing the instrument sensitivity considerably. Such a gas bench is currently not available at NTNU, and only single samples of 1 mL gas can be analyzed by the instrument.

In brief, the test development included a) increased extraction volume by using the complete sample in the 100 mL crimp-sealed flasks for extraction, b) testing of a larger volumes sample (1-L), c) purification of CO_2 in the headspace sample by separating CO_2 from the quantitatively predominant N_2 gas in the sample by freeze-drying, and d) increasing the concentration of spiked $^{13}CH_4$ in the sample. These procedures and the results of the experiments are described in **Appendix A**. The outcome of these method developments resulted in a method described below, where $^{13}CO_2$ and $\delta^{13}CO_2$ ratios in $^{13}CH_4$-spiked samples could be quantified considerably higher than in non-spiked blank samples. This was a prerequisite for the determination of methane oxidation rates in the spiked samples.

Table 1: Summary of the stable isotope method development.

Method	Details	Results/conclusions
Original method Different incubation times	50 µL $^{13}CH_4$ in 117 mL SW Incubation 3, 7, and 14 days at 5 °C 1 mL sample acidified 10 mL headspace from 1 mL sample Headspace of N_2 and CO_2 (not purified) 1 mL headspace injected to the IRMS	Below IRMS $^{13}CO_2$ detection limit
Increased extraction volume Different incubation times	50 µL $^{13}CH_4$ in 117 mL SW Incubation of 3 and 28 days at 5 °C Appr. 100 mL sample acidified 10 mL headspace from 100 mL sample Headspace of N_2 and CO_2 (not purified) 1 mL headspace injected to the IRMS	Detectable IRMS $^{13}CO_2$ signals Not higher signals than in blank solutions (not spiked with $^{13}CH_4$)
Increased incubation volume	50 µL $^{13}CH_4$ in 117 mL SW Incubation of 3 days at 5 °C Appr. 1 L sample acidified 200 mL headspace from 1 L sample Headspace of N_2 and CO_2 (not purified) 1 mL headspace injected to the IRMS	Detectable IRMS $^{13}CO_2$ signals Not higher signals than in blank solutions (not spiked with $^{13}CH_4$)
Improved extraction method Freeze-drying of headspace samples	50 µL $^{13}CH_4$ in 117 mL SW Incubation of 3 days at 5 °C Appr. 100 mL sample acidified 10 mL headspace from 100 mL sample Headspace of pure CO_2 (N_2 removed) 1 mL headspace injected to the IRMS	Significantly increased IRMS $^{13}CO_2$ signals Not higher signals than in blank solutions (not spiked with $^{13}CH_4$)
Increased concentrations of spiked $^{13}CH_4$	250 µL, 500 µL and 1250 µL $^{13}CH_4$ in 117 mL SW Incubation of 3 days at 5 °C Appr. 100 mL sample acidified 10 mL headspace from 100 mL sample Headspace of pure CO_2 (N_2 removed) 1 mL headspace injected to the IRMS	Significantly increased IRMS $^{13}CO_2$ signals Significantly higher in all spiked solutions than in blank solutions (not spiked with $^{13}CH_4$)

3.1.2 Established method

The established method for stable isotope experiments used for providing stable isotope data in this project is described below with figures showing some of the systems used (**Figure 4 to Figure 7**), and with an illustration of the method in **Figure 8.**

Spiking of SW with $^{13}CH_4$ gas

HiQ methane was pre-incubated in natural or sterilized SW at concentrations 50 nmol/L in 100 mL crimp-sealed flasks (both test, control, and blank solutions) at a 5°C for 7 days (see **section 5.2**). Some flasks were sacrificed for methane analyses by GC-FID analyses (see **section 5.3**). Flasks with pre-incubated methane were then spiked with $^{13}CH_4$ from the low-pressure lecture bottle (**Figure 10A**). Volumes of at least 250 µL $^{13}CH_4$ was transferred directly from the valve of the lecture bottle to a gas-tight syringe (**Figure 4**) and applied with the syringe to each of the crimp-sealed flask, except for the blank samples. Some flasks were then

sacrificed for methane analyses by GC-FID. Test solutions were prepared in 5 replicates, and control and blank solutions in 3 replicates.

Figure 4: Transfer of 13CH4 from lecture flask to gas-tight syringe

Incubation and extraction

All flasks were incubated upside-down at 5°C for 3 days. After incubation a volume of 10 mL was removed from each flask with a syringe, while the removed liquid volume was replaced with HiQ N_2 gas by a cannula coupled to a N_2 flask (**Figure 5**). Each flask was then acidified with 5 mL H_3PO_4 (85vol% phosphoric acid) and incubated overnight at room temperature for oxidation of all DIC to CO_2. The flasks were transported to the National Laboratory for Age Determination at NTNU for extraction and IRMS analyses. Each flask was connected directly to an extraction unit for freeze-drying of the headspace (**Figure 6**), and pure CO_2 gas separated from N_2 by the freeze-drying process was transferred to IRMS tubes (**Figure 7**) mounted in the extraction unit.

Figure 5: Sample removal and replacement with nitrogen.

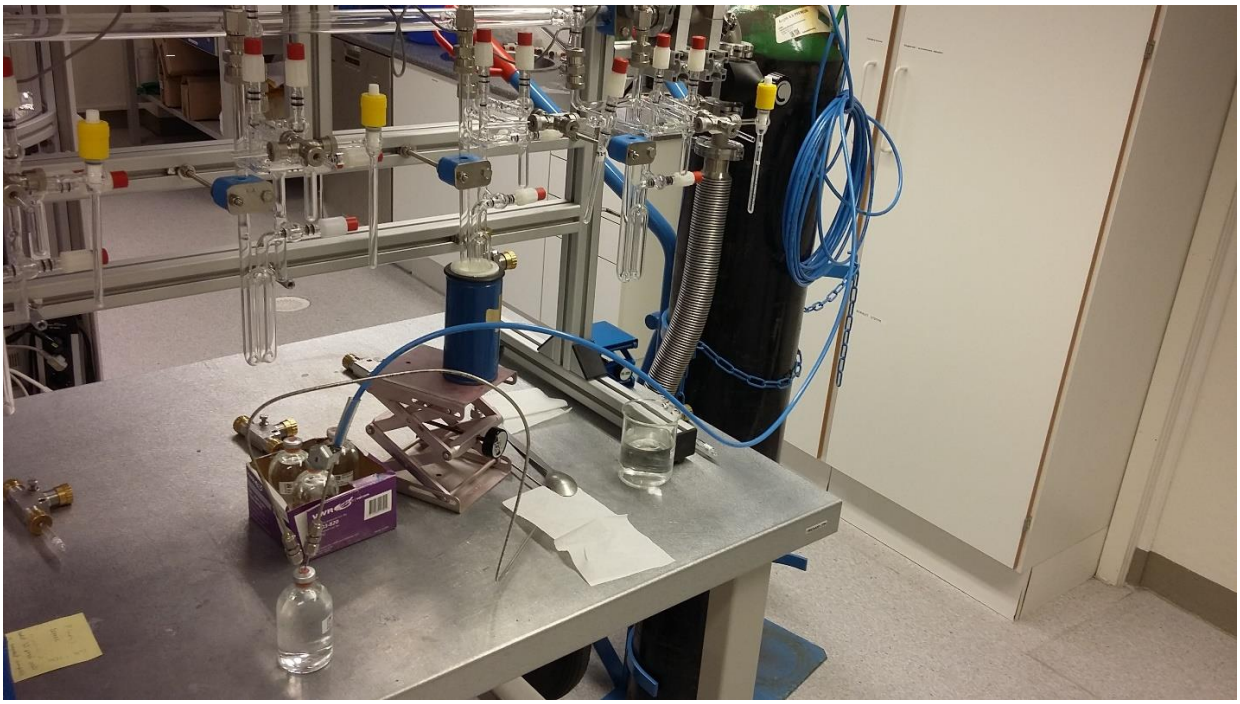

Figure 6: Samples extracted directly in an extraction unit at NTNU before IRMS analyses.

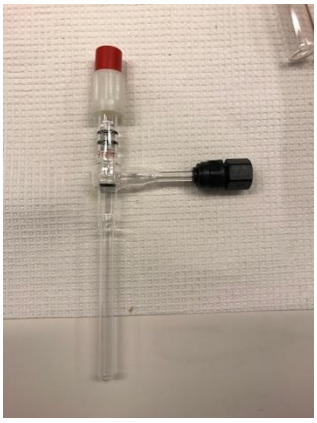

Figure 7: IRMS tube

IRMS analyses

The principles of the IRMS analyses are described above (see **section 4.1**). Volumes of 1 mL gas samples were injected in the IRMS instrument (Thermo 131 Delta V Advantage isotope-ratio mass spectrometer). The results were reported as relative $\delta^{13}C$ isotopic ratios, based on separate analyses of $^{12}CO_2$ (m/z = 44) and $^{13}CO_2$ (m/z = 45), and relative to the VPDB standard isotope ratio of 0.0112372 (IAEA, 1993). Calculations of oxidation rates where then performed from the reported $\delta^{13}C$ isotopic ratios as described in **sections 4.1** and **4.3**.

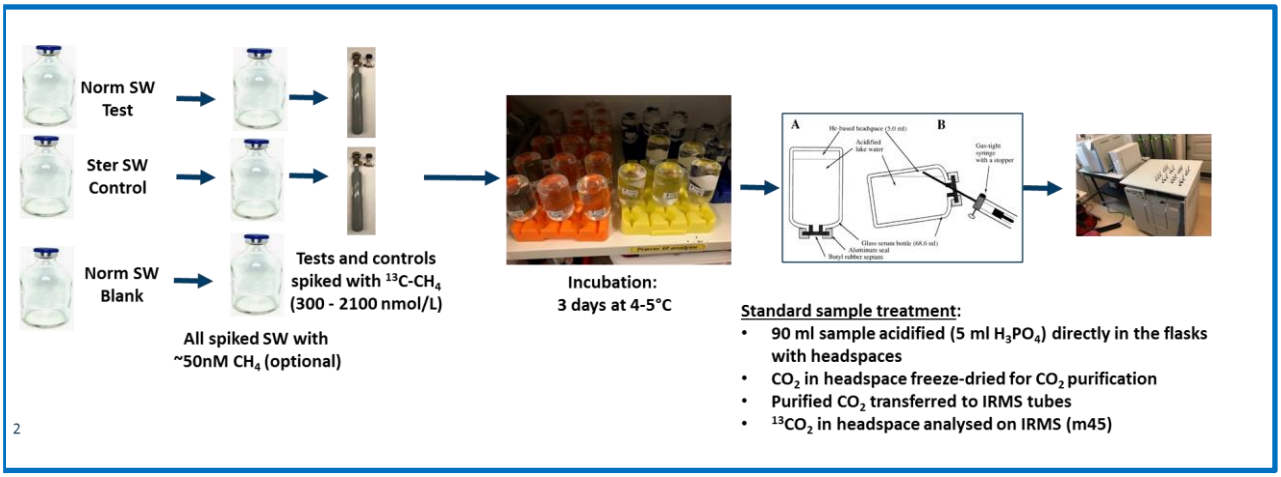

Figure 8: Overview of the experimental outline established for determination of methane oxidation by stable isotope analyses.

4. Principles of methods used

The methods used in this study included stable isotope analyses with samples spiked with $^{13}C\text{-}CH_4$ and experiments with radioactively labelled methane ($^{3}H\text{-}CH_4$). The method principles are presented below, while the technical details are described in the Materials and Methods.

4.1 Stable isotope analyses

In nature, carbon is distributed between ^{12}C-, ^{13}C- and ^{14}C- isotopes with relative distributions of 98.9% ^{12}C, 1.1% ^{13}C and 10^{-10} % ^{14}C. While neglecting the fraction of ^{14}C, the ^{13}C signatures can be determined as the $\delta^{13}C$ of a sample:

$$\delta^{13}C\text{sample } (‰) = \left(\frac{13C/12Csample}{13C/12Cstandard} - 1\right) \times 1000 \quad \text{(Eq5)}$$

The ratio between ^{13}C and ^{12}C in the sample is determined analytically on a mass spectrometer dedicated for these analyses (see below), while the ratio between ^{13}C and ^{12}C of the standard is established as an internationally accepted $\delta^{13}C$ unit for a reference material. The ratio between ^{13}C and ^{12}C ratio for the reference material VPDB ('Vienna Pee Dee Belemnite') approved by the International Atomic Energy Agency (IAEA) defines a $\delta^{13}C$ value of zero is 0.01123720 (IAEA, 1993).

Stable isotopes may be used as tracers for oxidation processes. By spiking a sample with pure $^{13}CH_4$, methane oxidation can be determined by measuring $^{13}CO_2$. These analyse are performed in an Isotope Ratio Mass Spectrometer (IRMS). In this instrument, the different isotopes are specifically analysed as exemplified with different carbon isotopes in **Figure 9**. For these analyses, all inorganic carbon, including HCO^- and CO_3^{2-} must be converted to CO_2 by sample acidification. Since the sample also will contain a natural background $^{13}CO_2$, the analysed ^{13}C in the samples must corrected for background values in material not spiked with $^{13}CH_4$.

$$^{13}CO_2/^{12}CO_2(ox) = {}^{13}CO_2/^{12}CO_2(sample) - {}^{13}CO_2/^{12}CO_2(blank) \quad \text{(Eq6)}$$

As a consequence of the methane oxidation process, the $^{13}CO_2/^{12}CO_2$ ratio will became higher in the spiked sample ($^{13}CO_2/^{12}CO_2$(sample)) than in the non-spiked blank ($^{13}CO_2/^{12}CO_2$(blank)).

The IRMS calculates and records the $\delta^{13}C$ value directly, and for determination of CH_4 oxidation back-calculations are performed from the $\delta^{13}C$ values, as raw isotopic ratios ($^{13}CO_2/^{12}CO_2$), using the known isotope ratio (0.0112372) of the standard (IAEA, 1993):

$$^{13}CO_2/^{12}CO_2 = (\frac{\delta 13CO2}{1000} + 1) \times 0.0112372 \text{ (Eq7)}$$

The $^{13}CO_2/^{12}CO_2$ ratio is then converted to the fraction (F) of $^{13}CO_2$ in the CO_2 sample (i.e. $^{13}CO_2/(^{13}CO_2 + ^{12}CO_2)$). And by subtracting F of the ''blank" control from the F of the inoculated/incubated samples, the fraction of ^{13}C generated through the oxidation of the $^{13}CH_4$ tracer (DF) was determined. The concentration of CO_2 produced in each sample following acidification was multiplied by DF to determine the concentration of excess $^{13}CO_2$, produced by $^{13}CH_4$ oxidation (Leonte et al., 2017).

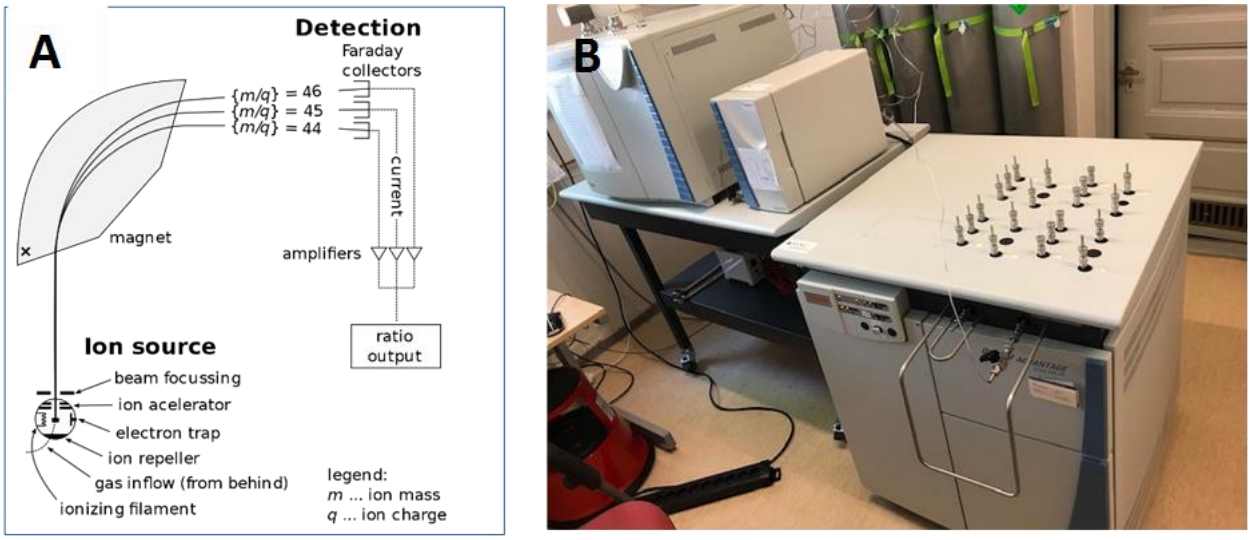

Figure 9: IRMS system for separation between carbon isotopes (A) and IRMS instrument located in the National Age Determination Laboratory at the NTNU Science Museum (B).

4.2 Tritium-method

Tritium is a radioactive isotope of hydrogen (H), with a half-life of 12 years. Tritium-labelled CH_4 (^3H-CH_4) is commercially available as gas or dissolved in a solvent (e.g. hexane). 3H-CH4 is oxidized the as follows:

$$^3H\text{-}CH_4 + 2\ O_2 = CO_2 + 2\ ^3H\text{-}H_2O \text{ (Eq. 8)}$$

During the oxidation, tritium is therefore transferred from gas to water molecules. After introduction of ^3H-CH_4 gas in the medium and incubation, residues of ^3H-CH_4 gas must be removed from the medium to determine the radioactivity of ^3H-H_2O formed. The best way of doing this will be to compare radioactivity in a sample with the radioactivity in a sterilized control after creating a headspace and removing as much as possible of the ^3H-CH_4 gas from samples and controls. This will result in lower radioactivity in the sterilized controls, where no ^3H-H_2O has been formed, compared to the samples. The radioactivity in the controls can then be subtracted from the radioactivity in the samples:

$$^3H\text{-}H_2O(\text{sample}) = (^3H\text{-}CH_4(\text{sample}) + {}^3H\text{-}H_2O(\text{sample})) - {}^3H\text{-}CH_4(\text{control}) \text{ (Eq. 9)}$$

4.3 Methane oxidation rates in seawater

Oxidation rates of methane in SW is determined by first-order rates (Eq.2), up to certain methane concentrations, where the rates become independent of methane concentrations (zero-order rates). As described above, the first-order rates of methane oxidation was determined up to concentrations of several µmols/L during the Deepwater Horizon oil spill (Kessler et al., 2011). By first-order rates, no non-responsive lag-periods (period from start of exposure to the onset of biodegradation) occur, and rate coefficient (*k*) can be determined as the fraction of methane oxidized per unit time (Valentine et al., 2001):

$$k = \frac{[CH4]ox}{[CH4]+[CH4]ox} / t \text{ (Eq10)},$$

where $[CH_4]ox$ is the concentration CH_4 oxidized, $[CH_4]$ is the ambient concentration of CH_4, and *t* is the time. Oxidation rates of a measured CH4 concentrations (MOX) and turnover time (τ) can then be determined (Bussmann et al., 2015):

$$MOX = k[CH_4] \text{ (Eq 11)}$$

$$\tau = 1/k = [CH_4]/MOX \text{ (Eq. 12)}$$

5. Materials and Methods

5.1 Seawater and methane

Natural subsurface SW was used as inoculum in the studies and was provided from 80 m depth in a local Norwegian fjord (Trondheimsfjord), outside the harbor area of Trondheim (63°26'N, 10°24'E). This subsurface SW is transported to the laboratory of SINTEF Ocean though a pipeline system. The depth of the pipeline inlet (80 m) is well below the thermocline, securing a stable temperature of 6-8 °C all the year around, and the SW is not considered to be influenced by seasonal variations (Brakstad et al., 2004). Some variations in microbial communities have been measured, as described in **section 6.1.2.1**. The SW holds an average salinity of 34. The SW passes a sand filter to remove coarse particles, before entering our laboratories. Mineral nutrient analyses have shown concentrations of 19 µg/L total-P, 16 µg/L o-PO_4-P, 130 µg/L NO_2+NO_3-N, and 3 µg/L NH_4-N, and < 0.05 mg/L Fe (Brakstad et al., 2015). The SW always shows 100% oxygen saturation when collected (appr. 10 mg/L dissolved oxygen at 6-8 °C).

High quality (HiQ) methane gas was purchased from Linde Gases Division, Pullach, Germany. The methane purity was ≥99.5%, and with ≤3000 mg/L of other hydrocarbons, according to information from the supplier.

^{13}C-methane stable isotope gas (Methane-^{13}C – 99 atom% ^{13}C; product no. 490229) was purchased from Sigma-Aldrich (St. Louis, MO, USA). The gas purity was ≥ 99.5 mole%, according to information from the supplier. The stable isotope methane gas was stored on a low-pressure 1-L lecture bottle gas cylinder (2.6 atm pressure), stored at room temperature (**Figure 10A**). The low positive pressure resulted in an atmospheric pressure in the cylinder after relieving 10% (appr. 100 mL). Relieved gas volume was increased by placing the cylinder in hot water (approximately 80 °C) when spiking samples with gas from the cylinder.

Tritium-labelled methane (^3H-CH_4) was purchased from American Radiolabeled Chemicals, Inc., St. Louis, MO, USA). The chemical was supplied on gas in a break-seal ampoule (**Figure 10B**) with a specific activity 1mCi (1-20 Ci/mmol 0.37-0.74 TBq/mmol). No information about concentration was provided by the supplier. The gas ampoule was stored inside an outer cylinder. The ampule was stored at 5 °C in a laboratory dedicated for work with radioactivity, and the ampoule equilibrated to room temperature before use.

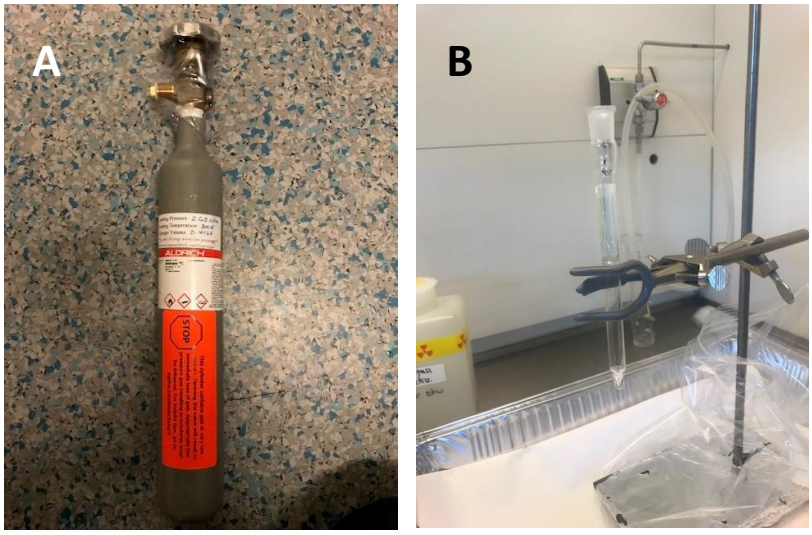

Figure 10: Lecture bottle with ^{13}C-methane (A) and break-seal ampoule with tritium-labelled methane (B).

5.2 Preparation of samples with HiQ methane in normal seawater

Preparation of HiQ methane was conducted in SW without any additional nutrient amendment, and in 100 mL crimp-sealed serum flasks with butyl rubber stoppers (total volume 117 mL).

5.2.1 Stock solutions of methane

Stock solutions of methane were prepared by injecting HiQ methane by a gas-tight syringe.

The procedure was conducted by filling the crimp-sealed serum flask with SW. A long gas-tight cannula connected to the stop-valve of the methane gas flask, was penetrated the rubber septum of serum flask, with the tip in the bottom of the flask. Gas was bubbled into the SW for 120 seconds, while another cannula was penetrated through the septum to relieve pressure in the flask. Air bubbles in the flasks were removed by adding SW with a syringe. The flasks with stock solutions were incubated for 2 hours at the relevant test temperature (4 °C or 13 °C, respectively).

The stock solutions were used for dilutions in methane test solutions in natural SW, or in sterilized controls (see below).

5.2.2 Test and control solutions with methane

Test and control solutions in 100 mL crimp-sealed serum flasks were prepared by filling each flask with SW. A gas-tight syringe was filled with stock solution, and the rubber septum of the crimp-sealed flask penetrated with the syringe, with the needle in the bottom of the flask, while another empty syringe with cannula was penetrated through the septum to collect the replaced SW out of the flask (equal volume as applied stock

solution). The headspace in the flasks were completely removed by adding SW with a syringe. Test solutions were provided with normal SW, and sterilized controls with poisoned SW (100 mg/L $HgCl_2$). Volumes of stock solutions were added to the test and control flasks with a syringe to achieve pre-defined methane concentrations, based on GC-FID analyses of stock solutions, while removing the same volume of headspace with a during used for relieving the pressure in the flasks. Typically, 10 mL stock-solution was added to obtain concentrations of 50 nmol/L methane. If higher methane concentrations were to be achieved, lower SW volumes were introduced prior to stock solution application. The flasks were then completely filled with SW (normal SW to test solutions, and sterilized SW to sterile control solutions) without air bubbles, while relieving the pressure with an extra cannula through the septa.

5.3 GC-FID analyses of methane

Quantifications of methane in the 100 mL serum flasks were routinely performed by gas chromatographic analyses. Volumes of 20 mL liquid were removed from the flasks with a syringe. While removed, the liquid was replaced with N_2 gas by a needle penetrating the rubber stopper, which connected to a hose from a gas cylinder with N_2 gas flask. The flasks were then shaken vigorously for 1 minute and incubated upside down for at least 2 hours. Volumes of 1 mL were then removed from the headspace and injected in the gas chromatograph coupled to a flame ionization detector (GC-FID; Agilent 6890N with J&WCP-Al2O3/Na2SO4 50m, 0.32 µm x 5 µm column; Agilent Technologies). An external calibration curve was prepared of 0.05 µL/mL to 2.5 µL/mL HiQ N_2 gas (Linde Gases) in air.

GC-FID results given as ppmV (µL/L) determined by linear regression analyses from the external calibration curve, were then converted to µmol/L for the volume in the headspace, using the gas constant (0.082):

$$\text{nmol/mL (headspace)} = \frac{ppmV(measured)x\ P(atm)}{0.082\ x\ Temperature\ (K)} \quad \text{(Eq13)}$$

The concentration was calculated for the total volume in the flask (117 mL):

$$\text{nmol/117 mL (sample)} = \text{nmol/L (headspace)} \times 20/117 \quad \text{(Eq14)}$$

The final the concentrations were then determined as nmol/L for the sample.

5.4 Tritium method

The tritium method was used to determine the transformation of $^3H\text{-}CH_4$ to $^3H\text{-}H_2O$ as a measure of methane oxidation. The method(s) used was modified from previously described use of $^3H\text{-}CH_4$ to determine methane oxidation rates in field samples (Bussmann et al., 2015; Mau et al., 2013; Pack et al., 2015). In brief, their methods included sampling of SW which was transferred to completely filled (no headspace) crimp-sealed serum vials, spiked with ^3H-labelled methane gas in N_2, and incubated in the dark at selected temperatures. Stoppers were then removed, some of the liquid discarded, and the sample sparged with N_2 gas to remove residual $^3H\text{-}CH_4$. Samples of 1-2 mL were then mixed with scintillation liquid (5-10 mL) and analyzed by liquid scintillation counting.

All work with the radiolabeled material was conducted in a laboratory dedicated for this type of work, and by a scientist trained and approved to work with radiolabeled material. All work with the radiolabeled material was performed in a fume hood.

Some experiments were performed to establish the final method, partly in association with HSE, and to avoid release if radioactive material outside the sample units. These included a) preparation and application of ^3H-CH_4 to test and sterilized control solutions, b) selection of incubation time, and c) establishment of method for sparging samples with N_2 gas and avoiding release of residual ^3H-CH_4 to the atmosphere outside the test and control flasks. These experiments are described in some detail in **Appendix B** and summarized in **Table 2** below.

5.4.1 Method development

The method was established by performing several experiments, as described in **Table 2** and in **Appendix B**. Some of the designed equipments are shown in **Figure 11 and Figure 12**, and an illustration of the established method is shown in **Figure 13**.

Table 2: Summary of the tritium method establishment.

Factor tested	Details	Results/conclusions
Storage of stock solutions	Screw-capped or crimp-sealed GC-glasses	Leakage testing showed that crimp-sealed GC-glasses did not result in leakage, while this was measured from several screw-capped glasses.
Stock solution volume in test and control samples	50 µL, 100 and 200 µL ^3H-CH_4 in 100 mL crimp-seal test and control flasks	50 µL of stock solutions resulted in acceptable radioactivity
Solubility of ^3H-CH_4 in hexane solvent	Comparison of radioactivity when stock solutions (50 µL) were transferred to 100 mL hexane and SW	Samples of 1 mL from samples of hexane and SW spiked with stock solutions did not differ significantly in measured radioactivity
Trapping of residual ^3H-CH_4 during sparging of samples with N_2-gas	Residual ^3H-CH_4 trapped in columns (syringes) of activated carbon	Experiments showed that columns trapped methane with 99% efficiency if used two times. Efficiencies slightly reduced (to 95% if used 4 times).
Volume of sample used for N_2-sparging	Sample volumes of 40 mL and 10 mL compared	Volumes of 10 mL sample resulted in higher differences between test and control radioactivity than 40 mL.
Incubation time	Incubations for 4, 13, 17 and 27 days compared	Most of the ^3H-CH_4 occurred after 4 days of incubation

5.4.2 Established method

Preparation of stock solutions of ^{3}H-labelled methane

Radiolabeled methane (^{3}H-CH_4) was purchased as gas in break-seal ampoules as shown in **Figure 10B** (**section 5.1**). Stock solutions of the gas dissolved were prepared in the solvent hexane in crimp-sealed GC-vials of 2 mL. Stock solutions in hexane were prepared as follows: The ampule was placed vertically in a clamp, and 5-6 ml of the solvent placed in the space above the inner break-seal. A large magnet (magnetic hammer) was placed in the solvent (**Figure 10B**). With a magnet outside the tube, the hammer was raised in the solvent and forced to fall in order to break the seal. The solvent then passed in the opened ampoule, and the methane gas became dissolved in the solvent. The solvent was left for at least 15 minutes to allow the mixture to equilibrate. The solvent was then distributed in vials in the 2-mL crimp-sealed GC-glasses with 1 mL stock solution in each glass. The stock solutions were stored at room temperature in a fume hood.

Test and control solutions

Solutions of HiQ methane were prepared in SW as described in **section 5.2**, and methane concentrations determined by GC-FID analyses. Methane concentrations was first determined in the stock solutions (**section 5.2.1**) by GC-FID analyses (**section 5.2.3**), and the determined concentrations used to dilute the stock solutions in normal SW (test) or in poisoned ($HgCl_2$) SW (sterilized controls) at concentrations of approximately 50 nmol/L (**section 5.2.2**) in 100 mL crimp-sealed serum flasks. Some flasks were sacrificed and analyzed by GC-FID to control the validate nominal methane concentrations. The test and control solutions were incubated for periods (see Results and Discussion under each section) before spiking samples with ^{3}H-CH_4.

Each test and sterilized control sample was spiked with 50 µL of ^{3}H-CH_4 from the stock solutions (^{3}H-CH_4 in hexane). Spiking was performed with a gas-tight syringe. The flasks were completely filled, controlling that no visible gas bubbles occurred. The flasks were the incubated in the dark in a refrigerator at 5 °C, or with the temperature of the refrigerator set at a minimum (approximately 8.5 °C). Incubations were performed for periods of 2 or 4 days, depending on the temperature (see Results and Discussion).

Sampling and analyses

When sampled, volumes of liquid were removed. Vials of the removed liquid was analyzed by liquid scintillation counting to determine the sum of generated ^{3}H-H_2O and residual ^{3}H-CH_4 in the samples. The rest of the solutions were discarded to obtain a final volume of 10 mL liquid in the samples. The discarded volumes were treated as radioactive waste (see **section 5.5.4**). The 10-mL volumes left in the test and control solutions were sparged with N_2 gas for 2 hours. This sparging was performed from a custom-made tower connected to the gas flask, and with 12 outlet units to sparge 12 bottles simultaneously (**Figure 11**).

Figure 11: Unit for sparging of samples with N_2 gas before analyses

Cannulas penetrating to flask septa to release pressure in the flasks during sparging, were connected to syringes filled with active carbon (**Figure 7)**.

After sparging with N_2 gas, volumes of 1 mL liquid were mixed with 10 mL Ultima Gold scintillation cocktail (Perkin Elmer Inc.) in 20 ml scintillation vials and counted in a LS 6500 multi-purpose scintillation counter (Beckman Coulter, Inc., USA). The results were recorded as disintegrations per minute (dpm)

Figure 12: Sparging of samples and trapping of radioactive material in headspace in columns with activated carbon.

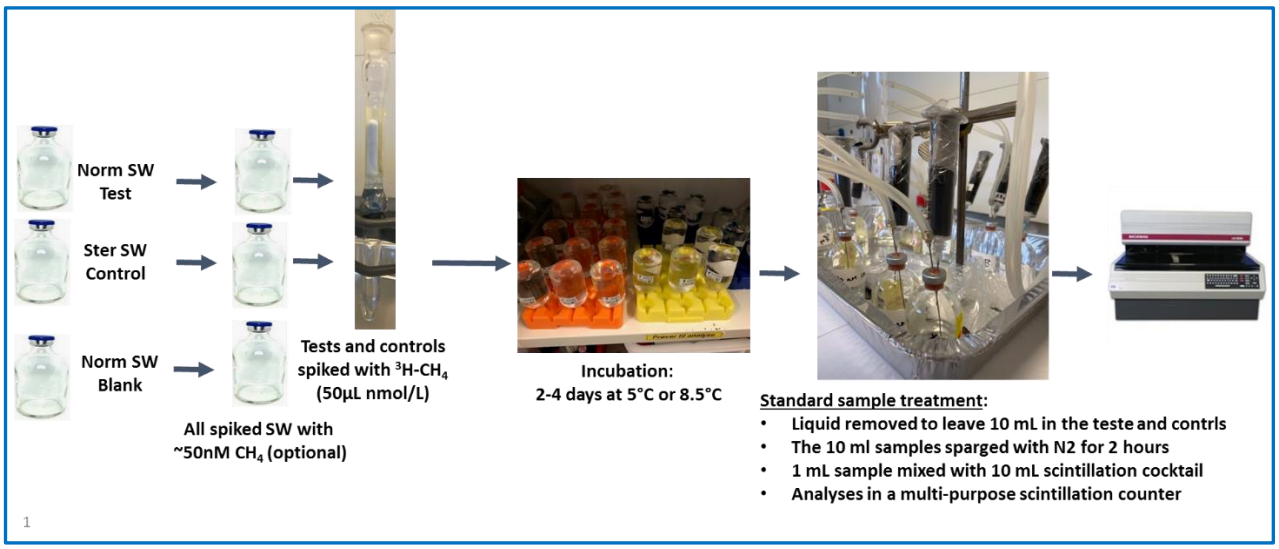

Figure 13: Overview of the experimental outline for determination of methane oxidation by tritium-labelled methane.

5.4.3 HSE in relation to work with radiolabeled material

Precautions were made to avoid emissions and accidents with the tritium-labelled materials. As mentioned, all work as performed in a lab dedicated for work with radioactive materials, and by a scientist trained and approved for this type of work. The work was conducted in accordance with SINTEF's procedures with chemicals and operations associated with health risk.

An HSE plan was established specifically for this project. This plan included the general procedures for work with the isotope, procedures in case of an accidental release, registration of work with the isotope, risk-reducing efforts. The plan also included calculations of radiation risks in relation to Norwegian regulations.

Waste treatment was separated between solid and liquid waste, and in three categories, based on radiation (Bq):

1. Units for storage of equipment with radioactivity >10^6 Bq – requires depositing at an approved supplier of these types of services
2. Units for storage of equipment with radioactivity between 10^2 and 10^6 Bq – requires delivery as radioactive material, but is not mandatory for deposition
3. Units for storage of equipment with radioactivity < 10^2 Bq – treated as 'dangerous material' but is not mandatory for deposition.

5.5 Microbiology

The microbiology analyses were performed with the intention to detect and quantify the *pmoA* gene responsible for microbial methane oxidation (Luesken et al., 2011; McDonald and Murrell, 1997).

5.5.1 Samples and filtering

For initial analyses, verification of methodology, 3 x 1L of seawater from a seawater tap at SINTEF Ocean was used. The water inlet is situated at 70 m water depth in the fjord outside the SINTEF-localities. From the following laboratory experiment, seven flasks with 500 ml seawater added varying concentrations of methane (3 flasks with 25 ml, and two flasks each with 12,5- and 6-ml methane), and one flask with 1 L seawater without methane (blank-sample) was received at the laboratory. The content of the flask with seawater without methane was split in two flask and the water from all flasks were filtered on separate 0,2 um Millipore filters.

5.5.2 DNA extraction

Filters were cut in smaller pieces and each sample added 1 ml DNA/RNA shield before being stored at -20 °C until extraction of DNA. ZymoBIOMICS DNA Miniprep kit was used for DNA extraction according to the producers' manuals, and samples eluted in 70 ul Dnase/Rnase free water. The DNA-concentration of the samples were quantified using a NanoDrop 1000 Spectrophotometer (ThermoFisher Scientific), and a Qubit 3.0 Fluorometer (Invitrogen) with dsDNA High Sensitivity kit (ThermoFisher Scientific). Extracted DNA was further analysed using digital PCR (dPCR) and quantitative PCR (qPCR).

5.5.3 Quantification of the pmoA- and 16S rRNA-genes

For quantification of 16S rRNA- og pmoA-genes in the samples, digital-PCR (dPCR) and quantitative PCR (qPCR) was used. For quantification of the total numbers of bacteria the V7–8 region of the 16S rRNA gene was amplified using the primer pair 1055f (5'-ATGGCTGTCGTCAGCT-3') and 1392r (5'-ACGGGCGGTGTGTAC-3') in qPCR. dPCR and qPCR for quantification of the ratio of methane oxidizing bacteria was performed using the primer pair 189f (5'-GGNGACTGGGACTTCTGG-3') and mb661r (5'-CCGGMGCAACGTCYTTACC-3') for amplification of the gene pmoA encoding particulate monooxygenase (pMMO) (Holmes et al., 1995; Lyew and Guiot, 2003).

dPCR (digital PCR) was performed on a Naica system from Stilla Technologies, using PerfeCTa Multiplex qPCR ToughMix. EVAGreen was used as fluorophore for detection, and the PCR conditions were as follows: 50 °C for 2 minutes followed by initial denaturation for 5 minutes at 95 °C. 30 cycles*(95 °C for 30 seconds, 55 °C for 30 seconds, and 72 °C for 30 seconds), and a final step of 72 °C for 7 minutes.

qPCR was performed on a QuantStudio 5 Real-Time PCR System, using PowerTrack SYBR Green Master Mix from Applied Biosystems (A46012). Standard curves were established using ZymoBIOMICS HMW DNA Standard from Zymo Research (D6322) and genomic DNA fra *Methylococcus capsulatus* NCIMB 11132 for quantification of the 16S rRNA- and pmoA-genes respectively. The same HMW DNA-standard was used as negative control in qPCR using the 189f/ mb661r primer pair for amplification of pmoA. Conditions as follows: 50℃ for 2minutes, 95 °C for 2minutes, followed by 40 cycles*(95 ℃ for 15 seconds, 55 ℃ for 60 seconds), with a final melt-curve step: (95 ℃ for 15 seconds, 60 ℃ for 1minute and 95 ℃ for 15 seconds). The annealing temperature was adjusted between 54-65 ℃ for optimization of the PCR conditions. PCR products were controlled on an Agilent 4150 TapeStation System (Aglient Technologies) using either a High Sensitivity D1000 ScrenTape Assay or Genomic DNA ScreenTape Assay for TapeStation Systems.

5.6 Calculations and statistics

5.6.1 Stable isotope oxidation

Calculations of oxidation rates with stable isotopes were performed, based on IRMS data:

DIC concentrations were first determined as vol% of the complete sample, based on analyzed vol% in the sample corrected for the complete sample volume:

$$\text{DIC vol\% test units (DIC\%)} = CO_2 \text{ vol\% headspace x } \frac{vol\ headspace}{vol\ test\ unit} \text{ (Eq15)}$$

where CO_2 vol% headspace was the percentage CO_2 measured in the sample by IRMS analyses, vol headspace the volume headspace formed in the test units (mL), and vol test unit was the total volume of the test unit (e.g. 117 mL in the 100-mL crimp-sealed serum flasks). DIC concentrations were then converted from vol% to ppmV (DIC ppmV = DIC vol% x 1 x 10^4).

The DIC concentrations were then determined in nmol/L (DIC nmol/L):

$$[DIC]nmol/L = \frac{P\ x\ (DIC\%\ x\ 1000)}{R\ x\ T} \text{ (Eq16)}$$

where P is the atmospheric pressure, R is the universal gas constant (0.082), and T is the temperature in Kelvin (K) of the measured sample.

The IRMS analyses included the $\delta^{13}C$ isotope ratios in the samples, and these data were used to determine the ratios between $^{13}CO_2$ and $^{12}CO_2$ and the fraction (F) of $^{13}CO_2$ in the samples:

$$^{13}CO_2/^{12}CO_2 = ((\frac{\delta 13C\ ratio}{1000}) + 1) \text{ x } 0.0112372 \text{ (Eq17)}$$

where 0.0112372 is the isotope ratio of the standard (IAEA, 1993).

$$F = \frac{13CO2}{13CO2+12CO2} \text{ (Eq18)}$$

where F is the fraction of $^{13}CO_2$ as part of the complete CO_2 in the samples.

The fractions of $^{13}CO_2$ in the samples spiked with $^{13}CH_4$ were then corrected for the fractions of $^{13}CO_2$ in the blanks not spiked with $^{13}CH_4$:

$$\Delta F = F_{sample} - F_{blank} \text{ (Eq19)}$$

where ΔF is the concentration of excess $^{13}CO_2$, produced by $^{13}CH_4$ oxidation.

The concentration of $^{13}CH_4$ oxidized was then determined from Eq 19, since, since 1 mole CH_4 is oxidized to 1 mol CO_2 (see Eq 1):

$$[CH_4]ox = [DIC] \times \Delta F \text{ (Eq20)}$$

Oxidation rate coefficients (k), oxidation rates based on measured CH_4 concentrations (MOX), and turnover times (τ) could then be determined as described in Eqs 10-12 (Bussmann et al., 2015).

5.6.2 Statistics

Unpaired and paired t-tests and one-way ANOVA were performed by the statistics module in GraphPad Prism version 9.3.1 (GraphPad Software, San Diego, CA, USA).

5.6.3 Oxidation of tritium-labelled methane

Oxidation of tritium-labelled methane (^3H-CH_4) was performed by determination of ^3H-H_2O by comparison of normal and sterilized SW samples after removing residues of ^3H-CH_4.

$$^3H\text{-}H_2O_{sample} = (^3H\text{-}H_2O_{sample} + {}^3H\text{-}CH_{4\ sample}) - {}^3H\text{-}CH_{4\ sterile\ controls} \text{ (Eq21)}$$

$$k1 = (^3H\text{-}H_2O/^3H\text{-}H_2O + {}^3H\text{-}CH_4))/t \text{ (Eq22)},$$

where k1 is the first-order rate coefficient, ^3H-CH_4 is the radioactivity in the applied tritium-labelled methane, and *t* is the incubation time (Bussmann et al., 2015). MOX and turnover times (τ) are then determined as described in Eqs 10-12.

6. Results

In this project, efforts were made to determine methane oxidation by two approaches, by the use of a) stable isotopes as $^{13}CH_4$ or as b) tritium-labelled methane (^3H-CH_4). Both methods were used to determine methane oxidation as mineralization of dissolved gas in natural SW, either into $^{13}CO_2$, or into ^3H-H_2O. In most of the experiments, the SW was pre-incubated with natural methane gas ($^{12}CH_4$) dissolved in the SW at a low concentration, to expose (and adapt) the microbial communities to methane before spiking with the labelled compound. Since low concentrations were used, we did not consider any need for additional nutrient amendment of the SW, in the form of nitrogen, phosphorus or iron sources, since the natural concentrations in the SW of these nutrients were expected to be high enough for the bacteria during the oxidation process. We have previously performed biodegradation studies with oil concentrations of 2-3 mg/L without the need for nutrient supplements (Brakstad et al., 2015). The low methane concentrations used in the experiments should also infer that oxygen anomalies should not occur during oxidation. Typically, the dissolved oxygen (DO) concentrations in the SW at 5 °C is 9-10 mg/L at 100% saturation. Since the theoretical oxygen demand

(ThOD) for methane oxidation is 4.0 mg/L O_2 (OECD, 1992), up to 1.2 mg/L methane is oxidized before DO in the SW is reduced to 50% saturation.

The methods used in this project were adapted from field studies. Several method modifications were needed. These modifications are described and discussed in **Appendix A** (stable isotope method) and **Appendix B** (tritium method).

6.1 Pre-adaption of SW with methane

The SW used in these experiments were collected from a 'pristine' source in relation to methane exposure. The background concentration in this SW was determined to be 0.72 ± 0.03 nmol/L, based on GC-FID analyses of 4 replicates. This is considerably lower than concentrations determined in most marine environments in seep areas, which may reach concentrations from 10 nmol/L to >100 nmol/L (Uhlig et al., 2018; Ward et al., 1989; Pack et al., 2015; Weinstein et al., 2016; Leonte et al., 2017; Valentine et al., 2001, 2010). It was therefore decided to introduce a 'standard' methane concentration of 50 nmol/L which should represent a concentration corresponding to *in situ* concentrations in SW close to methane seeps. This concentration be used to 'pre-adapt' the microbial communities in the SW to methane prior to introduction of labelled methane ($^{13}CH_4$ or ^{3}H-CH_4). Methane for pre-adaption was introduced as HiQ methane prepared as a stock solution, which was measured by GC-FID before diluted in test, sterilized controls, and blank samples. Concentrations of introduced methane in stock and test solutions are shown in **Figure 14** for 6 replicates. The measured concentrations in stock solutions were 906 ± 47 nmol/L methane, i.e. a standard deviation (SDs) of 5% of the average concentration. When 10 mL and 7 mL stock solution was diluted in 100 mL SW, concentrations of 49 ± 0.2 nmol/L and 57 ± 3 nmol/L were obtained, respectively **(Figure 14**), with 0.4% and 5% SDs, respectively. Based on these SDs we considered the repeatability of this method to be acceptable. In subsequent experiments, volumes of 8 mL stock solution were used to obtain final concentrations methane for pre-adaption of microbial populations.

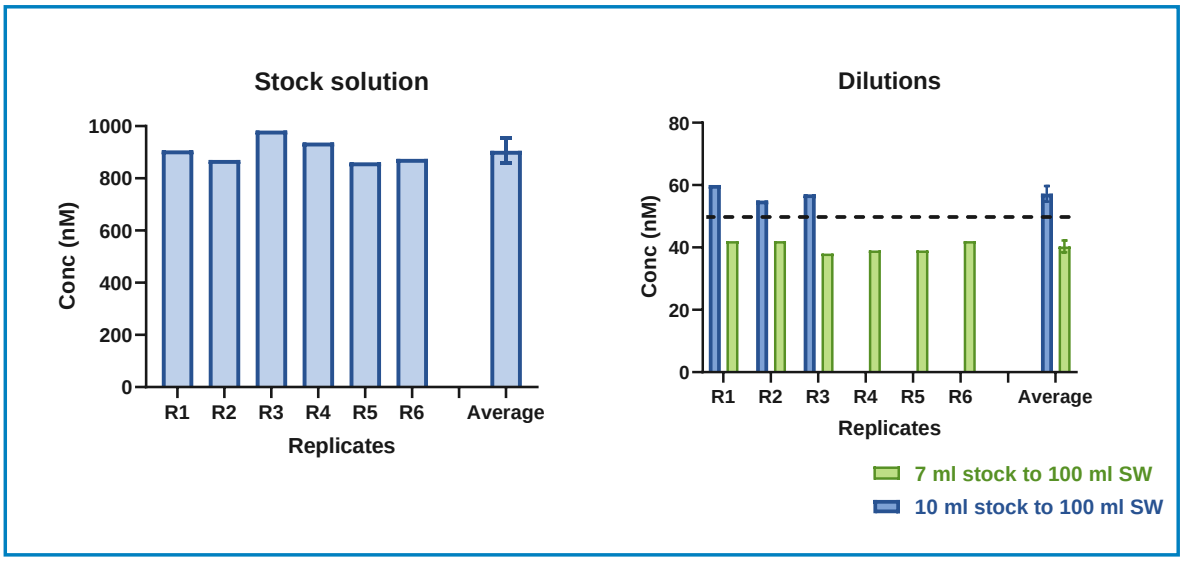

Figure 14: Methane concentration in 6 replicates of stock solutions prepared (25 mL methane injected over 120 seconds into 100 mL SW) and in dilutions by injecting 7 mL or 10 mL of stock solution to 100 mL SW.

6.2 Studies with SW spiked with stable isotope ($^{13}CH_4$)

The objectives of these studies were to determine methane oxidation rates related to incubation time, methane concentration, and incubation temperature. Test, sterilized control, and blank solutions were mainly pre-adapted HiQ methane (50 nmol/L) before spiked with $^{13}CH_4$ stable isotope. Analyses were performed with IRMS to determine $\delta^{13}CO_2$ ratios to be used for determination of $^{13}CH_4$ oxidation.

The intentions of these experiments were originally to determine $^{13}CH_4$ oxidation rates related to:

- Incubation times
- SW temperature
- Methane concentrations
- Test robustness

6.2.1 Method establishment

However, most of the experiments were performed as part of method development, as described in **Table 1** and in **Appendix A**. Experiments with different incubation times were performed with 50 µL of spiked $^{13}CH_4$. GC-FID analyses of blank samples with appr. 50 nmol/L HiQ methane, but not spiked with $^{13}CH_4$, and test and control samples with both 50 nmol/L HiQ methane and 50 µL $^{13}CH_4$ are shown in **Figure 15.**

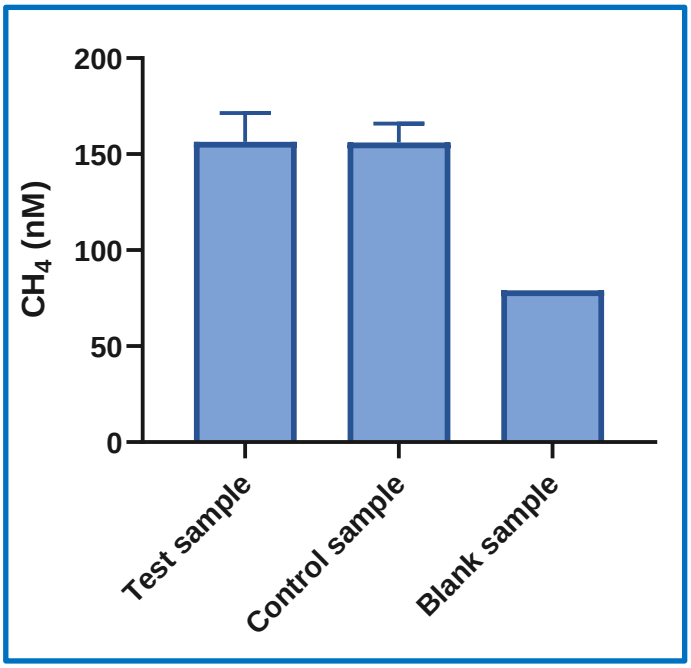

Figure 15: Methane concentrations in flasks with test and sterilized control samples (both pre-adapted with normal HiQ methane and spiked with 50 µL $^{13}CH_4$) and in Blanks (only pre-adapted with 50 nmol/L nominal concentrations of normal CH_4).

The GC-FID results verified that blank samples not spiked with $^{13}CH_4$ contained methane concentrations close to the nominal 50 nmol/L concentrations, with measured concentrations of 79-83 nmol/L methane. Spiking with $^{13}CH_4$ resulted in concentrations of 158 ± 4 nmol/L in sterilized controls, and the spiked stable isotope of methane therefore represented a concentration of appr. 76 nmol/L.

When experiments were performed with these concentrations of $^{13}CH_4$, and samples collected during incubation times of 3, 7, 14 and 28 days of incubation at 5°C, the concentrations of spiked material proved to be too low to clearly separate between $\delta^{13}CO_2$ ratios in spiked test and control samples compared to non-spiked samples (**Appendix A**). These experiments did not indicate that extended incubation times longer than the standard of 3 days improved the determination of $\delta^{13}CO_2$ ratios (**Appendix A**), and this incubation period was used during the rest of the experiments. It was further decided not to conduct experiments with different SW temperatures. Furter experiments with different test volumes for extraction and purification of CO_2 in samples did not result in determined $\delta^{13}CO_2$ ratios significantly different in $^{13}CH_4$-spiked test samples versus non-spiked blanks, as long as samples were spiked with 50 µL $^{13}CH_4$ (**Table 1** and **Appendix A**).

In the final experiment with different concentrations of $^{13}CH_4$, test and control samples were spiked with 250 µL, 500 µL or 1250 µL stable isotope. GC-FID analyses (**Figure 16)** showed that these volumes resulted in concentrations of 300 nmol/L, 570 nmol/L and 2150 nmol/L of $^{13}CH_4$, when corrected for the concentration of HiQ methane.

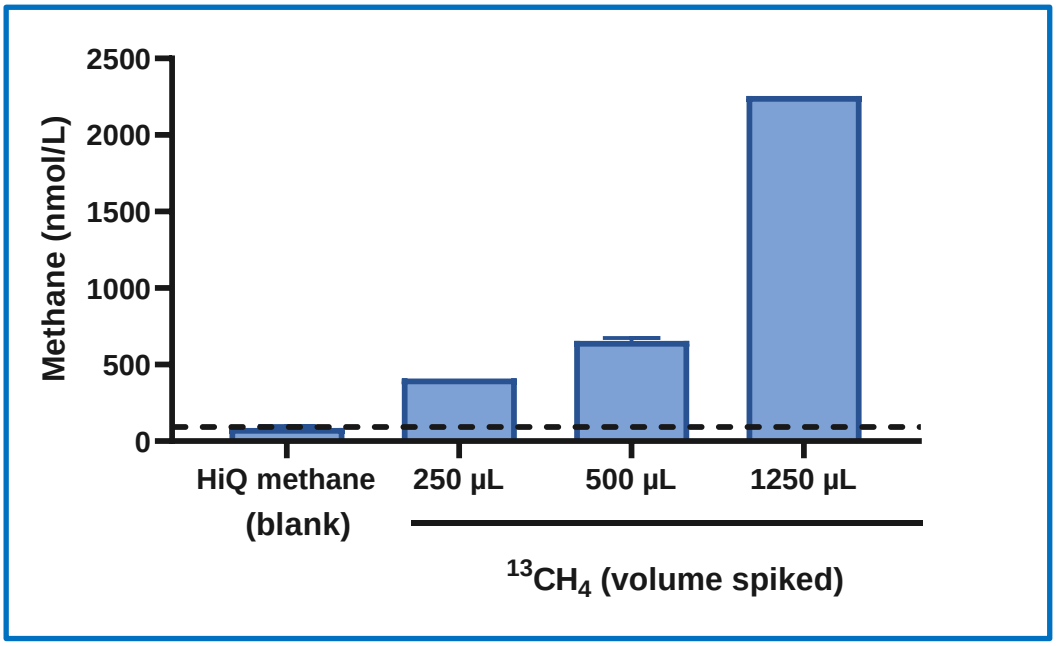

Figure 16: Methane concentrations measured by GC-FID in SW blanks pre-adapted with HiQ CH_4, and in pre-adapted samples spiked with 250 µL, 500 µL and 1250 µL $^{13}CH_4$. The broken line shows the concentration level of the blank not spiked with stable isotope.

As described in **Appendix A**, IRMS analyses now resulted in $\delta^{13}CO_2$ ratios significantly higher in test than in blank samples for all 3 volumes of spiked $^{13}CH_4$, and these data therefore enabled determinations of methane oxidation with all volumes of spiked material. The conclusion of the method establishment was that a combination of an extraction method with CO_2 purification by freeze-drying and spiking test samples with 300 nmol/L $^{13}CH_4$, worked acceptable for IRMS analyses (**Appendix A**). The final method used for determination of methane oxidation is described in **section 5.4.2** and summarized in **Figure 8**. Although the concentrations of 300 nmol/L - >2000 nmol/L are high, such concentrations can be related to methane concentrations in stratified SW of seep-areas and during the Deepwater Horizon oil spill (Kessler et al., 2011; Sansone and Martens, 1978; Ward et al., 1989).

6.2.2 Determination of methane oxidation by stable isotopes

The experiment performed for determination of $^{13}CH_4$ oxidation rates were determined as described in **section 5.4.2**, with volumes of 250 µL, 500 µL and 1250 µL $^{13}CH_4$ spiked to replicate 100-mL crimp-sealed flasks which had been pre-adapted with 50 nmol/L HiQ methane (**Figure 16**). The pre-adaption of test, control and blank flasks was performed at 5°C for 7 days, while incubation of tests and controls with $^{13}CH_4$ was performed at 5°C for 3 days. Test flasks included 5 replicates of each $^{13}CH_4$ volume applied, while 3 replicates of control (250 µL $^{13}CH_4$) and blank were included. The results of $\delta^{13}CO_2$ ratios for each replicate and the calculated oxidation of $^{13}CH_4$ are shown in **Table 3**, while average results of $\delta^{13}CO_2$ ratios replicates are shown in **Figure 17**. The sterilized controls spiked with 250 µL $^{13}CH_4$ showed significantly higher $\delta^{13}CO_2$ ratios ($P<0.0001$, paired *t*-test) than the corresponding values in test samples spiked with the same volume of stable isotope. This was expected, since $^{12}CO_2$ is formed faster than $^{13}CO_2$ during methane oxidation, and the $\delta^{13}CO_2$ ratios should therefore become reduced in oxidized samples when compared to sterilized controls. Since the of $\delta^{13}CO_2$ ratios in blanks and each of the tests showed significant differences ($P<0.01$ in all comparisons; paired *t*-tests), all spiked volumes could be used for determinations of $^{13}CH_4$ oxidation (**Table 3** and **Figure 18)**. However, the standard deviations increased with increasing volumes of $^{13}CH_4$ spiked, from 25% to 44% of average values from 250 µL to 1250 µL of spiked isotope. The calculated rate coefficients, half-lives, MOX and turnover are shown in **Table 4**. While rate coefficients decreased, and half-lives subsequently increased, by increasing $^{13}CH_4$ concentrations (**Table 4** and **Figure 19)**, MOX increased when applied $^{13}CH_4$ concentrations became higher (**Table 4** and **Figure 20**), in accordance with first-order rate kinetics (see Eq. 2). Linear regression analyses of rate coefficients (k1) and MOX were also determined (**Figure 21**), since these estimates may be used in the OSCAR model for rate determination in relation to methane concentration measured. The slopes of the linear regression analyses were significantly different from zero ($P=0.0190$ for k1-determinations and $P<0.0001$ for MOX), while Goodness-of-fits (R2) of the regression analyses were 0.3555 (k1) and 0.6760 (MOX).

Table 3: Determination of methane oxidation caused by different volumes of $^{13}CH_4$ spiked to normal (T) or sterilized (C) SW in samples pre-incubated for 7 days with normal methane (nominal concentrations of 50 nmol/L) before spiking with 250 µL, 500 µL or 1250 µL of $^{13}CH_4$ gas. The samples were incubated for 3 days. The results are shown for individual replicates of test samples (Test1-Test5), for single samples in sterilized controls (Control), and blanks (Blank) containing only normal methane (50 nmol/L nominal concentrations; not spiked with $^{13}CH_4$). When sampled, the complete samples were sacrificed for analyses of CO_2 (DIC) and $\delta^{13}C$ ratios. For explanations, see Table 1.

Sample	$\delta^{13}C$	DIC (mM)	F ($^{13}CO_2/^{12}CO_2$)	ΔF	$[^{13}CH_4]ox$ (nmol/L)
Test1-250	1.102	2.507	0.011250	0.00001274	31.9
Test2-250	1.298	2.705	0.011252	0.00001494	40.4
Test3-250	0.653	2.771	0.011245	0.00000769	21.3
Test4-250	1.326	2.672	0.011252	0.00001526	40.8
Test5-250	1.397	2.551	0.011253	0.00001605	41.0
Test1-500	1.298	2.496	0.011252	0.00001494	37.3
Test2-500	1.543	2.749	0.011255	0.00001769	48.6
Test3-500	0.706	2.727	0.011245	0.00000829	22.6
Test4-500	0.751	2.749	0.011246	0.00000879	24.2
Test5-500	2.029	2.936	0.011260	0.00002316	68.0
Test1-1250	4.676	2.793	0.011290	0.00005290	147.8
Test2-1250	4.744	2.749	0.011291	0.00005367	147.5
Test3-1250	5.39	2.782	0.011298	0.00006092	169.5
Test4-1250	2.068	2.606	0.011260	0.00002359	61.5
Test5-1250	2.117	2.573	0.011261	0.00002414	62.1
Control1-250	3.334	2.727	0.011275	--	--
Control2-250	2.904	2.474	0.011270	--	--
Control3-250	3.395	2.298	0.011275	--	--
Blank1	-0.401	2.705	0.011233	--	--
Blank2	0.319	3.134	0.011241	--	--
Blank3	-0.013	3.178	0.011237	--	--

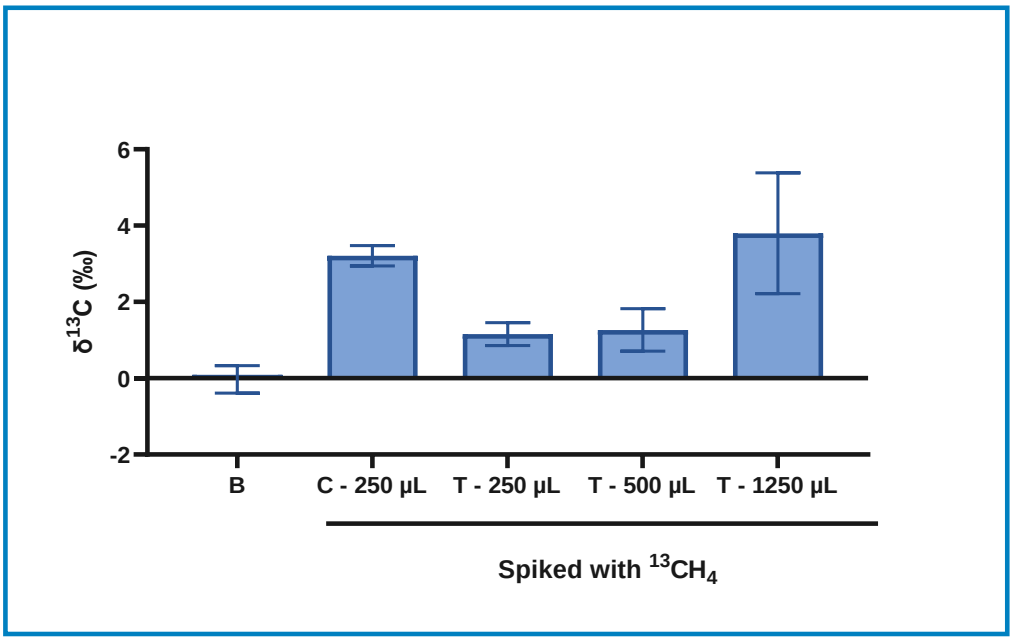

Figure 17: Average values ± standard deviations of $\delta^{13}CO_2$ ratio of blanks (B), sterilized controls (C) and test samples (T) of replicate values shown in Table 3.

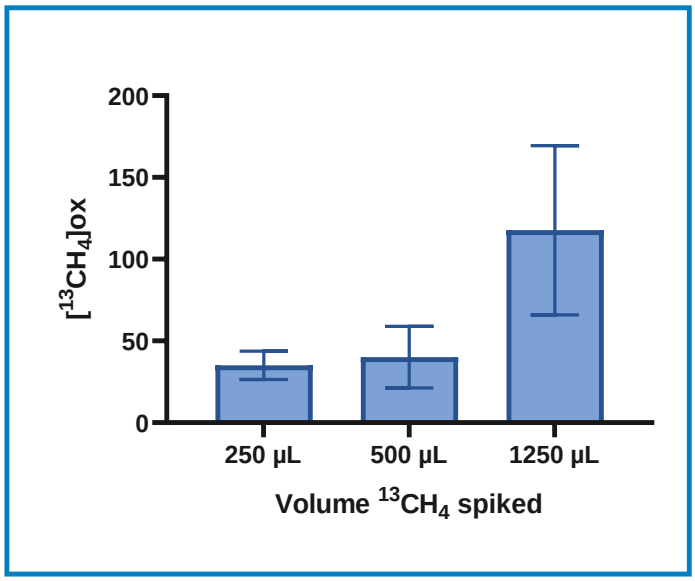

Figure 18: $^{13}CH_4$ oxidation related to spiked volumes of $^{13}CH_4$. The results are average ± standard deviations of replicate results shown in Table 3.

Table 4: Calculations of first-order rate coefficients, half-lives, methane oxidation rates (MOX) and turnover time for the replicates with positive ΔF after 3 days of incubation at 5 °C (Table 3). For explanations, see Table 2.

Sample	$[^{13}CH_4]ox$ (nmol/L)	Rate coefficient (k)[A)]	Half-life (days)[B)]	MOX (nmol/L d^{-1})[C)]	Turnover (days)[D)]
Test1-250	31.9	0.0312	22.2	9.6	32.0
Test2-250	40.4	0.0386	18.0	11.9	25.9
Test3-250	21.3	0.0215	32.2	6.6	46.5
Test4-250	40.8	0.0389	17.8	12.0	25.7
Test5-250	41.0	0.0390	17.8	12.1	25.6
Test1-500	37.3	0.0205	33.8	11.7	48.8
Test2-500	48.6	0.0263	26.4	14.9	38.1
Test3-500	22.6	0.0127	54.4	7.2	78.5
Test4-500	24.2	0.0136	51.0	7.7	73.6
Test5-500	68.0	0.0356	19.5	20.2	28.1
Test1-1250	147.8	0.0214	32.4	46.1	46.8
Test2-1250	147.5	0.0214	32.4	46.0	46.8
Test3-1250	169.5	0.0243	28.5	52.4	41.1
Test4-1250	61.5	0.0092	74.9	19.9	108.1
Test5-1250	62.1	0.0093	74.2	20.1	107.1

[A)] Calculated as described in Eq10; [B)] determined as ln2/k; [C)] calculated as described in Ew11; [D)] Calculated as described in Eq12.

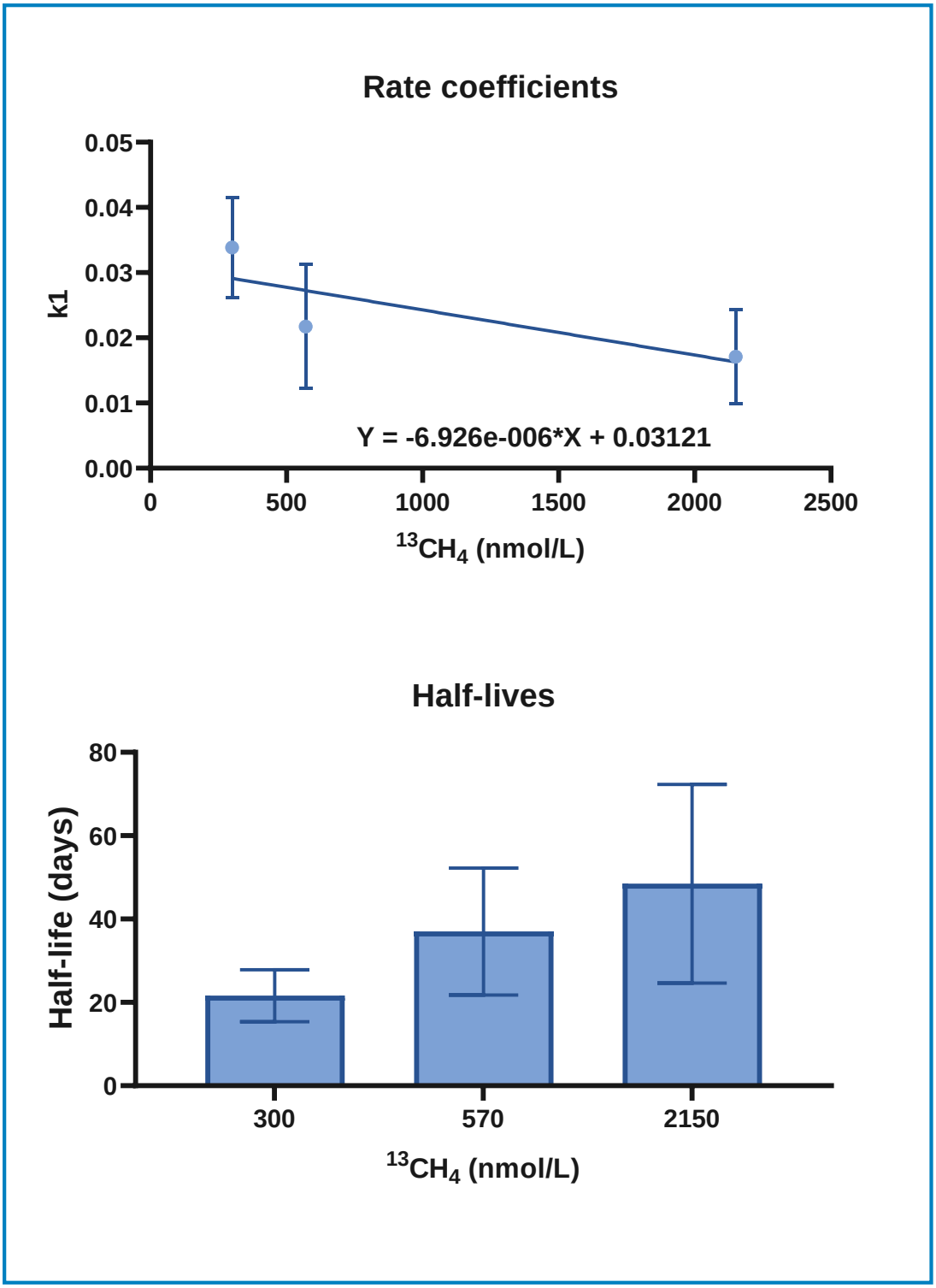

Figure 19: Rate coefficients and half-lives of $^{13}CH_4$ oxidation based on measured concentrations of stable isotope in the different volumes applied. The results are shown as mean ± standard deviations of replicate results presented in Table 4. Linear regression analyses of rate coefficients are also shown.

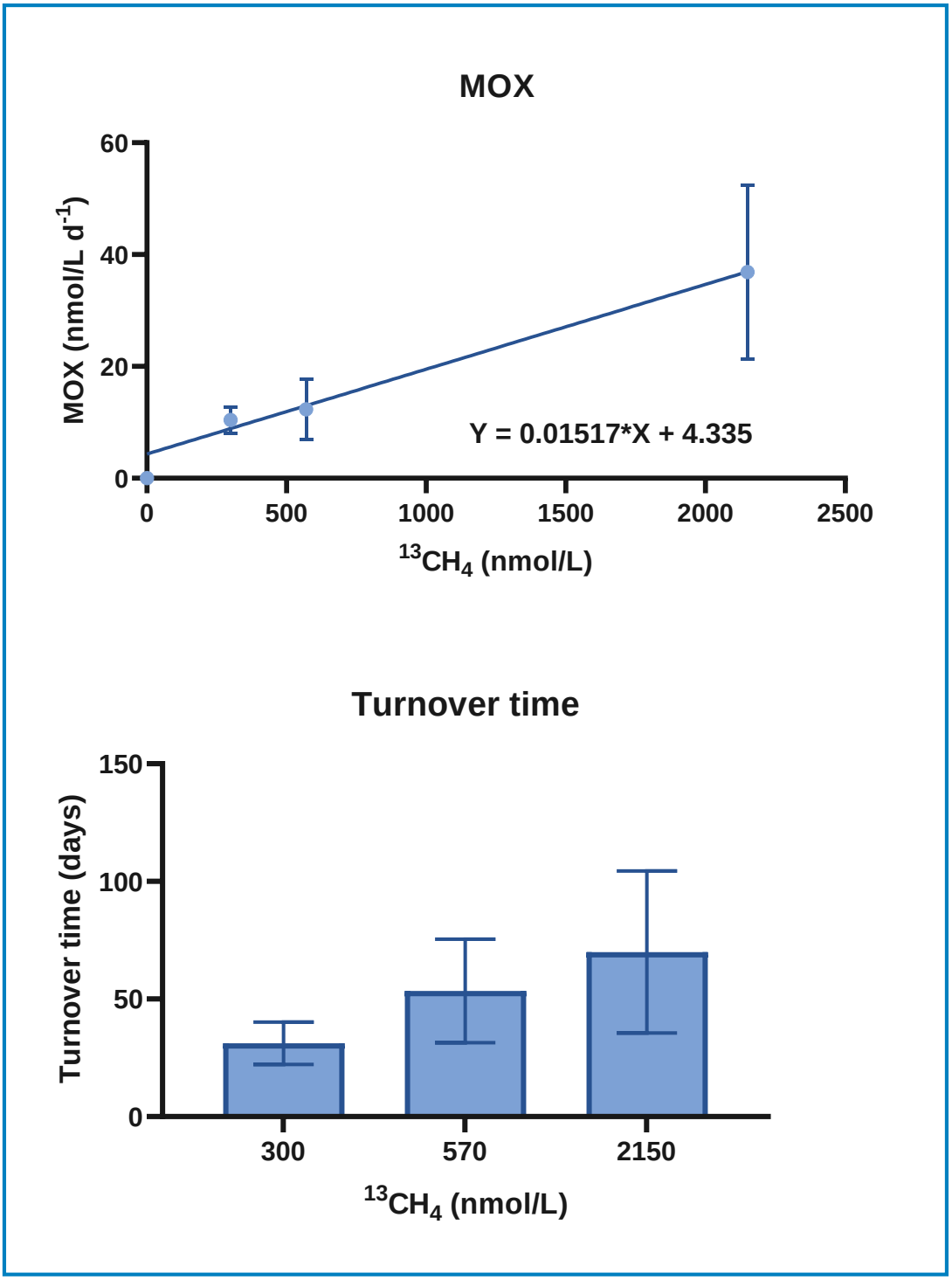

Figure 20: Methane oxidation rates shown as nmol/L oxidized per day (MOX) and turnover times determined from the MOX calculations of $^{13}CH_4$ oxidation, based measured concentrations in the different volumes of applied stable isotope. The results are shown as mean ± standard deviations of replicate results presented in Table 4. Linear regression analyses of MOX are also shown.

Since the standard deviations of the oxidation results decreased by increased volumes of spiked stable isotopes, we were more confident with the lower than the higher volumes applied. As mentioned above, all volumes applied resulted in much higher methane concentrations (300 to >2000 nmol/L) than will be relevant for SW close to leaking oil wells. We therefore extrapolated the rate coefficients and MOX down to more relevant concentrations of methane in the range of 1 to 100 nmol/L, by using the regression equations shown in **Figure 19** and **Figure 20.** The extrapolated results are shown in **Figure 21**. The estimated k1-values within this concentration range resulted half-lives from 22.2 to 22.7 days. Based on extrapolated MOX-data, turnover was estimated to be within 0.2 to 17 days within a concentration range of 1nmol/L to 100 nmol/L (**Figure 21**).

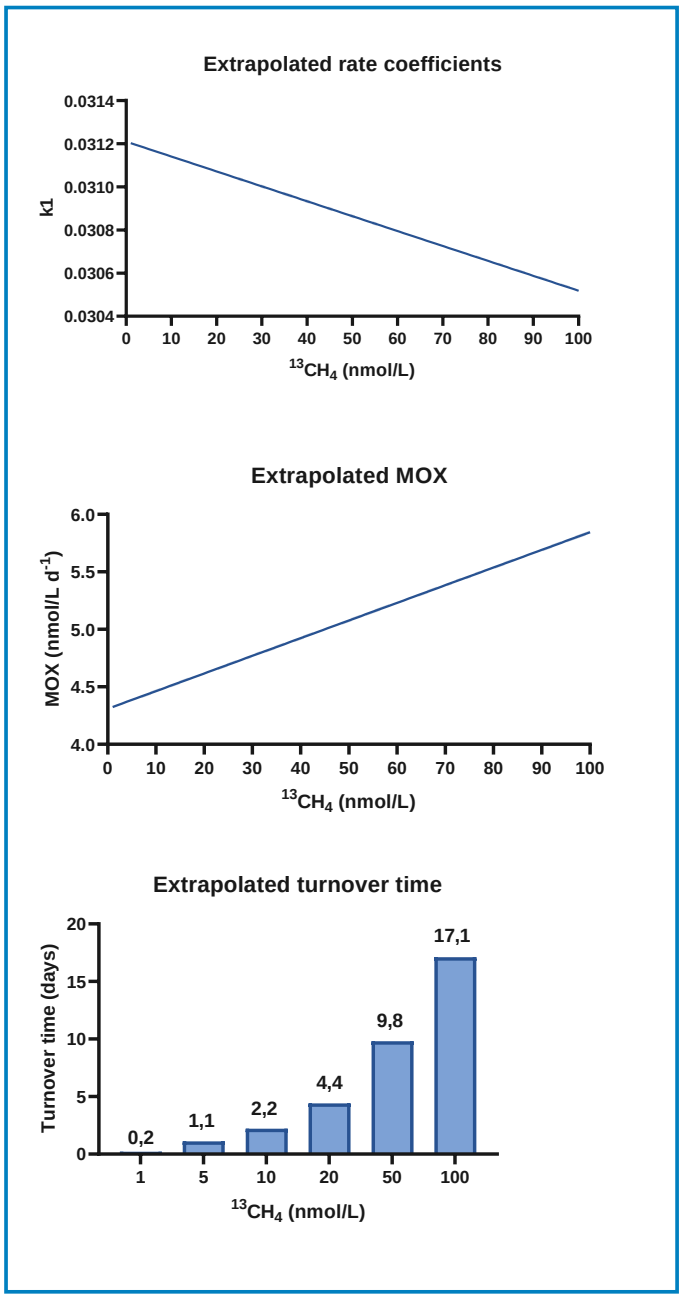

Figure 21: Extrapolations of k1 and MOX to methane concentrations in the range of 1 to 100 nmol/L, based on linear regression analyses performed in Figure 19 and Figure 20. Turnover times of selected methane concentrations are shown, with no. of days specified.

6.3 Studies with SW spiked by tritium-labelled methane (^3H-CH_4)

The studies with ^3H-CH_4 were designed to determine CH_4 oxidation in relation to incubation times, methane concentrations and incubation temperature. One objective of the studies was also to decide what oxidation method would provide the most suited data to be included in a fate model for methane released to the marine water column.

As with the stable isotope method, the original intentions were to determine ^3H-CH_4 oxidation rates in relation to incubation time, SW temperature, methane concentrations and test robustness. Compared to the stable isotope method, which required ^{13}CH4 concentrations of 300 nmol/L for determination of CH_4 oxidation, the tritium method required significantly lower ^3H-CH_4 concentrations. Since each batch contained 1 mCi 50 3H-CH4, which contained 15Ci/mmol, the nominal ^3H-CH_4 concentration was 67 nmol. A stock solution of 5 mL isotope should therefore contain a concentration of 13 nmol/mL ^3H-CH^4, and 50 µL stock solution in 100 mL test and control samples should then contain nominal concentrations of 6.5 nmol/L ^3H-CH_4.

6.3.1 Method establishment

Method establishment was needed also with the ^3H-CH_4 method, but not to the same extent as with the stable isotope method. However, considerable caution had be taken with respect to HSE requirements for working with radioactive materials. The different tests for final establishment of this method are described in **Appendix B**. These included a) preparation of stock solutions with ^3H-CH_4 stored in the solvent hexane, b) storage vials and temperature, c) the effect of ^3H-CH_4 stored in a poorly soluble solvent on measured radioactivity in SW, d) selection of stock solution volumes to be used in test and control samples, e) establishment of systems for sparging of sampled to remove residual ^3H-CH_4 and avoid releases of radioactivity to the environment outside the test vials, and f) selection of incubation times with samples and controls spiked with ^3H-CH_4. The steps for the method establishment tested in **Appendix B**, which are summarized in **section 5.5.1** and in **Table 2**, resulted in a test method described in **section 5.5.2** and illustrated in **Figure 13**.

6.3.2 Incubation times

As shown in **Appendix B**, rapid oxidation of ^3H-CH_4 occurred, and when an experiment was performed at a SW temperature of 5 °C, and samples were collected after 4, 13, 17 and 27 days of incubation, most of the measured 3H-CH4 oxidation had occurred after 4 days of incubation (see **Appendix B**, **Figure B.7**). Based on the radioactivities measured in test and control samples at the different sampling times, oxidation data were calculated and are described in **Table 5** and in **Figure 22**. These data were based on 4 replicate test samples and 2 control samples at each sampling time. The control samples were used to correct for residual ^3H-CH_4 in the test samples, for determination of ^3H-H_2O as the oxidation product (Eq21).

Based on the rate coefficients determined from 4 replicate samples after 4 days of incubation, and the complete methane concentration in the samples (50 nmol/L) the MOX rates were determined to be 6.2 ± 0,9 nmol/L d^{-1}, while the turnover rate was 8.2 ± 1.0 days.

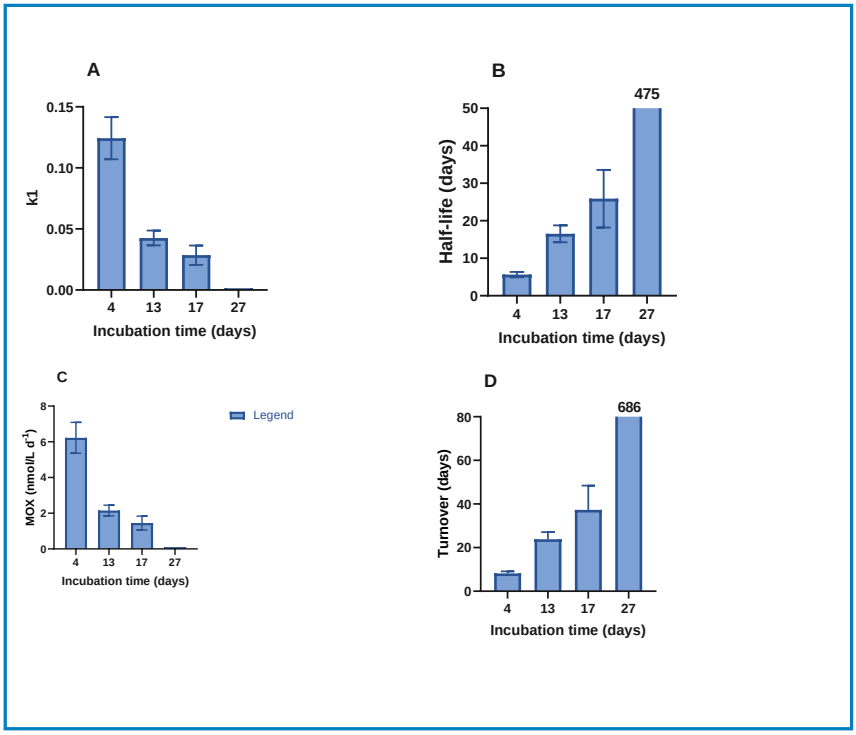

Figure 22: Rate coefficients (A), half-lives (B), MOX (C) and turnover (D) of test replicates (T1-T4) determined in experiment with different incubation times.

Table 5: Averages ± SDs of results for test (T) and control (C) replicates sampled during the 27-day incubation period.

Parameter	Incubation days T				Incubation days C	
	4	13	17	27	4	13
Raw data (dpm)	227403 ± 42914	264284 ± 57286	231057 ± 74449	311300	56052	124816
^{3}H-H_2O activity (dpm)	136969 ± 42914	173850 ± 57286	140623 ± 74449	220866	--	--
K1	0.1243 ± 0.0173	0.0426 ± 0.0060	0.0285 ± 0.0079	0.0015		
Half-life (days)	5.6 ± 0.7	16.6 ± 2.3	25.9 ± 7.7	475		
MOX (nmol/L d^{-1})[A)]	6.2 ± 0.9	2.1 ± 0.3	1.4 ± 0.4	0.1		
Turnover (days)[A)]	8.2 ± 1.0	23.8 ± 3.3	37.3 ± 11.1	686		

[A)] Based on a concentration of 50 nmol/L methane

6.3.3 Different methane concentrations

An experiment was performed in which normal and sterilized SW was preincubated with different concentrations of normal methane before samples were spiked with ^{3}H-CH_4. Since the available amounts of ^{3}H-CH_4 were limited, we decided to do this experiment with different concentrations of HiQ CH4, and not with different ^{3}H-CH_4 concentrations, which were spiked at 50 µL volumes to all test and control samples. The samples were preincubated with the different methane concentrations for 5 days at 5 °C. The nominal concentrations of methane in the pre-incubated samples were 0, 50, 100 and 200 ng/L methane. GC-FID analyses shown in **Figure 23** and were mainly within 20% agreement with nominal concentrations, except for the highest concentration, which was measured to be deviate 31% from the nominal concentration.

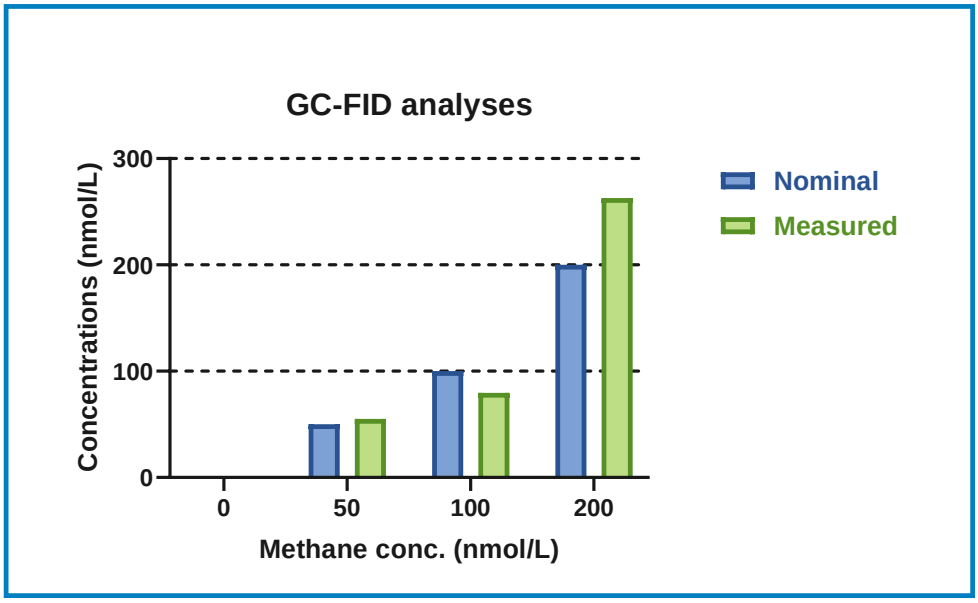

Figure 23: GC-FID analyses of methane concentrations in pre-incubated samples with nominal concentrations 0, 50, 100 and 50 nmol/L methane.

After preincubation, the samples were spiked with $^{3}H\text{-}CH_4$ and incubated at 5 °C for 4 days before sampling. The measured raw radioactivities of the replicates (samples and sterilized controls) are shown in **Figure 24A**. The replicate radioactivities varied considerably, as shown by the large standard deviations. The sterilized control at 50 nmol/L methane concentration showed very high activity and was even higher than the activities in the test samples (**Figure 24A**). This was the only sterilized control in all our experiments which showed higher activity than the corresponding test. We therefore excluded this control and used the data for sterilized control of 200 nmol/L to determine the radioactivity associated with $^{3}H\text{-}H_2O$ activities (**Figure 24B**).

The results of **Figure 24** further showed that the radioactivity was not affected by the preincubation with the different methane concentrations, since the counts did not differ significantly between the three preincubation concentrations (P=0.8905; one-way ANOVA).

Rate coefficients, half-lives, MOX and turnover estimations determined for replicate samples are shown in **Figure 22** and in **Table 6**. The data showed lower rates and higher half-lives/turnover than in the previous experiments. However, these data were hampered by large replicate variations, resulting in high standard deviations (**Table 6**), which varied between 36% and >100% of average values for the calculations (**Table 6**. The reliabilities of these data may therefore be questioned.

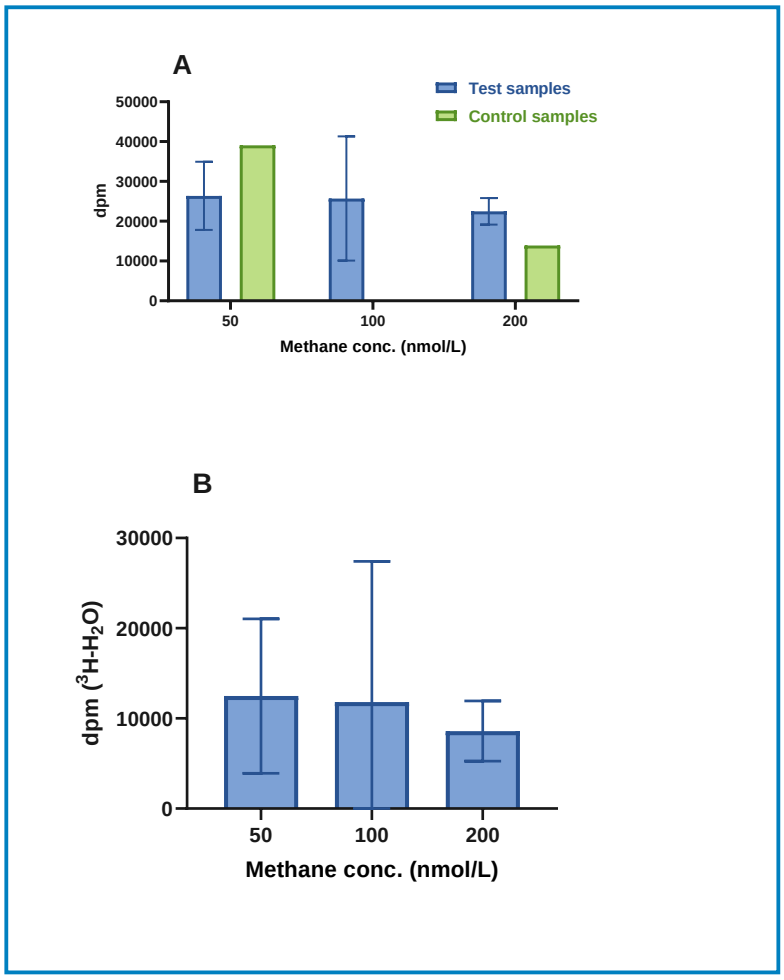

Figure 24: Radioactivity in replicate samples of test (n=3) sterilized control (n=1) samples (A) pre-adapted with different HiQ methane concentrations (50-200 nmol/L) and spiked with 50 µL ^{3}H-CH_4 (A). Radioactivity associated with ^{3}H-H_2O formation after subtracting activity in one selected sterilized controls (B). The results are showed as average ± SD.

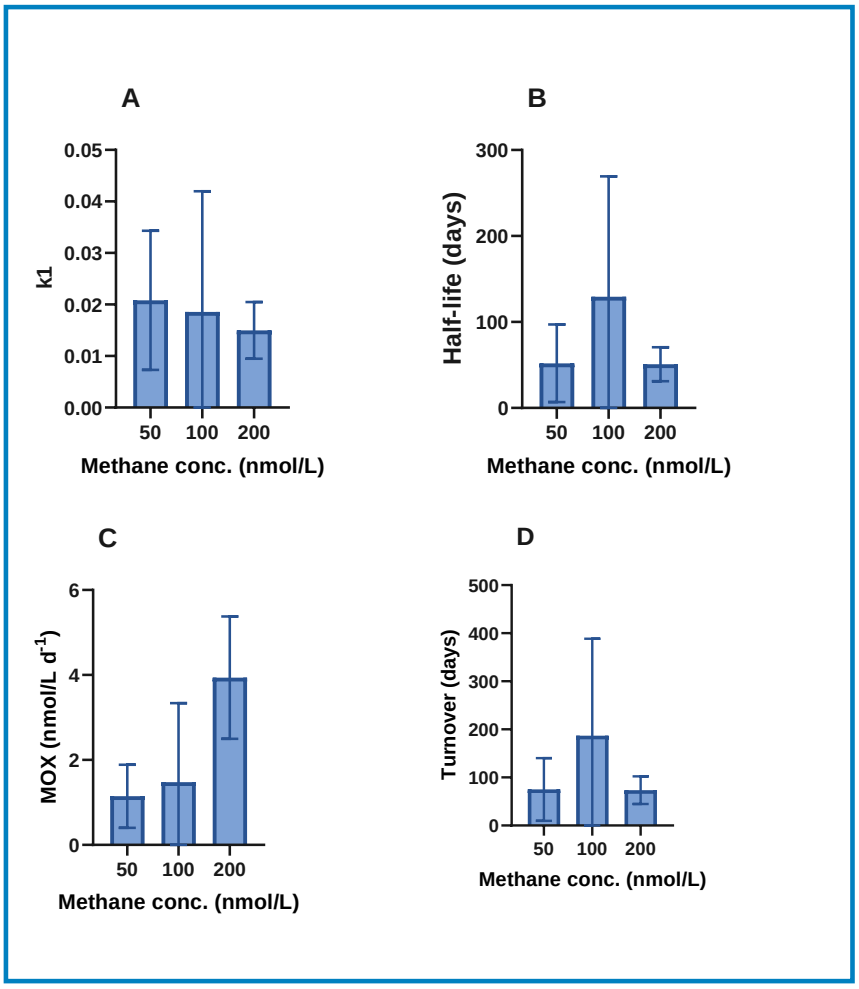

Figure 25: Rate coefficients (A), half-lives (B), MOX (C) and turnover times (D) of ^{3}H-CH_4 oxidation determined in test samples (n=3) replicates (T1-T3) in an experiment with different concentrations of pre-incubated methane. MOX and turnover times were based on the methane concentrations measured by GC-FID analyses (Figure 23). The results are showed as average ± SD.

Table 6: Averages ± SDs of results for test and control replicates shown in Figure 24 and Figure 25.

Parameter	Measured methane concentrations (nmol/L)					
	Tests			Controls		
	55.1	79.6	263	55.1	79.6	263
Raw data (dpm)	26365 ± 8565	25701 ± 15603	22484 ± 3333	39067	ND	13886
^{3}H-H_2O activity (dpm)	12479 ± 8565	11814 ± 15603	8598 ± 3333	--	--	--
K1	0.0208 ± 0.0135	0.0186 ± 0.0234	0.0150 ± 0.0055			
Half-life (days)	52.0 ± 45.2	129 ± 134	51.0 ± 19.8			
MOX (nmol/L d^{-1})[A)]	1.14 ± 0.74	1.48 ± 1.86	3.94 ± 1.44			
Turnover (days)[A)]	75.0 ± 65.3	187 ± 202	± 28.6			

[A)] Based on a concentration of measured methane concentrations

Despite the large replicate variations, regression analyses of rate coefficients and MOX were performed in the same way as previously described for stable isotope analyses (see **Figure 19** and **Figure 20** in **section 6.2.2**). K1 and MOX were plotted against their measured methane concentrations, and the results with regression equations are shown in **Figure 26**. From these data, the k1 and MOX were extrapolated within the range of 1 to 100 nmol/L methane, and turnover calculated for selected methane concentrations (**Figure 27**). Comparison of data in **Figure 21** and **Figure 27** showed that the extrapolated turnover was faster by factors of 3 to 12 from the data with stable isotope analyses than with tritium. However, the tritium data were highly questionable due to the large replicate variations.

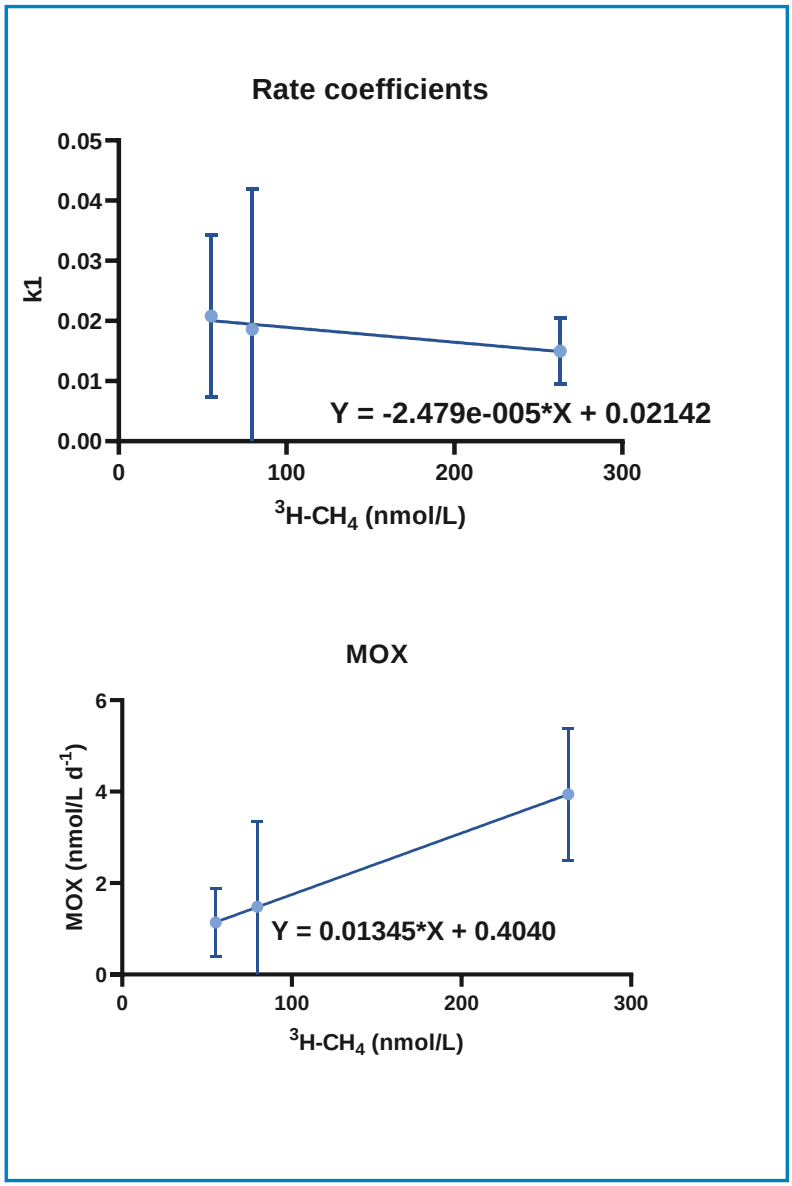

Figure 26: Rate coefficients and MOX of ^{3}H-CH$_4$ oxidation based on the measured concentrations of methane in the samples. The results are shown as mean ± standard deviations of replicate results presented in Table 6. Linear regression analyses of rate coefficients and MOX are shown.

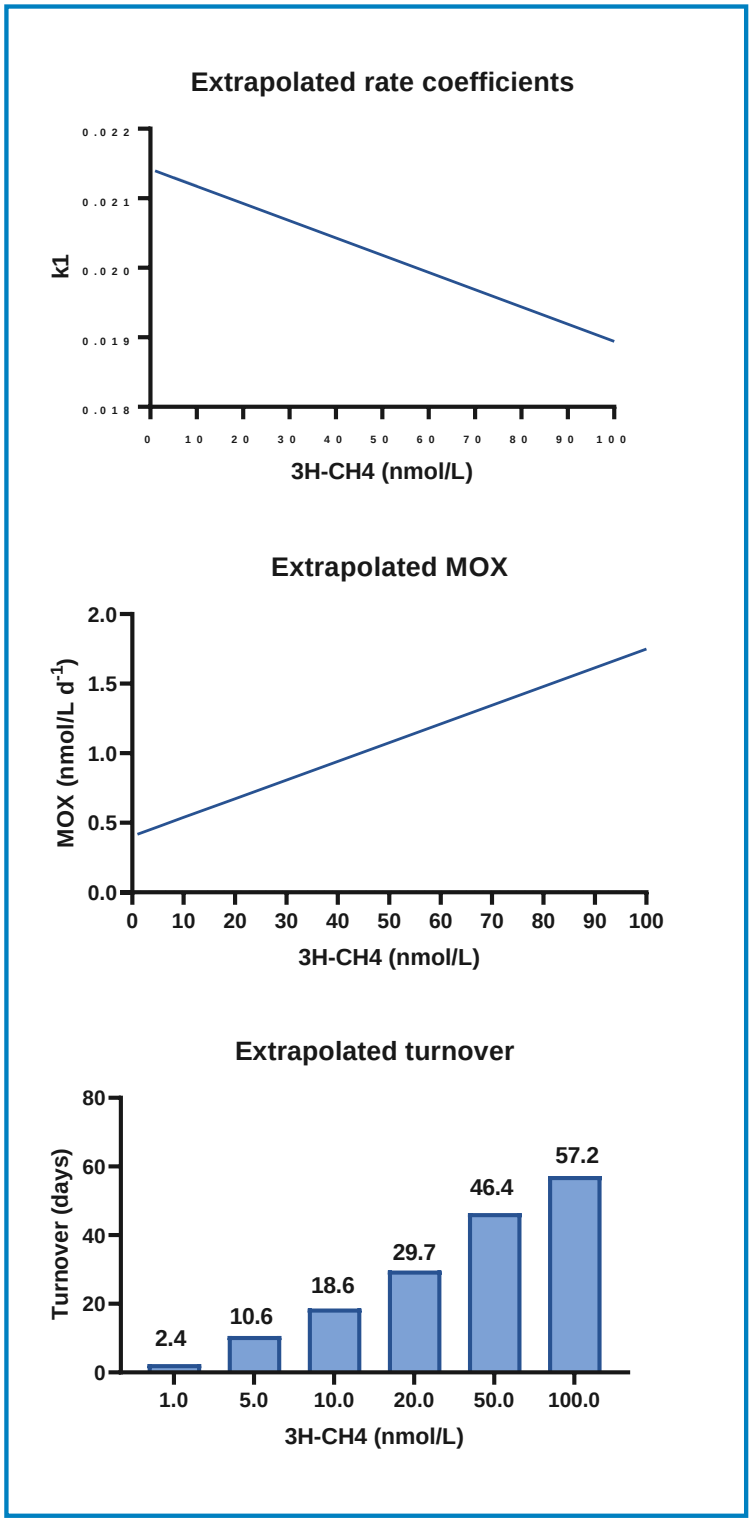

Figure 27: Extrapolations of K1 and MOX to methane concentrations in the range of 1 to 100 nmol/L based on linear regression analyses performed in Figure 26. Turnover rates of selected methane concentrations are shown, with no. days specified.

6.3.4 Temperatures

An experiment was performed with a higher temperature than 5 °C, which may be relevant for methane reaching SW above a thermocline in a summer season. The intention was to perform an experiment with an incubation temperature of 13 °C. The SW (normal and sterilized) was pre-acclimated to 13 °C in in 2 days and pre-incubated with 50 nmol/L normal methane for 4 days at 13 °C. The pre-adapted SW was then spiked with 50 µL ^3H-CH_4 and incubated in a refrigerator at the isotope lab that was set on minimum temperature. However, we did not achieve 13 °C, but a temperature of 8.5 °C. The samples with spiked isotope were incubated at this temperature for a shorter time than the incubations at lower temperature, since we suspected a faster oxidation at the higher temperature. An incubation of only 2 days was therefore used before sampling and analyses. The radioactivity in test and sterilized controls are shown **Figure 28**, and oxidation rated in **Table 7.**

Comparison of the results from **Table 5** (4 days incubation at 5 °C) and **Table 7** showed result similarity for of rate coefficients, half-lives, MOX and turnover (P=0.9898; paired *t*-test).

Temperature variations of biodegradation rates have also been estimated by QSAR methods, and in a study of methane oxidation rates in the North Pacific Ocean water column, a Q10 values varied between 1.0 (no correction) to 2.4 (Pack et al., 2015). In the OSCAR model, temperature calibration is determined with a Q_{10} of 2.0. If a value of Q10 = 2 is used on the k1 value in **Table 7**, temperature-corrected k1, half-lives, MOX and turnover will be as shown in **Table 7**.

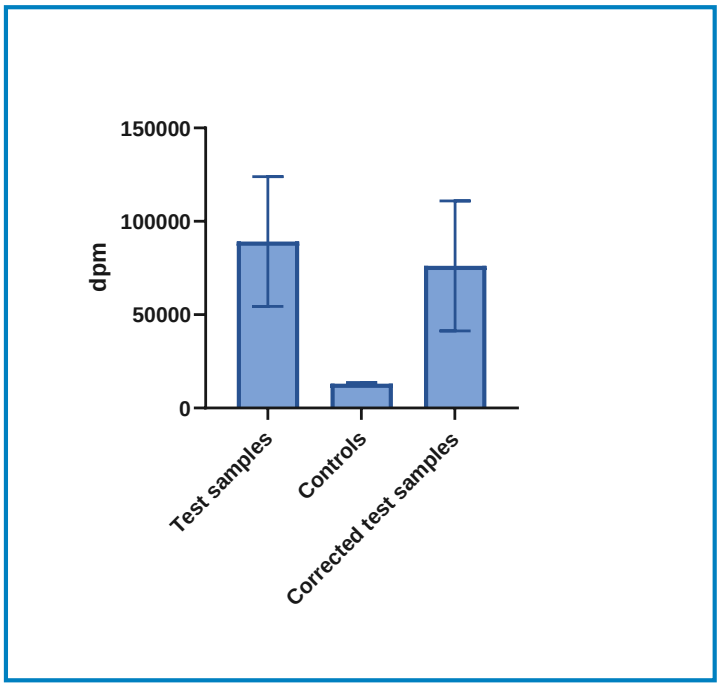

Figure 28: Radioactivity (dpm) in test samples (n=4) and sterilized controls (n=3), and in test samples corrected for the residual ^3H-CH_4 after incubation in SW pre-adapted with 50 nmol/L at 13 °C and spiked with 50 µL ^3H-CH_4. The results are shown as average ± SD of the replicates.

Table 7: Results from experiment with higher temperature, including dpm-results and rate data. The results are based on data from 4 replicates. Q10-calbrated values to 13 °C (from the temperature of 8.5 °C) of k1, half-life, MOX and turnover are shown in brackets.

Parameter	Results/calculations (mean ± SD)	
	Normal SW	Sterilized SW
Raw data (dpm)	89199 ± 34767	13061 ± 666
^{3}H-H_2O activity (dpm)	76138 ± 34767	--
K1	0.1735 ± 0.0619 (0.2370 ± 0.0845[B)])	
Half-life (days)	4.6 ± 2.5 (3.4 ± 1.8[B)])	
MOX (nmol/L d^{-1})[A)]	8.7 ± 3.1 (11.8 ±4.2[B)])	
Turnover (days)[A)]	6.7± 3.4 (4.9 ± 2.6[B)])	

[A)] Based on a concentration of 50 nmol/L methane; [B)] Q10-corrected values from 8.5 °C to 13.0 °C).

6.4 Methane-oxidizing microbes

6.4.1 Testing and optimalisation of methodology.

Initial experiments were performed to establish methodology for quantification of methane oxidising microorganisms in seawater.

As described in **section 5.6.1**, flasks with 500 ml seawater were added varying concentrations of methane, 6 mL, 12.5 mL, or 25 mL injected over a period of 120 seconds. These treatments resulted in average methane concentrations of 17 nmol/L, 37 nmol/L and 53 nmol/L, respectively, when measured by GC-FID analyses.

The 16S rRNA gene are used for identification of bacteria (and archaea) as the gene has conserved variable and hypervariable regions. Although an exact number of genes per cell cannot be determined for all bacterial communities, conversion factors between 2,4 and 4,2 have been suggested for quantification of cells based on the number of copies of the 16S rRNA gene (De Paula et al., 2021; Louca et al., 2018; Větrovský and Baldrian, 2013). Microbiome profiling can also include quantitative analyses of key functional genes. Methanotrophic bacteria produce the enzyme methane monooxygenase (MMO), that exists in two variants: soluble MMO (sMMO) and as particulate MMO (pMMO) (Hanson and Hanson, 1996). Quantification of the pmoA-gene encoding particulate monooxygenase (pMMO) can therefore be a target gene for quantification of the relative amount of methane oxidizing bacteria in the total bacterial composition. It should be noted that the selection of primers for amplification of these genes will strongly affect the outcome of the analyses. dPCR and qPCR was hence used for amplification of the pmoA-gene encoding particulate monooxygenase (pMMO).

In initial experiments using dPCR for quantification, the rain-effect was observed to a strong degree **(Figure 29**). Consequently, it was not possible to distinguish between positive- and background amplification. No further experiments using dPCR were performed.

For quantification of the target genes using qPCR, establishment of a standard curve is necessary. In the initial qPCR experiments, no standard curve or positive control was used (not available at the current time), but amplification from the seawater samples were achieved. No amplification from the negative control (HMW DNA-standard) nor the non-template control (PCR-grade water) was observed.

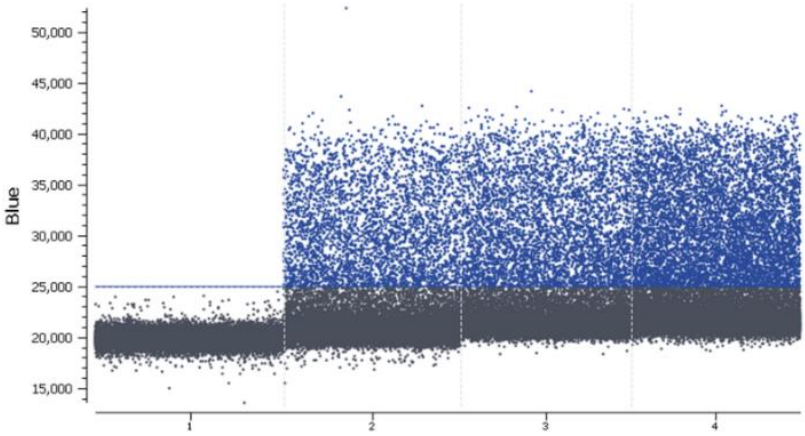

Figure 29: Results from digital PCR. Samples are (from left): non-template control, parallels 1 to 3.

6.4.2 Quantification of pmoA- and 16S rRNA-genes, laboratory samples

Standard curves for quantification of pmoA- and 16S rRNA-genes were later established using genomic DNA from *Methylococcus capsulatus* NCIMB 11132 and ZymoBIOMICS HMW DNA Standard from Zymo Research (D6322) respectively.

Water samples for analyses were filtered and DNA extracted from the filters. Low concentrations of DNA were obtained from these samples. Quantification of 16S rRNA-gene copies were performed using qPCR and the number of cells calculated based on a conversion factor of 2.4. The estimated number of cells pr ng DNA extracted is shown in **Figure 30.**

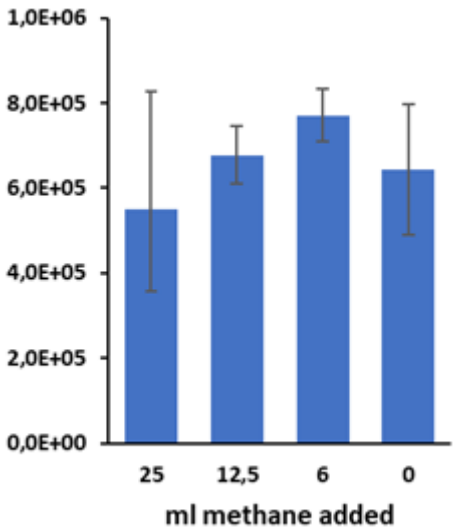

Figure 30: Number of cells pr ng DNA extracted

No or low specific amplification of the pmoA-gene from the experimental samples were achieved. This could be caused by both by the low DNA concentrations, but suboptimal primers or conditions for detection could also be affecting the amplification efficiency. It should be noted that the relative amount of methane oxidizing bacteria in seawater used in the initial analyses (roughly estimated to lower than 0,005%) were at the detection limit of the analyses, indicating that the low or no specific amplification of the test samples were mainly due to the low DNA concentrations.

16S rRNA gene amplicon sequencing for studies of the microbial community compositions could indicate the presence of methane oxidizing bacteria in the samples.

7. Modelling

Methane is released from sea-floor seeps in many locations around the world, including at the Norwegian Continental Shelf. Methane is also a powerful greenhouse gas, with 28–34 times the Global Warming Potential of CO_2, on a 100-year timeframe. Hence, it is of some interest to be able to predict the fate of the methane released in sea-floor seeps. To model the fate of methane released from seeps at the sea floor, a range of parameters and processes must be considered, including:

- Release rate
- Release depth
- Initial bubble size
- Bubble rise
- Dissolution of methane from bubbles to the water column
- Mass transfer of other dissolved gases from the water column to the bubbles
- Vertical turbulent mixing of dissolved methane
- Biodegradation of dissolved methane
- Mass transfer of dissolved methane from the sea surface to the atmosphere

Some of these processes are well understood (e.g. bubble rise and dissolution of methane), and some parameters are straightforward to measure (e.g. release rate and release depth). However, vertical turbulent mixing and biodegradation rates of dissolved methane are both relatively uncertain and have a large impact on the predicted fate of the released methane. The biodegradation rate of dissolved methane in particular has been quite uncertain, with half-lives reported in the literature ranging from days to years. Recent experiments aiming to reduce this uncertainty are described elsewhere in this report.

7.1 Modelling of bubble rise, dissolution and fate of dissolved methane

When a bubble of methane is released from the sea floor, several processes must be understood to predict the fate of the methane. First, the size of the bubble depends on the amount of methane, and the pressure, and the size impacts the rise velocity. Second, methane will dissolve from the bubble into the surrounding water, at a rate which depends on pressure, temperature, bubble size, and the presence of surfactants in the water. At the same time, other gases that are dissolved in the water column will enter the bubble, via mass transfer. This mainly applies to nitrogen and oxygen, which are the most abundant dissolved gases in the ocean. As a consequence of this two-way exchange of gases, a bubble which initially contains pure methane may at a later time contain nitrogen and oxygen, and little or no methane (Olsen et al., 2019).

As the methane from the bubble dissolves into the water column, the rate of dissolution will be highest near the bottom when the bubble is nearly pure methane. Hence, most of the methane is dissolved into the water column close to the sea floor. In our model runs, using conditions representative for the Norwegian Continental Shelf, we found that essentially all the methane will dissolve within the first 50-100 meters from the sea floor. If the methane is released in depths of less than this, then some fraction of the methane will

be transported directly to the atmosphere with the bubbles, while the remainder is dissolved. The dissolved methane is then re-distributed throughout the water column by vertical turbulent mixing (eddy diffusivity). The vertical mixing changes in intensity depending on local conditions, but in general the mixing is faster during winter than during summer.

Once methane has been dissolved into the water column, we consider two fate processes: Biodegradation into water and CO_2 or escape to the atmosphere via mass transfer. Note that we ignore hydrate formation, which is only relevant for greater depths than what is found on the Norwegian Continental Shelf. Biodegradation is described in more detail in the next section. Mass transfer to the atmosphere requires the dissolved methane first to be mixed by diffusion to reach the surface, from where the methane can escape across the surface into the atmosphere. The rate of escape can be parameterized as a function of near-surface methane concentration, and the wind speed.

An illustration of the relevant processes is shown in **Figure 31**, and additional details on our modelling approach are found in the report from the earlier desktop study on methane fate (Nordam et al., 2020).

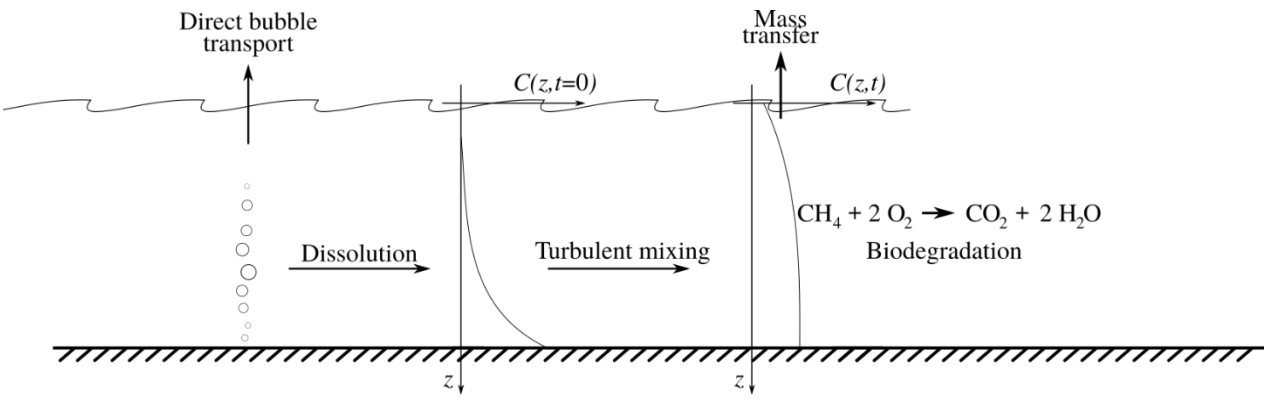

Figure 31: An illustration of the processed affecting methane from sea-floor seeps, which have been accounted for in our model. Methane bubbles are released from the sea floor, and some of the methane dissolves, while some may reach the atmosphere directly. The dissolved methane is then redistributed throughout the water column by turbulent mixing. The dissolved methane may biodegrade or escape to the atmosphere via mass transfer.

7.2 Modelling approaches for biodegradation

Different approaches exist for modelling the biodegradation of dissolved methane in the water column. The simplest approach is to assume that the oxidation of methane is a first-order decay process, where the instantaneous rate of degradation is equal to the concentration times a rate constant, k_1:

$$\frac{\mathrm{d}\,[\mathrm{CH_4}]}{\mathrm{d}t} = -k_1 \cdot [\mathrm{CH_4}] \quad \text{(Eq23)}$$

In this case, the concentration will decay exponentially, with a half-life equal to $t_{1/2} = \frac{1}{k}\ln 2$.

More advanced approaches include the abundance of degrading bacteria as a variable, in addition to the concentration of methane. A well-known example is the Monod equation for the specific growth rate μ of bacteria (growth rate per unit of biomass),

$$\mu = \mu_{max}\frac{S}{K_S+S} \quad \text{(Eq24)}$$

where μ_{max} is the maximal specific growth rate, S is the concentration of the limiting nutrient, and K_S Is the concentration of nutrient at which the specific growth rate is half of the maximum, see, e.g. (Liu, 2007).

We consider methane degradation and combine the Monod equation with an ODE for methane concentration. Here we assume that methane is the limiting nutrient for methane degrading bacteria, and the rate of methane degradation is assumed to be proportional to the product of the concentration of methane, $[\mathrm{CH_4}]$ and the concentration of bacteria, $[\mathrm{B}]$. Then we get a coupled system of two ODEs

$$\frac{\mathrm{d}[B]}{\mathrm{d}t} = \mu_{max}[\mathrm{B}]\frac{[\mathrm{CH_4}]}{K_S+[\mathrm{CH_4}]} \text{ (Eq25a)}$$

$$\frac{\mathrm{d}[\mathrm{CH_4}]}{\mathrm{d}t} = -k[\mathrm{CH_4}][\mathrm{B}] \text{ (Eq25b)}$$

which describe the time development of both methane and bacterial concentration. Note that this set of equations can give rise to apparently different progressions of methane decay, depending on the parameters and the initial values. This is illustrated in **Figure 32**. In the left column, the initial concentration of methane is low, relative to the concentration of bacteria. In this case, the concentration of bacteria remains approximately constant, and the methane decay is essentially a first-order reaction giving rise to the standard exponential decay. In the right column, the initial concentration of methane is high, relative to the concentration of bacteria. In this case, the concentration of methane remains approximately constant for a while ("lag phase"), until the bacteria have grown to a point where they can oxidize the methane more rapidly. Eventually, the methane is depleted, and the bacterial abundance remains constant (note that death of bacteria is not included as a mechanism in the Monod equation).

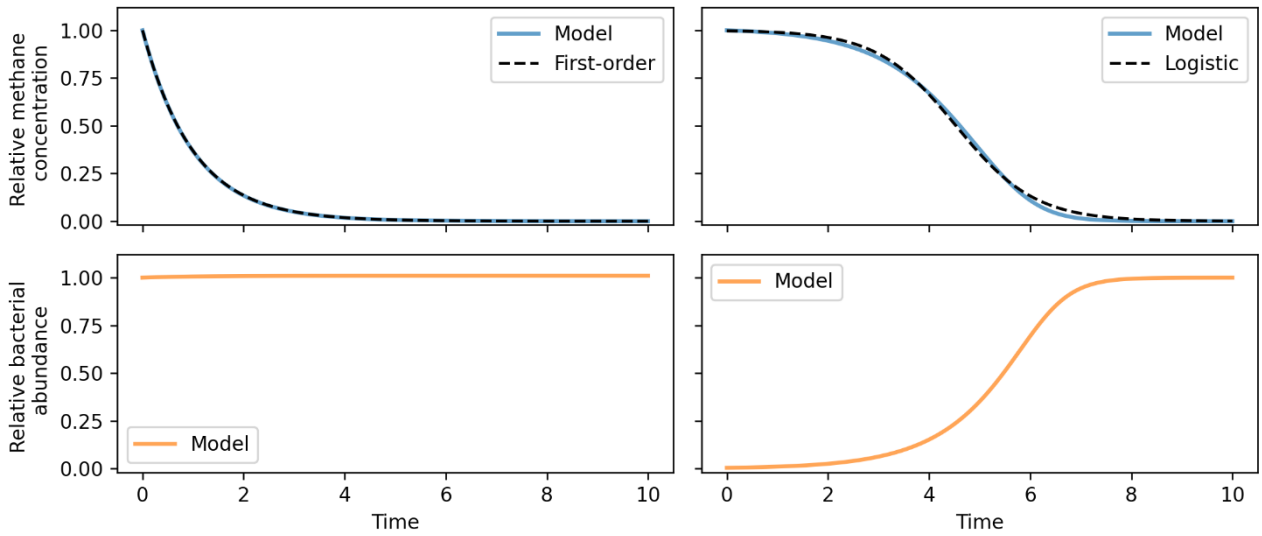

Figure 32: Time development of methane concentration and bacterial abundance as modelled by the system of coupled equations above, for two different initial conditions. With initially high bacterial abundance relative to methane, the model displays approximately first-order kinetics (left column). With initially low bacterial abundance relative to methane, the methane decay follows approximately a logistic curve.

The lag phase displayed in the right-hand column of **Figure 32**, where the nutrient concentration remains approximately constant for a while before degradation begins, is also found experimentally in some cases. Note, however, that no distinct lag phase was observed in the experiments described elsewhere in this report. This could mean that the lag phase was so short that it was not seen at the chosen sampling times, or it could mean that the bacterial abundance was high enough that there was no lag phase.

Since the two-variable model is more general, it may be assumed that this type of model is a more faithful representation of reality than the simple one-variable first-order decay. On the other hand, the two-variable model presented above requires three parameters, as well as initial concentrations for both methane and methane-degrading bacteria. Contrast this to the first-order model, which requires only one parameter, and only the initial concentration of methane. This means that the two-variable model requires more experimental data to fit the parameters (including measurements of bacterial abundance at different times, for different initial concentrations of methane), and it also requires information about the background concentration of methane-degrading bacteria in seawater at the relevant locations. Hence, the two-variable model is more demanding, and in practice the increased realism of the model may be negated if the required parameters are not accurately determined.

7.3 Model results

From the current experiments, there is not enough data available to fit the parameters of the two-variable model. In **Figure 33**, we show results for the one-variable (first order) decay model. The results shown are mass balances for methane seeps at the sea floor, at three different depths. The model takes into account bubble rise and dissolution, methane being carried by bubbles to the surface, vertical mixing and biodegradation of dissolved methane, and finally mass transfer of dissolved methane from the sea surface to the atmosphere.

The bubble rise and gas exchange were modelled with TAMOC (Socolofsky et al., 2015), while the fate of the dissolved methane was modelled by solving the advection-diffusion-reaction equation, with a reaction term for the biodegradation, and a prescribed-flux boundary condition for the mass transfer. The results have been averaged over 1 year, assuming a well-mixed water column in the winter, and a stronger stratification in summer. The vertical mixing (eddy diffusivity) was described by idealized profiles, with seasonal differences based on historical CTD profiles for different positions in the North Sea. For additional details of the model and the assumptions that were made, see the report from the previous desktop study (Nordam et al. 2020).

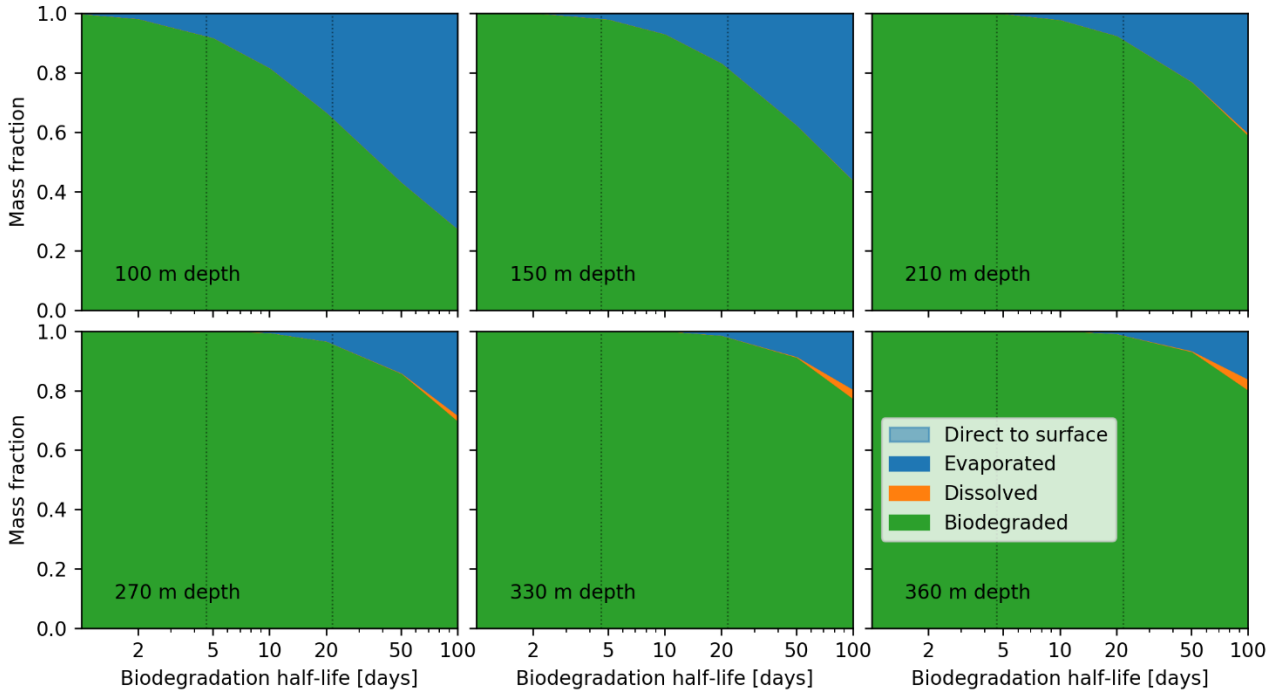

Figure 33: Mass balance for methane from seafloor seeps, for six different depths, shown as a function of biodegradation half-life. The vertical dotted lines indicate half-lives of 4.6 and 21.6 days. The mass balance

is calculated from bubble rise and dissolution, vertical mixing and biodegradation of dissolved methane, and mass transfer of dissolved methane across the sea surface into the atmosphere, averaged over 1 year. See the text and Nordam et al. (2020) for additional details.

In the experiments described in Sections 4, 5, and 6 of the current report, biodegradation half-lives of methane were found to range from 21.6 days to 4.6 days (see Table 12). As can be seen from **Figure 33**, with these half-lives essentially all the released methane can be expected to dissolve and biodegrade in the water column for the deeper releases. For the release at 270 m depth, and assuming a half-life of 20 days, more than 96% of the methane will biodegrade. At a shallower release of 100 m depth, up to about 34% of the released methane may reach the atmosphere for a half-life of 20 days. Additional numbers are presented in the table below (**Table 8**).

Table 8: Biodegradation and atmospheric emissions of methane from different release depths, based on selected microbial methane oxidation half-lives determine from laboratory experiments performed in this project.

	4.6 days half-life		21.6 days half-life	
Depth	Biodegraded [%]	Atmosphere [%]	Biodegraded [%]	Atmosphere [%]
50	60.5	39.5	26.3	73.7
100	92.2	7.8	64.2	35.8
150	97.9	2.1	81.3	18.7
210	99.5	0.5	91.1	8.9
270	99.8	0.2	95.6	4.4
330	99.9	0.1	97.8	2.2
360	99.9	0.1	98.5	1.5

7.4 Future work

There are several good reasons to want to use a two-variable model describing the coupled time-development of methane and methane-degrading bacteria. For example, the model can be assumed to be applicable across a wide range of different concentrations, and it can describe the “lag-phase” where the methane concentration remains approximately constant for some time before degradation picks up speed. However, there are also challenges involved in the use of such a model, mainly related to estimation of the required parameters from experiments.

If one has some idea of the parameters and timescales involved in the degradation process, it is possible to use the model itself to inform choices about experimental setup and sampling times. The idea is to assume a set of parameters for the model, and then generate a set of “data” by evaluating the model for different times. Then, noise is added to the data, to simulate random variations in experiments and measurements, and finally one attempts to fit the same model to the synthetic data. The degree to which one is successful in recovering the assumed parameters can tell us something about the power of the proposed sampling scheme to constrain the model parameters.

For a future, more extensive estimate of the net transport of methane from sea floor seeps to the atmosphere, a two-variable model accounting for both bacterial growth and methane degradation could be a useful tool. However, it would have to be informed by experimental work on degradation rates, where the experiments should span a range of initial methane concentrations, a range of different sampling times, and the samplings should include both methane concentration and abundance of genes associated with methane degradation. In the planning of such a set of experiments, the model should be used to assess the proposed sampling plan.

8. General Discussion

In this project microbial methane oxidation data were determined in natural SW at low methane concentrations. In previous studies, we determined methane oxidation rates at high concentrations, i.e. in µM levels. These concentrations may be relevant for subsurface spill conditions with large emissions of natural gas, like the Deepwater Horizon spill (Kessler et al., 2011), but are not relevant for the Norwegian Continental Shelf. Releases from seeps and abandoned oil wells will be rapidly diluted in the SW column to concentrations well below 100 nmol/L (Mau et al., 2013; Vielstädte et al., 2017; von Deimling et al., 2015, 2011), except in release areas with stratified water, where methane gradients may occur (Ward et al., 1989). In order to follow biodegradation at these low concentrations, most studies have been performed with labelled methane, either in the form of $^{14}C\text{-}CH_4$ or $^{3}H\text{-}CH_4$. Alternatively, stable isotope analyses have been performed with $^{13}CH_4$. As shown in **Figure 3**, the biodegradation half-lives seem to vary between the methods, and the $^{14}C\text{-}CH_4$ methods in particular showed variable results. In this project two methods, based on labelled methane, were selected for methane oxidation studies, the $^{3}H\text{-}CH_4$ (tritium labelled methane) and the $^{13}CH_4$ (stable isotope) method. None of these methods were established at SINTEF Ocean, and efforts were therefore put on method establishments.

8.1 Method developments and challenges

The stable isotope method was performed in collaboration with the National Laboratory of Age Determination at NTNU, where analyses are conducted on routine basis. Methods with stable isotope were performed by pre-adapting natural SW with methane at a concentration close to 50 nmol/L, which was relevant for areas close to natural methane releases (Leonte et al., 2017; Mau et al., 2013; Weinstein et al., 2016). The pre-adapted SW in 100 mL vials was then spiked with 50 µL $^{13}CH_4$, (2.1 µmol), and acidify test volumes of 1 mL after the oxidation experiment (Leonte et al., 2017; Weinstein et al., 2016). However, analyses at NTNU revealed that for $\delta^{13}CO_2$ ratios were not raised significantly above the background (SW without spiked $^{13}CH_4$) at these conditions. The reason was different extraction conditions, including the use of an automated gas bench which pumped 10 mL pure CO_2 into the IRMS instrument (Leonte et al., 2017; Weinstein et al., 2016), while the instrument at NTNU could only analyse 1 ml volumes. Two approaches were first evaluated to increase CO_2 concentrations, extracting the complete CO_2 in each sample (100 mL instead of 1 mL) and purify the gas by freeze-drying to remove the excess of nitrogen in the gas samples (by still spiking sample with 50 µL $^{13}CH_4$). However, it was still difficult to determine the $\delta^{13}CO_2$ ratios at significant levels above the background levels in SW, and higher concentrations of $^{13}CH_4$ were therefore introduced to the samples. At volumes of 300 µL $^{13}CH_4$ (12.6 µmol), the $\delta^{13}CO_2$ ratios in the spiked samples finally raised significantly above the background in the SW blanks. This also inferred that most of the work with the stable isotopes were used for method establishment. However, the method is now well established. In addition to be used as a laboratory method, the stable isotope method is relevant on field cruises with research vessels adequately equipped for gas analyses. Differently from tritium and ^{14}C-labelled methods, the stable isotopes do not represent any particular HSE challenge.

The establishment of the tritium method included both a methodological and HSE challenge. The most obvious challenges were represented by accidental spills and avoiding release of tritium to the atmosphere during sampling sparging with N_2 to remove residual $^{3}H\text{-}CH_4$ from the water phase. The last challenge was eliminated by trapping release tritiated methane in activated carbon filters. However, an accidental spill situation occurred, which was considered serious and reported internally in SINTEF, to the project partners, and to the Norwegian Radiation and Nuclear Safety Authority. Since the $^{3}H\text{-}CH_4$ gas was suppled in break-seal ampoules, and equipment for transferring and storing the sample in gas form, stock solutions of $^{3}H\text{-}CH_4$ dissolved in a solvent (hexane) were prepared instead. Storage vials were also investigated since we experienced problems with destructed septa in screw-capped vials first used, and these were replaced by

crimp-sealed vials, where the septa are better fastened. Since samples needed to be sparged with an inert gas (N_2) for 2 hours, a unit was built for sparging 12 samples simultaneously.

8.2 Incubation periods and first-order rates

Biodegradation experiments are normally performed over extended time periods, often for several months. However, all reported methane oxidation studies with $^{13}CH_4$ and $^{3}H\text{-}CH_4$ spiked into SW have used incubation times varying from 1 to 4 days. In all these studies, biodegradation rates are described by Eq2 ($Rox=k1[CH_4]$), i.e. by first-order rate coefficients k1). The methane oxidation rates have been estimated to follow these concentration-dependent rates up to concentrations of µM levels, after which concentration-independent zero-order rates occur (Kessler et al., 2011; Valentine et al., 2010), due to microbial enzyme saturation. First order rates infer immediate depletion of the substate without any non-responsive lag-periods (Alexander, 1985). In a laboratory-based methane oxidation study in natural SW, we measured increased oxidation rates by a factor of 2.4 even increasing methane concentrations from 24 µmol/L to 1720 µmol/L (Brakstad et al., 2017), i.e. zero-order rates were not reached at least at 24 µmol/L methane.

Time-related degradation was intended to be performed both by stable isotope and tritium-methods, although the experiment with stable isotope was performed with low concentrations of $^{13}CH_4$, where results in spiked and blank samples could not be properly separated (see **Appendix A**). However, the results from a 4-week experiment with tritium-labelled methane showed rapid oxidation of $^{3}H\text{-}CH_4$ after 4 days of incubation, resulting in a plateau already after this incubation time (see **Appendix B**, **Figure 22** and **Table 5**). It was therefore concluded that first-order rates were followed without any non-responsive lag-period, and that experiments thus could be performed with short incubations.

As shown by Eq2, first-order rates should be concentration-dependent, and methane oxidation rates (MOX) should increase by increased concentrations. This was shown both in experiments with stable isotope ($^{13}CH_4$) and tritium ($^{3}H\text{-}CH_4$), where rates increased by concentrations (see **Figure 21** and **Figure 26**). Several field studies have also shown higher oxidation rates related to increased methane concentrations, including data from oxidation of SW from the Pacific Ocean, Arctic SW near Svalbard, and from the Deepwater Horizon oil spill (Kessler et al., 2011; Mau et al., 2013; Valentine et al., 2001).

8.3 Temperature

Temperature may play a role for biodegradation rates, and it is generally assumed that increased temperatures will affect biodegradation rates positively. And as a 'rule of thumb' it is estimated that a 10 °C water temperature increase will increase the biodegradation rate coefficient by a factor of 2 (Q_{10}=2). However, this model has been challenged many times. Since microbes adapt to their environments and develop for instance cold adapted enzymes, biodegradation of chemicals may occur faster at low SW temperatures than anticipated from the Q_{10}-model (Bagi et al., 2014).

In our study it as attempted to compare methane oxidation at two temperatures, 5 °C and 13 °C. These experiments were to be performed with tritium-labelled methane ($^{3}H\text{-}CH_4$). Since the experiments were restricted to be performed in a dedicated laboratory, we had to use the only incubator present in the room, a refrigerator. By setting the temperature setting to the minimum, we hoped to achieve as high temperature as possible during $^{3}H\text{-}CH_4$ incubation. Although the pre-incubation with normal methane was performed at 13 °C, we were not able to increase incubation temperature above 8.5 °C, and at this temperature the oxidation rates were comparable to the rates at 5 °C. Rate differences were determined to be insignificant

between 5 °C and 8.5 °C. Q_{10} calculations were performed to theoretically evaluate possible degradation data at 13 °C, based on the temperature differences between the measured 8.5 °C and 13 °C.

Results from methane oxidation field studies have shown conflicting results with respect to SW temperatures. Some of the fastest oxidation rates have been determined in Arctic SW with oxidation half-lives of 10-75 days (Mau et al., 2013; Uhlig et al., 2018), while long half-lives (116 days) have been determined in warm SW at 25 °C (Sansone and Martens, 1978). Whether these differences are real or caused by methodological differences are not known to us.

8.4 Data reliability and comparison of methods

The analytical reliabilities of data will be related to the numbers of replicates used and the similarities of the data between the replicates. In most biodegradation studies, the use of three replicates is normal, including most of the field studies referred to in this report. The standard approach in most of the studies referred to have been one blank, one sterilized control and three replicates of test samples. In our experiments, 3 to 5 replicates of test samples were used in the experiments, while 1 to 3 replicates of blanks and sterilized controls were used. In a comparison of test qualities of results from several field experiments, it was conclude that more than 3 replicates were necessary for obtaining acceptable precision and discriminatory power (Bussmann et al., 2015).

Although both the $^{13}CH_4$ and $^{3}H\text{-}CH_4$ methods analyzed the oxidation product, either as $^{13}CO_2$ or as $^{3}H\text{-}H_2O$, the methods have their limitations. In our study, the $^{13}CH_4$ concentrations required were higher than expected in most environmental samples, since the $^{13}CO_2$ concentrations and the $\delta^{13}CO_2$ ration should be significantly higher than in the SW blanks. In addition, the use of $^{13}CH_4$ as tracer for methane oxidation results in slightly slower oxidation than $^{12}CH_4$ oxidation, since ^{12}C-uptake in biomass is faster than ^{13}C-uptake. However, one advantage of the method is the direct measurement of the oxidation product ($^{13}CO_2$) by the IRMS analyses. With the $^{3}H\text{-}CH_4$ methods the measurements can be performed at isotope concentrations relevant for environmental methane concentrations. One limitation of the $^{3}H\text{-}CH_4$ method is the presence of residual $^{3}H\text{-}CH_4$ in the samples, which are removed by sparging of the samples with an inert gas. However, the effectiveness of this sparging is only determined indirectly by comparison to measurements in sterilized controls (see Eq21). The oxidation product measurements in the test samples then become dependent on the measurement in the sterilized control.

During the experiments we have realized the importance of the reference materials. In the experiments with stable isotopes, the blanks are important, since these represent the reference to the test samples for calculations (see Eq6), while sterilized controls before and after sparging to remove residual $^{3}H\text{-}CH_4$ are correspondingly important in the experiments with tritium-labelled methane (see Eq9). During the experiments with tritium-labelled methane, we lost some control samples, and the numbers of sterilized controls could have been expanded. However, in the experiment with higher temperatures, 3 control replicates were includes, showing standard deviations of 5% of the average. Some controls were lost during the experiments with tritium, which also potentially reduced the data reliability of some experiments. We have now learned that a weakness with our and several other studies is that the number of control samples used are limited and should ideally have been expanded. This would have increased the reliability of our data. As mentioned, tests were performed with 3 to 5 replicates. Despite the limited sample material in this study, a comparison of $\delta^{13}CO_2$ ratios and dpm from tritium experiments showed that standard deviations became lower when determined as percentages of median replicate values when the numbers of replicates were increased from 3 (average standard deviation 59%) to 4 or 5 replicates (average standard deviation 28-34%).

8.5 Comparison of experiments and results

Since several of the experiments were parts of methods establishment, particularly for the stable isotope analyses, only a few experiments provided data which could be used with reliability for predicting methane oxidation rates. Based on an evaluation of the data, we have considered the qualities of the experiments in **Table 9** below. Of the 6 planned experiments, we considered the outcome of three experiments to be acceptable.

Table 9: Experiments performed in the study and their suggested "qualities", based on some quality criteria described for each experiment.

Experiment	"Quality"	Replicates	Controls	Other
$^{13}CH_4$_Incubation times	Poor	3	1	Low conc $^{13}CH_4$
$^{13}CH_4$_Flask volumes	Poor	3	1	Low conc $^{13}CH_4$
$^{13}CH_4$_Increased $^{13}CH_4$ conc	Acceptable	5	3	Rates determined
^{3}H-CH_4_Incubation time	Acceptable	4	2	Rates determined
^{3}H-CH_4_Different CH_4 concentrations	Questionable	3	1	High replicate variabilities
^{3}H-CH_4_Increased temperature	Acceptable	4	3	Rates determined

We have further summarized the rate data from the three experiments which we considered be of acceptable quality in **Table 10**.

Table 10: Methane oxidation data of the three experiments considered be of acceptable quality, (see Table 8).

Parameter	$^{13}CH_4$_Increased $^{13}CH_4$ conc[A)]	^{3}H-CH_4_Incubation time[B)]	^{3}H-CH_4_Increased temperature[C)]
K1	0.0338 ± 0.0077	0.1243 ± 0.0173	0.1735 ± 0.062
Half-life (days)	21.6 ±6.2	5.6 ± 0.7	4.6 ± 2.5
MOX (nmol/L d^{-1})[D)]	10.4 ±2.4	6.2 ± 0.9	8.7 ± 3.1
Turnover (days)[D)]	31.1 ± 9,9	8.2 ± 1.0	6.7 ± 3.5

[A)] Test with 250 µL $^{13}CH_4$ applied; [B)] Incubation period 4 days; [C)] Incubation period 2 days; [D)] MOX and turnover based on the methane concentrations in the experiments.

As shown, the use of tritium labelled CH_4 resulted in faster oxidation rates than the use of stable isotope. In **Figure 3**, the range of methane oxidation half-lives were shown, based on data from filed studies. In **Figure 34**, we have included our half-life data described in **Table 10.**

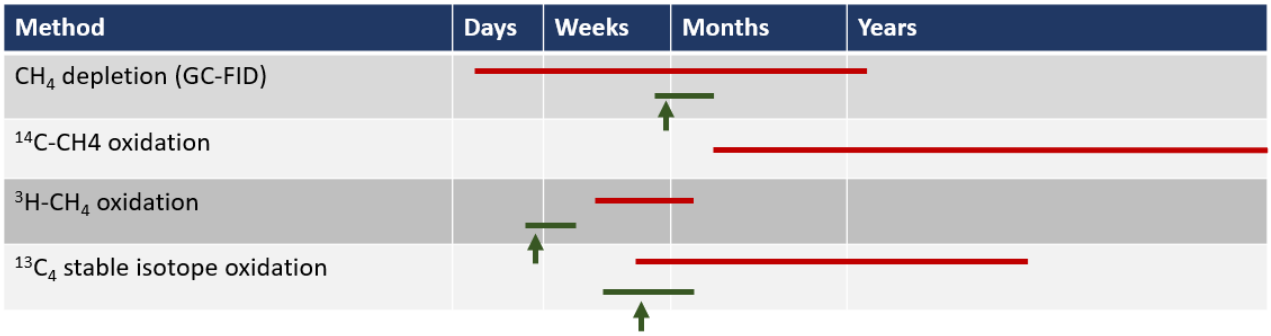

Figure 34: Ranges of methane oxidation half-lives related to the use of different analytical methods. The red lines describe the ranges of half-lives from literature data, and the green lines include the data with our laboratory studies with local SW. The data included for CH_4 depletion by GC-FID analyses refer to a biodegradation study with methane concentrations (Brakstad et al., 2017). The vertical arrows show the average half-lives from the laboratory experiments conducted at SINTEF Ocean.

The reported field data showed faster oxidation by the tritium- than the stable isotope method, in agreement with our data. However, comparison of these results both by paired one-way ANOVA, and by paired t-tests did not show significant differences between the results. The comparison in **Figure 34** also shows that the half-life results determined in the current study were in the lower part of data ranges provided from most other studies. Particularly the results with oxidation of $^{3}H\text{-}CH_4$ showed faster oxidation (and lower half-lives) then results reported from other studies (**Figure 34**). However, the data obtained from the experiment with $^{13}CH_4$ oxidation were in mainly in agreement with results from field studies, for instance a study performed in Storfjorden at Svalbard, which showed half-lives of 2-4 weeks by stable isotope and tritium methods (Mau et al., 2013).

8.6 Methane-oxidizing bacteria

The *pmoA* gene was amplified as a potential measure of methane-oxidizing bacteria during incubation of SW with low methane concentrations. However, qPCR analyses revealed that concentrations of this gene remained below detection limits of the method. These results indicated continuously low concentrations of methane-oxidizing bacteria during the experiment period, or that the selected conditions were not optimal for the gene amplification. Initial analyses indicated that the fraction of methane oxidizing bacteria constituted <0.005% of the total bacterial population in the samples. The methane concentrations in the sampled ranged from 17 nmol/L to 53 nmol/L, and we expect that higher methane concentrations than those used in this experiment would increase the possibilities for quantification of the gene during the incubation period (14 days).

8.7 The use of the oxidation rates data on relevant field data

The methane oxidation rate data provided from this project may also be used to estimate methane oxidation rates and half-lives in Norwegian SW. Two environments were selected, the Haltenbanken and Svalbard. To estimate oxidation rates, methane field concentrations were used. The Haltenbanken data are based on analytical data on samples from a cruise in 2021, where methane was quantified by GC-FID analyses performed at SINTEF Ocean. The analyses showed low methane concentrations, in the range of 1.99-0.56 nmol/L, and with mean concentrations of 0.66±0.29 nmol/L (Brakstad et al., 2022). Analyses from Svalbard were based on data from a water column study around gas flares at the West Spitsbergen continental shelf (Gentz et al., 2014). Vertical sampling of the Svalbard water revealed methane concentrations of 42±2

nmol/L close to the seabed (250 m depth), decreasing in concentrations to approximately 10 nmol/L at 175 m depth up to the surface (Gentz et al., 2014).

To estimate oxidation rates, we used first-order rate coefficients from experiments of acceptable quality (see **Table 8** and **Table 9**). For the $^{3}H\text{-}CH_4$ data, we used the lowest rate coefficient of the described in **Table 9**, 0.1243 ± 0.0173. We included the standard deviations for the rate coefficient determination:

- $^{13}CH_4$ rates coefficient: 0.0338 (– 0.0077) = 0.0261 (half-life 26.6 days)
- $^{3}H\text{-}CH_4$ rate coefficient: 0.1243 (-0.0173) = 0.107 (half-life 6.5 days)

The estimated methane oxidation data for Haltenbanken and Svalbard data are shown in **Table 11**:

Table 11: Methane oxidation in SW from Haltenbanken and Svalbard, based on rate coefficient determined in the current project, and methane concentrations determined in field samples.

Parameter		Haltenbanken			Svalbard	
Sample		R6-14 ca200m	KA 5 10m 7/6	IR-2 10m 1/6	250 m	175 m
CH_4 conc. (nmol/L)		0.66	1.99	0.56	42	10
$^{13}CH_4$ k=0.0261	MOX (nmol/L d^{-1})[A)]	0.0172	0.0519	0.0146	1.0962	0.2610
$^{3}H\text{-}CH_4$ k=0.107	MOX (nmol/L d^{-1})[B)]	0.0706	0.2129	0.0599	4.494	1.070

[A)] Half-life 26 days based on k-values, turnover 38 days based on MOX and CH_4 concentrations; [B)] Half-life 7 days based on k-values, turnover 9 days on MOX and CH_4 concentrations.

The MOX calculations with the Svalbard samples could be compared with MOX data from field samples performed with the $^{3}H\text{-}CH_4$ method (Gentz et al., 2014). In the sample with 42 nmol/L methane, a methane oxidation rates of 0.77 nmol/L d^{-1} were reported, while rates of <0.22 nmol/L d^{-1} were reported in the water with low methane concentrations. The data provided by the $^{13}CH_4$ method were therefore closer to the field data than the $^{3}H\text{-}CH_4$ data from our study.

By comparing our data to methane oxidation field trials, it may seem that the stable isotope method resulted in rates closer to data from field trials than the tritium method, as shown both in **Figure 34**, and by the comparison of **Table 10** and **Table 11**. We may therefore anticipate that the fast oxidation rates achieved by the $^{3}H\text{-}CH_4$ may represent an overestimation of methane oxidation, and that the $^{13}CH_4$ oxidation rates from this project may be more relevant to use. The $^{13}CH_4$ oxidation rates are more in agreement with reported field data (**Figure 34**).

In the case of the use of the stable isotope and tritium methods for field studies, a list of necessary equipment and chemicals are described in **Appendix C**.

9. Conclusions

The main conclusions from the results of this project can be summarized as follows:

- Both methods (stable isotope and tritium methods) strongly indicated that methane was oxidized by first order rates, since oxidation occurred rapidly without measurable non-responsive lag-periods
- Since there were considerable requirements for method developments, relatively few oxidation input data were available for the release model
- While stable isotopes experiments required $^{13}CH_4$ concentrations significantly higher than relevant environmental methane concentrations, tritium experiments were performed at more environmentally relevant $^{3}H\text{-}CH_4$ concentrations
- Despite the different methane concentrations in the experiments, both experimental setups resulted in comparable methane oxidation rates
- While reported methane oxidation half-lives varies from days to years, our data indicated half-lives in the range of 1 to 4 weeks
- When our data were compared to selected oxidation field data from Svalbard, the stable isotope oxidation data were from our experiments were in closer agreement with the field data than the tritium data.
- The stable isotope method has now been established and may be feasible for use in field studies
- The gene encoding for the particulate methane monooxygenase (*pmoA*) was not possible to detect in experiments with low methane concentrations and detection may require higher methane concentrations.
- When the oxidation data provided from the laboratory studies were used for model simulations of methane released from seafloor seeps at different depths, almost all methane may be dissolved and biodegraded from seeps at 300 m depth, while 30% may reach the atmosphere from 120 m depth and 40-75% from 50 m depth.

10. Acknowledgements

We want to thank Marie-Josée Nadeau and Martin Seiler at the National Laboratory of Age Determination at NTNU for helping us with the stable isotope analyses. We will also thank Grethe Eggen and Arne Kjøsnes at the Institute for Biology at NTNU for help and guidance with the work with tritium-labelled methane, as well as making the isotope lab available for us.

11. References

Alexander, M. (1985). Biodegradation of organic chemicals. Laboratory tests using chemical concentrations greater than those found in nature may lead to erroneous conclusions about microbial transformation in nature. Environ. Sci. Technol. 18: 106-111.

Abdallah, R.Z., Adel, M., Ouf, A., Sayed, A., Ghazy, M.A., Alam, I., Essack, M., Lafi, F.F., Bajic, V.B., El-Dorry, H., 2014. Aerobic methanotrophic communities at the Red Sea brine-seawater interface. Frontiers in microbiology 5, 487.

Bagi, A., Pampanin, D.M., Brakstad, O.G., Kommedal, R., 2013. Estimation of hydrocarbon biodegradation rates in marine environments: a critical review of the Q10 approach. Marine environmental research 89, 83-90.

Bagi, A., Pampanin, D.M., Lanzén, A., Bilstad, T., Kommedal, R., 2014. Naphthalene biodegradation in temperate and arctic marine microcosms. Biodegradation, 25(1), pp.111-125.

Brakstad, O. G., Bonaunet, K., Nordtug, T., & Johansen, Ø. (2004). Biotransformation and dissolution of petroleum hydrocarbons in natural flowing seawater at low temperature. Biodegradation, 15(5), 337-346.

Brakstad, O. G., Nordtug, T., & Throne-Holst, M. (2015). Biodegradation of dispersed Macondo oil in seawater at low temperature and different oil droplet sizes. Marine pollution bulletin, 93(1-2), 144-152.

Brakstad, O. G., Almås, I. K., & Krause, D. F. (2017). Biotransformation of natural gas and oil compounds associated with marine oil discharges. Chemosphere, 182, 555-558.

Brakstad, O.G., Hakvåg, S., Almås, I.K., Aas, M., & Ribicic, D. (2022). Analyses of methane in field samples from 2022 cruise. SINTEF Ocean Report (In Prep).

Bui, T.N.N. 2018. Dissolved methane distribution in seawater and its controlling factors in the polar regions. PhD thesis, Hokkaido University, 2018, pp. 147.

Bussmann, I., A. Matousu, R. Osudar, and S. Mau. 2015. Assessment of the radio 3H-CH4 tracer technique to measure aerobic methane oxidation in the water column: The 3H-CH4 tracer technique to measure aerobic methane oxidation. Limnol. Oceanogr.: Methods 13: 312–327.

DePaula, Renato M De, Lisa Gieg, Kathleen Duncan, Nicolas Tsesmetzis, Richard Eckert, and Torben Lund Skovhus. 2021. “Time to Agree: The Efforts to Standardize Molecular Microbiological Methods (MMM) for Detection of Microorganisms in Natural and Engineered Systems.” CORROSION 2021.

Gentz, T., Damm, E., von Deimling, J. S., Mau, S., McGinnis, D. F., & Schlüter, M. (2014). A water column study of methane around gas flares located at the West Spitsbergen continental margin. Continental Shelf Research, 72, 107-118.

Gutierrez, T., Aitken, M.D., 2014. Role of methylotrophs in the degradation of hydrocarbons during the Deepwater Horizon oil spill. The ISME journal 8, 2543-2545.

Haroon, M.F., Hu, S., Shi, Y., Imelfort, M., Keller, J., Hugenholtz, P., Yuan, Z., Tyson, G.W., 2013. Anaerobic oxidation of methane coupled to nitrate reduction in a novel archaeal lineage. Nature 500, 567-570.

Holler, T., Wegener, G., Knittel, K., Boetius, A., Brunner, B., Kuypers, M.M., Widdel, F., 2009. Substantial 13C/12C and D/H fractionation during anaerobic oxidation of methane by marine consortia enriched in vitro. Environmental microbiology reports 1, 370-376.

Holmes, A.J., Costello, A., Lidstrom, M.E., Murrell, J.C., 1995 Evidence that particulate methane monooxygenase and ammonia monooxygenase may be evolutionarily related. FEMS Microbiology Letters 132, 203-208.

IAEA, 1993. Reference and intercomparison materials for stable isotopes of light elements. Consultants Meeting on Stable Isotope Standards and Intercomparison Materials. IAEA, Vienna, Austria, p. 159.

Kessler, J.D., Valentine, D.L., Redmond, M.C., Du, M., Chan, E.W., Mendes, S.D., Quiroz, E.W., Villanueva, C.J., Shusta, S.S., Werra, L.M., 2011. A persistent oxygen anomaly reveals the fate of spilled methane in the deep Gulf of Mexico. Science 331, 312-315.

Leonte, M., Kessler, J.D., Kellermann, M.Y., Arrington, E.C., Valentine, D.L., Sylva, S.P., 2017. Rapid rates of aerobic methane oxidation at the feather edge of gas hydrate stability in the waters of Hudson Canyon, US Atlantic Margin. Geochimica et Cosmochimica Acta 204, 375-387.

Louca, Stilianos, Michael Doebeli, and Laura Wegener Parfrey. 2018. Correcting for 16S RRNA Gene Copy Numbers in Microbiome Surveys Remains an Unsolved Problem. Microbiome 6 (1): 41.

Luesken, F.A., Zhu, B., van Alen, T.A., Butler, M.K., Diaz, M.R., Song, B., den Camp, H.J.O., Jetten, M.S., Ettwig, K.F., 2011. pmoA primers for detection of anaerobic methanotrophs. Applied and environmental microbiology 77, 3877-3880.

Lyew, D. and Guiot, S.2003. Effects of aeration and organic loading rates on degradation of trichloroethylene in a methanogenic-methanotrophic coupled reactor, Appl. Microbiol. Biotechnol., 61, 2003.

Mau, S., Blees, J., Helmke, E., Niemann, H., Damm, E., 2013. Vertical distribution of methane oxidation and methanotrophic response to elevated methane concentrations in stratified waters of the Arctic fjord Storfjorden (Svalbard, Norway). Biogeosciences 10, 6267-6278.

McDonald, I.R., Murrell, J.C., 1997. The particulate methane monooxygenase gene pmoA and its use as a functional gene probe for methanotrophs. FEMS microbiology letters 156, 205-210.

Nauhaus, K., Treude, T., Boetius, A., Krüger, M., 2005. Environmental regulation of the anaerobic oxidation of methane: a comparison of ANME-I and ANME-II communities. Environmental microbiology 7, 98-106.

Naqvi, S.W.A., Bange, H. W., FarÃ-As, L., Monteiro, P. M. S., Scranton, M. I., & Zhang, J., 2010. Marine hypoxia/anoxia as a source of CH4 and N2O. Biogeosciences.

Niewöhner, C., Hensen, C., Kasten, S., Zabel, M., Schulz, H., 1998. Deep sulfate reduction completely mediated by anaerobic methane oxidation in sediments of the upwelling area off Namibia. Geochimica et cosmochimica acta 62, 455-464.

Nordam, T., Dissanayake, A., Brakstad, O.G., 2021. Methane seeps. A desktop study. SINTEF Ocean, p. 59.

Nordam, T., Lofthus, S., Brakstad, O.G., 2020. Modelling biodegradation of crude oil components at low temperatures. Chemosphere 254, 126836.

Olsen, J. E., Krause, D. F., Davies, E. J., & Skjetne, P., 2019. Observations of rising methane bubbles in Trondheimsfjord and its implications to gas dissolution. Journal of Geophysical Research: Oceans, 124

Pack, M.A., Heintz, M.B., Reeburgh, W.S., Trumbore, S.E., Valentine, D.L., Xu, X., Druffel, E.R., 2015. Methane oxidation in the eastern tropical North Pacific Ocean water column. Journal of Geophysical Research: Biogeosciences 120, 1078-1092.

Reeburgh, W.S., 2007. Oceanic methane biogeochemistry. Chemical reviews 107, 486-513.

Sansone, F.J. Martens, C.S., 1978. Methane oxidation in Cape Lookout Bight, North Carolina, Limnology and Oceanography, 23

Socolofsky, S.A., Dissanayake, A., Jun, Gros, J.,Arey, J.S. and Reddy, C., 2015. Texas A&M Oilspill Calculator (TAMOC): Modeling suite for subsea spills. Proceedings of the 38th AMOP Technical Seminar on Environmental Contamination and Response. 153-168.

Steinle, L., Schmidt, M., Bryant, L., Haeckel, M., Linke, P., Sommer, S., Zopfi, J., Lehmann, M.F., Treude, T., Niemannn, H., 2016. Linked sediment and water-column methanotrophy at a man-made gas blowout in the North Sea: Implications for methane budgeting in seasonally stratified shallow seas. Limnology and Oceanography 61, S367-S386.

Uhlig, C., Kirkpatrick, J.B., D'Hondt, S., Loose, B., 2018. Methane-oxidizing seawater microbial communities from an Arctic shelf. Biogeosciences 15, 3311-3329.

Valentine, D.L., Blanton, D.C., Reeburgh, W.S., Kastner, M., 2001. Water column methane oxidation adjacent to an area of active hydrate dissociation, Eel River Basin. Geochimica et Cosmochimica Acta 65, 2633-2640.

Valentine, D.L., Kessler, J.D., Redmond, M.C., Mendes, S.D., Heintz, M.B., Farwell, C., Hu, L., Kinnaman, F.S., Yvon-Lewis, S., Du, M., 2010. Propane respiration jump-starts microbial response to a deep oil spill. Science 330, 208-211.

Větrovský, Tomáš, and Petr Baldrian. 2013. The Variability of the 16S RRNA Gene in Bacterial Genomes and Its Consequences for Bacterial Community Analyses. PLOS ONE 8 (2): e57923.

Vielstädte, L., Haeckel, M., Karstens, J., Linke, P., Schmidt, M., Steinle, L., Wallmann, K., 2017. Shallow gas migration along hydrocarbon wells–An unconsidered, anthropogenic source of biogenic methane in the North Sea. Environmental Science & Technology 51, 10262-10268.

von Deimling, J.S., Linke, P., Schmidt, M., Rehder, G., 2015. Ongoing methane discharge at well site 22/4b (North Sea) and discovery of a spiral vortex bubble plume motion. Marine and Petroleum Geology 68, 718-730.

von Deimling, J.S., Rehder, G., Greinert, J., McGinnnis, D., Boetius, A., Linke, P., 2011. Quantification of seep-related methane gas emissions at Tommeliten, North Sea. Continental Shelf Research 31, 867-878.

Ward, B., Kilpatrick, K., Wopat, A., Minnich, E., Lidstrom, M., 1989. Methane oxidation in Saanich Inlet during summer stratification. Continental Shelf Research 9, 65-75.

Weinstein, A., Navarrete, L., Ruppel, C., Weber, T.C., Leonte, M., Kellermann, M.Y., Arrington, E.C., Valentine, D.L., Scranton, M.I., Kessler, J.D., 2016. Determining the flux of methane into H udson C anyon at the edge of methane clathrate hydrate stability. Geochemistry, Geophysics, Geosystems 17, 3882-3892.

Appendix A – Stable isotope method development

A.1 Background

The stable isotope method development was based on procedures described by Leonte at al. (2017) and Valentine et al. (2001). The development progress is summarized in **Table 1** (**section 5.4.1**) but is described in more detail here. As shown in **Table 1**, different experiments were performed to a) be able to detect $^{13}CO_2$ by the IRMS analyses, and b) to quantify higher $^{13}CO_2$ concentrations in $^{13}CH_4$-spaked test samples than in SW blanks not spiked with $^{13}CH_4$. The method developments included:

- Extractions of different sample volumes
- Purification of CO_2,
- Comparison of $^{13}CH_4$ concentrations in spiked samples

A.2 Extractions of different sample volumes

A.2.1 IRMS analyses of 1 ml samples

A.2.1.1 Method

After pre-adaption of test samples, sterilized controls, and blanks with 50 nmol/L HiQ methane (see (see section 5.2.2), spiking of each 100 mL crimp-sealed flask of test and control solutions with 50 µL $^{13}CH_4$, and incubation at 5°C for 3, 7, or 14 days. Extractions and samples for IRMS analyses were performed with screw-capped GC tubes (12 mL volumes) with butyl rubber septa (see **Figure A.1**). The GC tubes were added 0.5 ml H_3PO_4 (85 vol%) each and flushed with HiQ N_2 to obtain a nitrogen headspace in the tubes. A volume of 1 mL sample was then applied to each tube with a gas-tight syringe, and the tubes were equilibrated overnight at room temperature. Headspace volumes were then transferred to custom-made IRMS tubes (see **Figure 7**). The transfer of headspace from 12-mL GC tubes to IRMS tubes were performed as follows: The IRMS tubes were first flushed with HiQ N_2 through the sidearm to generate a nitrogen atmosphere in the tubes. A volume of gas (headspace) was transferred from the 12-mL GC tube with a gas-tight syringe, while the removed headspace was simultaneously replaced with HiQ N_2 gas. The gas was applied into the IRMS tube, which was immediately closed (top screw cap closed). The sidearm of the IRMS tube was then flushed with HiQ N_2 and the sidearm capped and covered with parafilm. Spiking, incubation, and extraction for IRMS analyses are shown in **Figure A.1**. IRMS tubes with acidified headspace samples were transported to the National Laboratory for Age Determination at NTNU for IRMS analyses and determination of $\delta^{13}CO_2$ isotopic ratios and CO_2 (DIC) of the headspace samples. The analyses included 8 separate measurements of the sample and 9 corresponding measurements of a reference gas, each measurement of 1 mL gas volume. The data were provided as CO_2 at m=45 ($^{13}CO_2$) in mV and as $\delta^{13}CO_2$±SD in ‰. Further calculations are described in **section 5.7.1**.

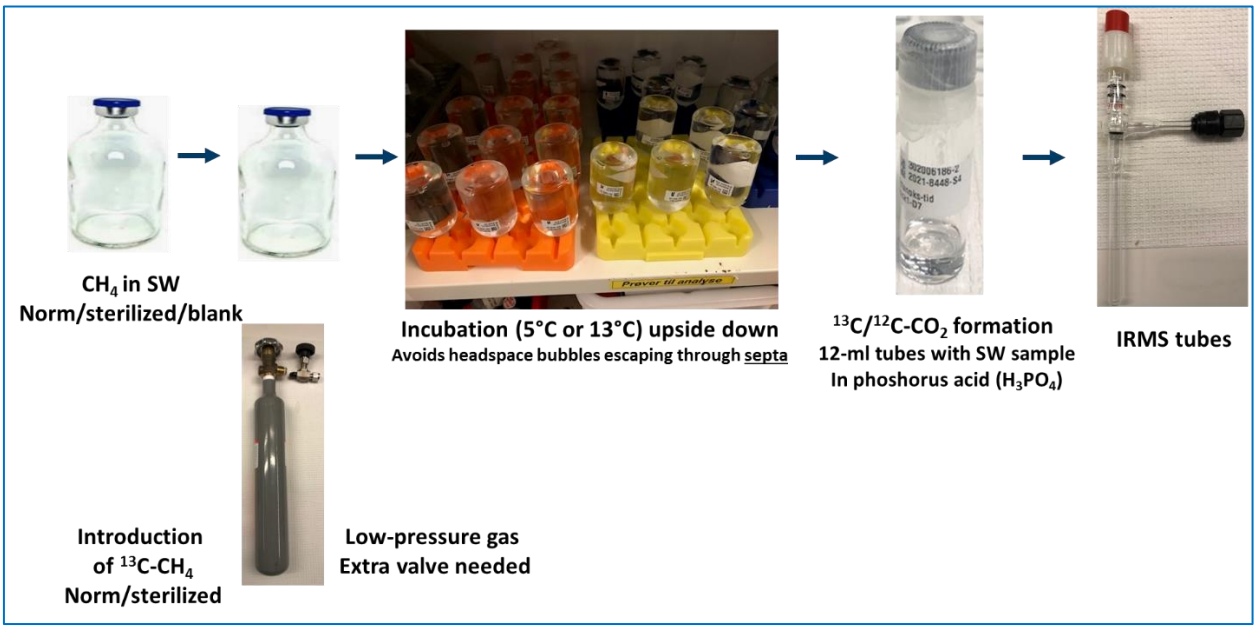

Figure A.1: Illustration of spiking, incubation, and extraction of stable isotopes for IRMS analyses using small sample volumes transferred to 12-mL GC tubes.

A.2.1.2 Results

When delivered for IRMS analyses to determine $\delta^{13}CO_2$ ratios, the signals were below detection limits in the instrument, even though the method was adapted from other studies, as described above. The reason for the poor detection limit in our method was the fact that the reported field studies used a Finnegan Gas Bench (Leonte et al., 2017). While the instrument used in our study could only analyse 1-mL sample volumes, the Gas Bench is mounted directly to the 12-mL GC vial, sampling the complete 10-mL headspace and flushes the sample through liquid nitrogen to purify the CO_2 gas. The complete gas volume is then sequentially injected into the IRMS in 1-mL pulses, and the results for the complete 10-mL sample is determined.

A.2.2 IRMS analyses of 100 ml samples

A.2.2.1 Method

Increased volumes for $\delta^{13}CO_2$ isotopic ratio determination were used by directly acidification of the samples in the 100 mL serum flasks. After adding normal methane ($^{12}CH_4$), spiking with stable isotope ($^{13}CH_4$) and incubation, 10 mL volumes were removed from the flasks with a syringe while the liquid volume was simultaneously replaced with HiQ N_2 with a cannula coupled to a N_2-flask (**Figure 5**).

Two separate experiments were performed:

1. An experiment with pre-adaption of HiQ methane (50 nmol/L) of test, control, and blank samples for 3 days at 5°C, spiking with 50 µL $^{13}CH_4$, and incubation a 5°C for 28 days.
2. An experiment with comparison of pre-adapted (50 nmol/L HiQ methane to test, control, and blank samples for 3 weeks at 5°C) and non-adapted samples. Both pre-adaption and non-adapted samples were spiked with 50 µL $^{13}CH_4$ and incubated for 3 or 7 days at 5°C.

After incubation were extraction performed directly in the crimp-sealed flasks. A volume of 10 mL sample was removed from each flask with a syringe, while the liquid volume was simultaneously replaced with HiQ N_2 gas with a cannula coupled to a N_2-flask (see **Figure 5**). The content of each flask was the acidified with 5 mL of H_3PO_4 and equilibrated overnight with flasks stored upside down. Samples of 10 mL headspace were then collected with a 10-mL syringe and was transferred to IRMS tubes, as described above. IRMS tubes with acidified headspace samples were transported to the National Laboratory for Age Determination at NTNU

for IRMS analyses and determination of $^{13}CO_2$ and $\delta^{13}CO_2$ isotopic ratios and CO_2 (see above) of the headspace samples. Further calculations are described in **section 5.7.1**.

A.2.2.2 Results

When near to complete contents of the samples were used for IRMS analyses, detectable levels of $^{13}CO_2$ were measured, and $\delta^{13}CO_2$ isotopic ratios could be analyzed in test, control, and blank samples. The results are shown in **Figure A.2 and tabulated in Table A.1**.

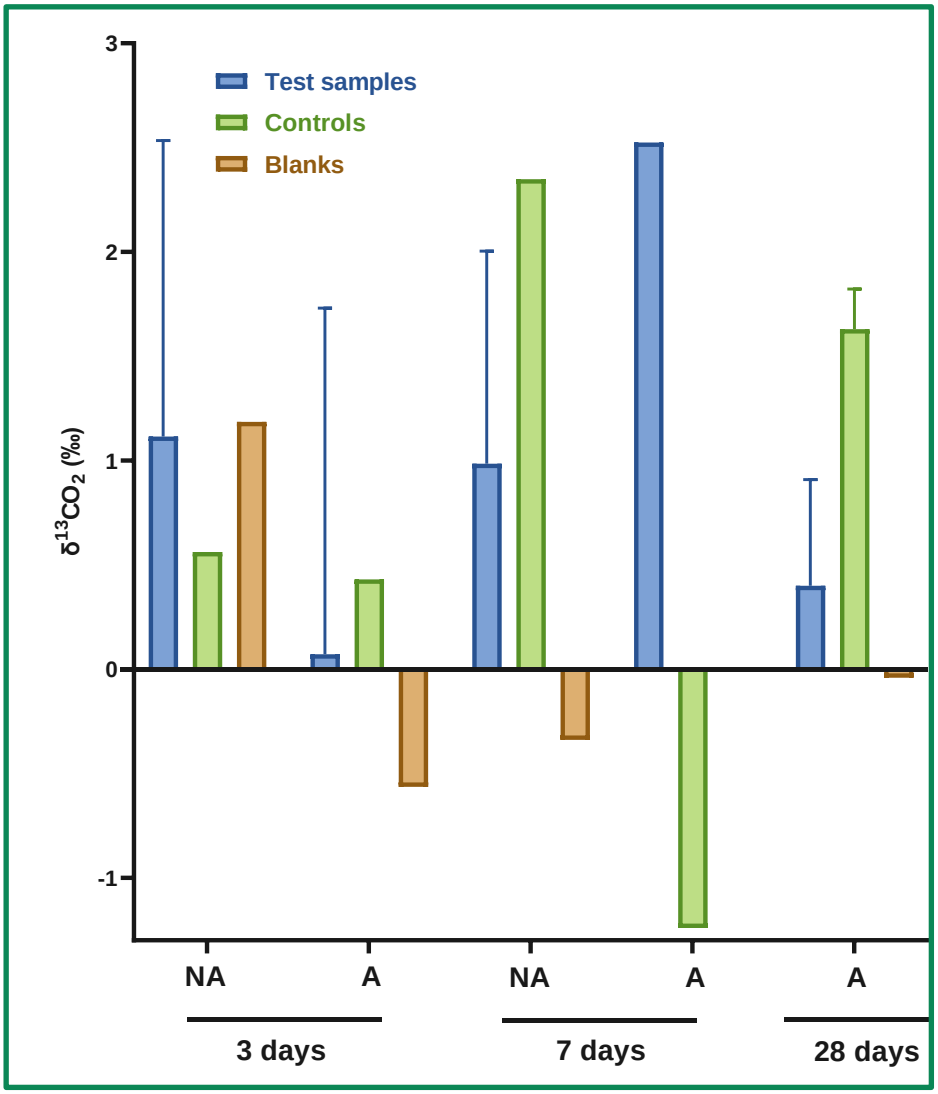

Figure A.2: δ^{13} C ratios determined from IRMS analyses in $^{13}CH_4$-spiked samples incubated for 3, 7 and 28 days at 5°C. The incubations were performed in samples pre-adapted to methane (A), or not pre-adapted (NA) prior to $^{13}CH_4$ spiking. The $\delta^{13}CO_2$ ratios were compared between samples in normal SW (Tests), in SW sterilized with $HgCl_2$ (Controls) and SW not spiked with $^{13}CH_4$.

Table A.1: Efforts made to calculate $^{13}CH_4$ oxidation from data described in Figure A.2. The results are shown for $^{13}CH_4$-spiked samples incubated at 5 °C for 3, 7 or 28 days. Experiments were performed with samples pre-adapted to methane (A), or not pre-adapted (NA) prior to $^{13}CH_4$-spiking. Test samples in normal SW (T) and sterilized controls (C) were spiked with $^{13}CH_4$, while blanks (B) were not spiked. For explanations of calculations, see Eqs 16-20). Experiments were performed with 3 replicate test samples and one replicate of control and blank samples.

Incubation	$\delta^{13}CO_2$	DIC (µmol/L)	F ($^{13}CO_2/^{12}CO_2$)	ΔF	[$^{13}CH_4$]ox (nmol/L)[A)]
3 days NA – T	1.115±1.418	77.4±38.4	0.01125±0.00002	0.00001±0.00001	0.55±0.78
3 days NA - C	0.561	37.3	0.01124	ND[B)]	ND[B)]
3 days NA - B	1.185	58.2	0.01125	ND[B)]	ND[B)]
3 days A – T	0.072±1.658	36.1±20.6	0.01123±0.00002	0.000012±0.00001	0.57±0.51
3 days A - C	0.430	25.2	0.01124	ND[B)]	ND[B)]
3 days A - B	-0.564	37.6	0.01123	ND[B)]	ND[B)]
7 days NA – T	0.985±1.019	19.7±18.2	0.01125±0.00001	0.00001±0.00001	0.27±0.43
7 days NA - C	2.349	0.34	0.011264	ND[B)]	ND[B)]
7 days NA - B	-0.339	21.7	0.011233	ND[B)]	ND[B)]
7 days A – T[C)]	2.524	0.33	0.011266	ND[B)]	ND[B)]
7 days A – C	-1.241	10.4	0.011223	ND[B)]	ND[B)]
7 days A – B[D)]	ND[B)]	ND[B)]	ND[B)]	ND[B)]	ND[B)]
28 days A – T	0.400±0.508	75.2±12.6	0.01124±0.00001	0.000002±0.000004	0.42±0.48
28 days A - C	ND[B)]	ND[B)]	ND[B)]	ND[B)]	ND[B)]
28 days A - B	-0.041	75.2	0.011237	ND[B)]	ND[B)]

[A)] $^{13}CH_4$ oxidation after incubation for 3, 7 or 28 days; [B)] not analyzed; [C)] only one replicate could be measured; [D)] Blank sample lost due to gas leakage in the IRMS instrument.

When the complete samples in the crimp-sealed flasks were used for acidification and headspace transfer to IRMS tubes, detectable levels of $^{13}CO_2$ were measured, and $\delta^{13}CO_2$ ratios could be determined. The comparison of $\delta^{13}CO_2$ ratios (**Figure A.2** and **Table A.1**) showed large standard variations, demonstrating considerable replicate variations. Paired t-test comparison of $\delta^{13}CO_2$ ratios in test and blank samples did not show significant differences (P=0.78653). These results were therefore not reliable for determination of methane oxidation. The calculated $^{13}CH_4$ oxidation ([$^{13}CH_4$]ox) after the different incubation times also indicated poor and variable oxidation.

A.2.3 IRMS analyses of samples in 1 L flasks

A.2.3.1 Method

An experiment was performed to determine if further increased volumes of SW from 100 mL crimp-sealed flasks to 1 L flasks could be used for improving $\delta^{13}CO_2$ isotopic ratios. The 1 L flasks (SCHOTT) were supplied with gas-tight screwcaps. The complete volume of the flasks was 1.3 L. SW was directly spiked with $^{13}CH_4$ without any pre-adaption with HiQ methane at an approximate concentration of 50 nmol/L. The spiked gas volumes were based on analytical data (GC-FID) where CH_4 concentrations were determined before and after spiking with $^{13}CH_4$. No sterilized controls were included in this experiment. Blanks samples were included, containing inly normal SW. The test and blank samples were completely filled (no headspace) and incubated upside down at 4°C for 7 days (**Figure A.3**). Volumes of 200 mL liquid were then replaced by HiQ N_2 gas, and 100 mL H_3PO_4 applied for CO_2 formation of DIC. After equilibrium overnight, 10 mL volumes were transferred to IRMS tubes as described above. IRMS tubes with acidified headspace samples were

transported the National Laboratory for Age Determination at NTNU for IRMS analyses and determination of $^{13}CO_2$ and $\delta^{13}CO_2$ isotopic ratios and CO_2 (see above) of the headspace samples. Further calculations are described in **section 5.7.1**.

Figure A.3: Incubation of 1-L flasks upside down.

A.2.3.2 Results

The $\delta^{13}CO_2$ results from IRMS analyses of the acidified headspace samples in test and blank samples from the 1 L flasks are shown in **Figure A.4**.

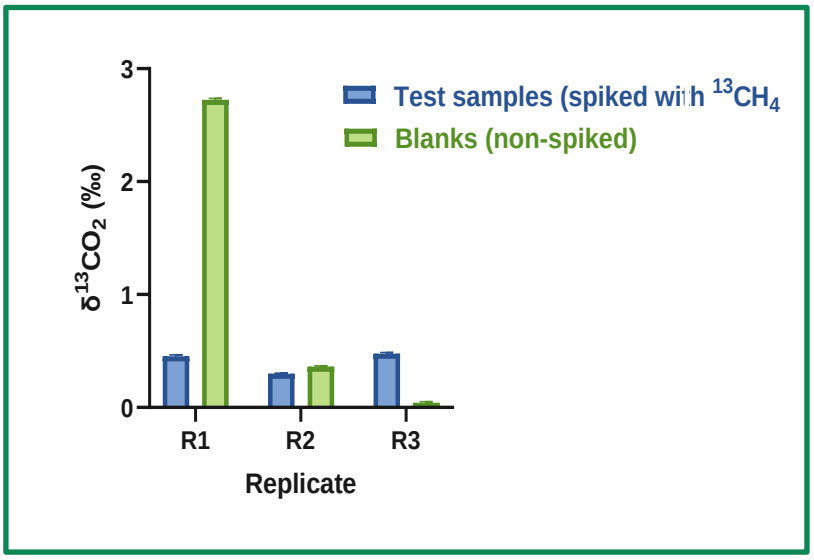

Figure A.4: $\delta^{13}CO_2$ ratios of three replicates (average ± SD of 8 IRMS measurements of each replicate) of SW test samples spiked with $^{13}CH_4$ and non-spiked SW blanks.

The result of **Figure A.4** showed that $\delta^{13}CO_2$ ratios in spiked samples varied between 0.299 ± 0.004 and between 0.476 ± 0.011, and between 0.04 ± 0.01 and 2.723 ± 0.01 in blanks. Unpaired t-test showed that spiked and blank samples did not differ significantly (P=0.4977). The $\delta^{13}CO_2$ ratios in the spiked samples were therefore within the $\delta^{13}CO_2$ ratios in natural SW. Spiking of SW with concentrations of 50 nmol/L $^{13}CH_4$ did

therefore not result in determinations of $\delta^{13}CO_2$ ratios which were significantly different from the background levels in natural SW.

A.3 Improvement of extraction method

When headspaces were prepared for IRMS analyses, the systems were flushed with HiQ N_2 gas as, described above. This resulted in samples with very high N2 concentrations, and the CO_2 fractions usually constituted <1 % of the headspace. Flasks with acidified samples and headspace were treated by freeze-drying to purify the separate CO_2 from N_2 and achieve near pure CO_2 samples for IRMS analyses.

A.3.1 Method

Acidified samples on 100 mL serum flasks with appr. Test samples in crimp-sealed flasks (100 mL) spiked with 50 µL $^{13}CH_4$ in normal SW, and non-spiked blank samples, were incubated for 3 days at 5 °C. The test and blank samples were acidified as described (see **A.2.2.1**), and the flasks were connected directly to an extraction unit at NTNU (see **Figure 6**). Headspace volumes were evacuated into the extraction unit, freeze-dried, and pure CO_2 samples were transferred to IRMS tubes. IRMS analyses included determination of $^{13}CO_2$ and $\delta^{13}CO_2$ isotopic ratios of the headspace samples. Further calculations are described in **section 5.7.1**.

A.3.2 Results

By changing extraction method and purifying CO2 in the headspace samples, the signal intensities increased by a factor of 67 (based on average values of replicates) in CO_2-purified samples and were significantly different from the signals in samples with low CO_2 concentrations (P<0.001; unpaired *t*-test). However, when $^{13}CO_2/^{12}CO_2$ ratios were determined from $\delta^{13}CO_2$ ratios (see Eq17), the test and blank results did not differ significantly (P = 0.4869), as shown in **Figure A.6**.

The conclusions from these experiments were that $^{13}CO_2$ concentrations in the samples were too low when stable isotope of $^{13}CH_4$ was spiked in a concentration of 50 nmol/L, since $^{13}CO_2/^{12}CO_2$ ratios in spiked samples were not significantly different from blank values at these concentrations. In order to obtain significantly different ratios between spiked and blank samples, the applied $^{13}CH_4$ concentration therefore needed to be increased.

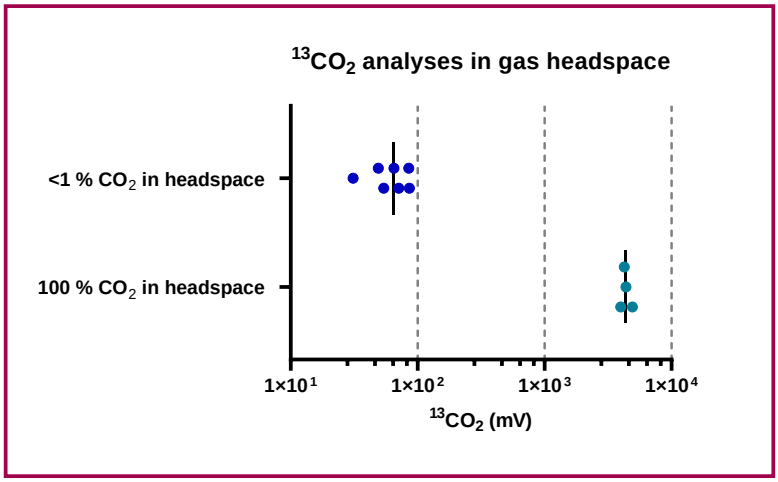

Figure A.5: IRMS analyses of $^{13}CO_2$ (mV) in single replicate samples from 100 mL crimp-sealed flasks with low CO_2 concentration (<1 % CO_2) compared with freeze-dried samples with 100% CO2. The average concentrations of the replicated are marked.

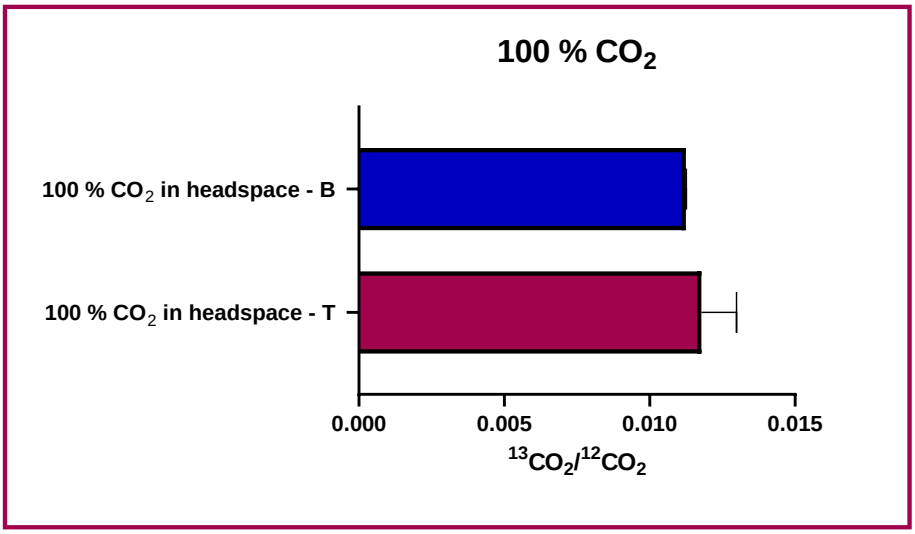

Figure A.6: $^{13}CO_2/^{12}CO_2$ ratios in samples with 100% CO_2 from blanks (B) not spiked with $^{13}CH_4$ and in $^{13}CH_4$-spiked test samples (T) extracted from 100-mL crimp-sealed flasks. The results are shown as average values with SDs.

A.4 Increased concentrations of spiked $^{13}CH_4$

To better separate $\delta^{13}CO_2$ ratios in test and blank samples, the concentrations of $^{13}CH_4$ spiked to the SW in test samples were increased above the 50 µL volumes used in each crimp-sealed flask in the previous experiments described here.

A.4.1 Method

Crimp-sealed flasks with test and blank samples in SW were first pre-adapted for 7 days at 5 °C with normal HiQ methane at the nominal concentrations of 50 nmol/L. Test samples were then spiked with 250 µL, 500 µL and 1250 µL $^{13}CH_4$ (5 replicates of each), while non-spiked blanks were incubated in triplicate. These $^{13}CH_4$-spiked volumes resulted in final methane concentrations of 300, 570 and 2150 nmol/L (see **Figure 13**). The samples were then incubated at 5°C for 3 days upside down. After sampling the complete samples were acidified as described (see **A.2.2.1**), and the flasks were connected directly to an extraction unit at NTNU (see **A.3.1** and **Figure 6)**. Headspace volumes were evacuated into the extraction unit, freeze-dried, and pure CO_2 samples were transferred to IRMS tubes. IRMS analyses included determination of $^{13}CO_2$ and $\delta^{13}CO_2$ isotopic ratios of the headspace samples. Further calculations are described in **section 5.7.1**.

A.4.2 Results

Determined $\delta^{13}CO_2$ ratios (**Figure A.7**) showed that test and blank samples differed significantly for all spiked concentrations ($P<0.01$ in all comparisons; paired *t*-tests). All spiked volumes could therefore be used for determinations of $^{13}CH_4$ oxidation.

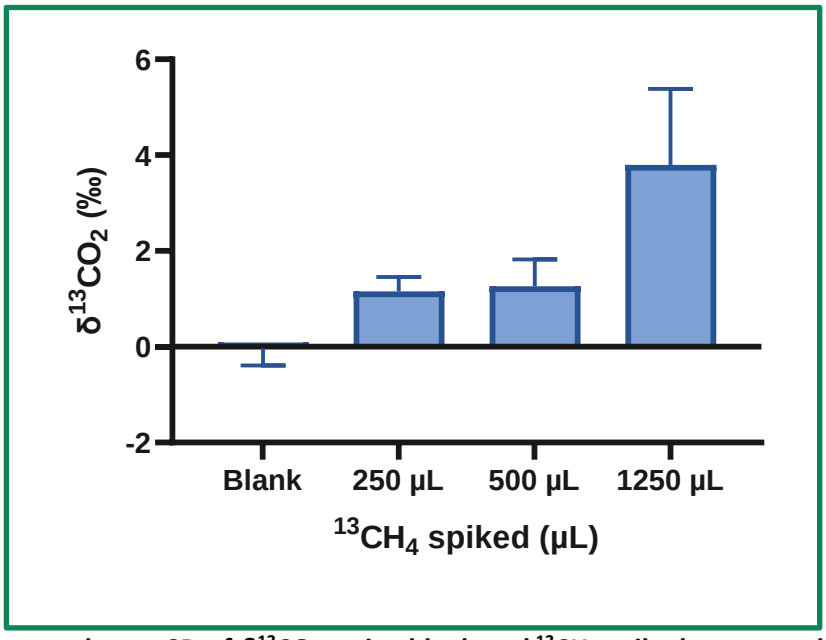

Figure A.7: Average values ± SD of $\delta^{13}CO_2$ ratios blank and $^{13}CH_4$-spiked test samples (250 µL, 500 µL or 1250 µL of $^{13}CH_4$ spiked).

A.5 Conclusions

The successive testing of the stable isotope method to be used for determination of methane oxidation in natural SW required that spiked concentrations of $^{13}CH_4$ resulted in significantly higher $\delta^{13}CO_2$ ratios in spiked test than blank samples, since determination of methane oxidation relied on the determination of a ΔF which describe an excess of $^{13}CO_2$ in test samples compared to blank samples (see Eq18 and Eq19). By combining an extraction method where CO_2 was purified and N_2 removed from the headspace samples, and spiked $^{13}CH_4$ concentrations of at least 300 nmol/L, it was possible to obtain this within the available IRMS instrument.

Appendix B – Tritium isotope method development

B.1 Background

The method with tritium-labelled methane (^3H-CH_4) was established based on procedures described by Bussmann et al. (2015), Mau et al. (2013) and Pack et al. (2015) for determination of methane oxidation rates in field samples. The development progress is summarized in **Table 2** (**section 5.5.1**) but is described in more detail here. As shown in **Table 2**, different experiments were performed for a) preparation and application of ^3H-CH_4 to test and sterilized control solutions, b) selection of incubation time, and c) establishment of method for sparging samples with N_2 gas and avoiding release of residual ^3H-CH_4 to the atmosphere outside the test and control flasks. The experiments included for method establishment included:

- Testing of measured radioactivity in prepared stock solutions and in different volumes of stock solutions used for test and sterilized control solutions
- Development of method to sparge samples after incubation to remove residual ^3H-CH_4
- Comparison potential oxidation of ^3H-CH_4 related to incubation times

B.2 Radioactivity in stock solutions and volumes for test and sterilized control solutions

Purchased ^3H-CH_4 was supplied from American Radiolabeled Chemicals (ARC) on a break-seal ampoule (see **Figure 2B**) in gas form at an activity of 1 mCi (see also **section 5.1**), and this activity was further reported to contain 15 Ci/mmol and thus 67 nmol $^3HCH_4$ in total. The radioactivity (1 mCi) corresponded 37000 kBq and 2.22 x 10^9 disintegrations per minute (dpm). One recommended option by the supplier was to transfer the ^3H-CH_4 as a stock solution to a solvent of hexane, which was easier to handle than the alternative of keeping the compound in gas form.

B.2.1 Method

The break-seal ampoule was placed vertically in a clamp, and 5-6 ml of the solvent hexane was applied in the space above the inner break-seal. A large magnet (magnetic hammer) was placed in the solvent (**Figure 2B**). With a magnet outside the tube, the hammer was raised in the solvent and forced to fall in order to break the seal. The solvent then passed in the opened ampoule, and the methane gas became dissolved in the solvent. The solvent was left for at least 15 minutes to allow the mixture to equilibrate. The solvent was then distributed in vials in tightly closed glass vials and stored in a refrigerator or at room temperature in the fume hood. Two types of 2-mL glass vials were compared, a) crimp-sealed GC-glasses and b) screw-capped GC-vials with rubber septa. The 2-mL vials were further placed in larger screw-capped glass GC-vials (40 mL volumes for extra security).

Application of volumes from stock solutions to test solution were compared before final decision on selected volume was made. The volumes tested were 50 µL, 100 µL and 200 µL stock solution to 100 mL of SW.

Samples for measurement of radioactivity were mixed with 10 mL Ultima Gold scintillation cocktail (Perkin Elmer) in 20 mL scintillation vials and counted in a LS 6500 multi-purpose scintillation counter (Beckman Coulter). The results were recorded as dpm.

B.2.2 Results

B.2.2.1 Storage conditions

When transferring volumes of ^3H-CH_4 in hexane from the break-seal ampoules to glass vials for stock solution storage, we observed that screw-capped GC-vials tolerated the solvent poorly during storage, and in-sunken septa were sometimes observed. A leakage test with normal methane dissolved in the solvent was therefore performed to compare screw-capped and crimp-sealed GC-vials as storage vials for the stock solutions. High concentrations of normal methane were applied to hexane in 2-mL vials of screw-capped or crimp-sealed GC glasses (6 replicates of each) and incubated at 4-5 °C in 14 days. The methane concentrations in the vials were then determined by GC-FID analyses (**Figure B.1**). The analyses revealed that methane concentrations

in the crimp-sealed vials were maintained at high concentrations, while the concentrations varied highly in the screw-capped vials. Some of the screw-capped vials were nearly emptied of methane, demonstrating serious leakage. We therefore decided to store the stock solutions in crimp-sealed vials placed inside the larger GC-vials. It was further observed that pressure differences when moving vials between room and refrigerator temperature could affect the septa, and stock solutions were therefore decided to be stored at room temperature in the fume head.

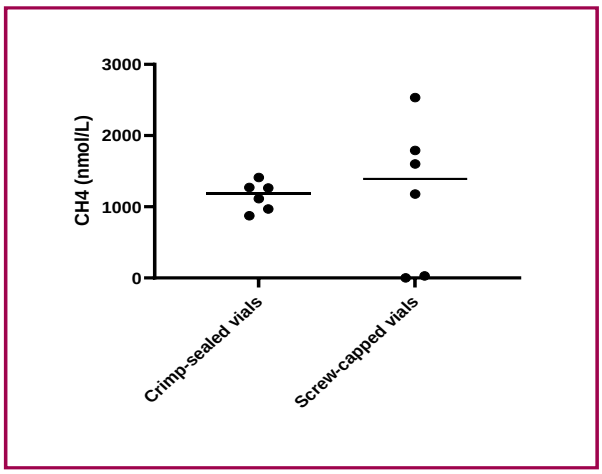

Figure B.1: Concentrations of methane gas dissolved in hexane and stored in crimp-sealed or screw-capped GC-vials (2 mL volumes) at 4-5 °C before analyses by GC-FID.

B.2.2.2 Volumes of stock solutions applied to test and control solutions

Different volumes of stock solutions (50 µL, 100 µL and 200 µL) were tested in 100 mL crimp-sealed serum flasks completely filled with SW (117 mL volumes). Volumes of 1 mL were then measured in the scintillation counter (**Figure B.2**). These results showed that a spiked volume of 50 µL resulted in a radioactivity of at least 400.000 dpm, which was adequate for the test. Based on the theoretical radioactivity calculated, the measured yield was 96.4% of the theoretical values for the 50 µL stock solution added to the test solution. The results also showed a linear relation between stock solution volumes added and measured radioactivity **(Figure B.2**). Subsequent experiments were then performed with 50 µL of spiked stock solutions added to generate test solutions.

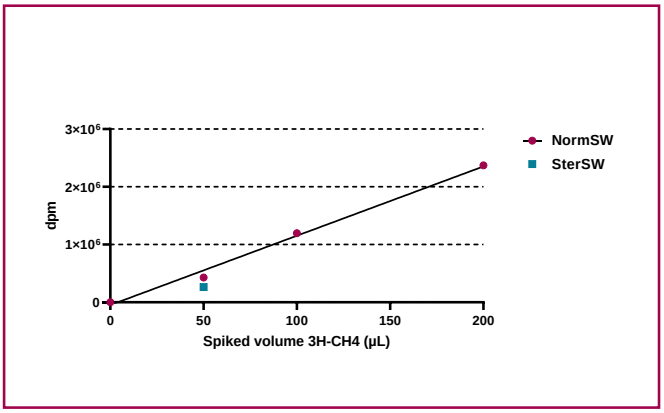

Figure B.2: Radioactivity measured in SW samples spiked with 50 µL, 100 µL and 200 µL stock solution in completely filled 100-mL crimp-sealed flasks. Volume of 50 µL was applied both to normal SW and to SW added 100 mg/L HgCl2 (Ster SW). The curve shows simple linear regression of the measured radioactivity.

B.3 Solvent impact of radioactivity measurements

Hexane is poorly soluble in water, and we therefore tested if this could affect measurement. One possibility was that when stock solutions were transferred to test and control samples, the solvent with the ^3H-CH_4 would not dissolve in the SW and that most of the radioactivity would remain in a solvent fraction separated from the SW phase.

B.3.1 Method

To determine if the poor solvent solubility affected measurements of radioactivity, crimp-sealed flasks (100 mL) were filled with SW or hexane (4 replicates of each) and each flask spiked with 50 µL stock solution of ^3H-CH_4. The flasks were incubated for 2 hours to secure mixing of the samples, and samples of 1 mL samples were collected from each flask.

Samples for measurement of radioactivity were mixed with 10 mL Ultima Gold scintillation cocktail (Perkin Elmer) in 20 mL scintillation vials and counted in a LS 6500 multi-purpose scintillation counter (Beckman Coulter). The results were recorded as dpm.

B.3.2 Results

The analyses (**Figure B.3**) showed that the radioactivity in SW was 74% of the activity in the hexane samples, The difference between the activities in SW and hexane was not significantly different between samples in hexane and SW (P=0.1603; paired *t*-test)

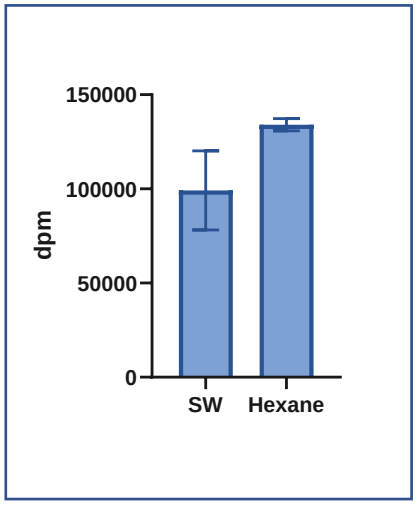

Figure B.3: Radioactivity in 50 µL ^3H-CH_4 applied to crimp-sealed flasks with SW and hexane.

B.4 Sparging of the samples

The principle of the tritium method is based on the measurement of labelled oxidation product in the SW phase, in the form of ^3H-H_2O. This means that before measurements, residual parent compound (^3H-CH_4) must be removed from the solutions. This is performed by forming a headspace in the sample and sparging the sample with N_2 to remove the residual ^3H-CH_4 to the headspace volume. To release pressure during the sparging, cannulas penetrated the septa. However, to further avoid ^3H-CH_4 from being released to the atmosphere outside the test vials, the headspace with radioactive CH_4 must be trapped. This was done by connecting the cannulas used for pressure release to syringes of activated carbon (see **Figure 10**).

To facilitate the sparging process, a custom-made tower was built and connected to the test units. This tower was connected to the N_2 source in the top and had 12 outlets to sparge 12 samples simultaneously **(Figure 5**).

B.4.1 Activated carbon

B.4.1.1 Method

A high concentration of methane gas (1000 ppmV) was prepared in SW, and 50 mL of this solution pumped through syringes with 5 g activated carbon. This was repeated up to four times, by pumping new solutions (1000 ppmV) through the same filter. The gas passing the activated filter columns were collected and analyzed by GC-FID analyses

B.4.1.2 Results

The results in **Table B.1** showed that the same filter adsorbed >98% CH4 by 1 to 4 filtrations, while some capacity became lost at the fourth filtration, where adsorbance capacity was reduced to 95%. We therefore expected activated carbon to efficiently hinder release of $^3H\text{-}CH_4$ to the atmosphere in the fume head during aeration.

Table B.1: Testing of CH_4 adsorbance capacities of activated carbon filters by repeated pumping of SW with high CH_4 concentrations (1000 ppmV) for 1 to 4 times. The results are shown as GC-FID response and % removal after filtration relative to CH4 response in the SW before adsorbance (reference).

CH4 passages (no.)	Response	Removal (%)
Reference	29.8	--
1	0.16	99.5
2	0.16	99.5
3	0.41	98.6
4	1.6	94.6

B.4.2 Sparging with N_2 gas

B.4.2.1 Method

Stock solutions of $^3H\text{-}CH_4$ were spiked in SW test and sterilized control solutions, with 50 µL stock solution in each sample. The flasks were incubated for 4 days at 5 °C. After incubation, liquid was removed from test and control samples, so either 40 mL or 10 mL liquid was left in test and control samples. The flasks were then sparged with N_2 gas for 2 hours, and samples of 1 mL mixed with 10 mL Ultima Gold scintillation cocktail (Perkin Elmer) in 20 mL scintillation vials and counted in a LS 6500 multi-purpose scintillation counter (Beckman Coulter). The results were recorded as dpm.

B.4.2.2 Results

In the samples 40 mL liquid sparged, comparison of radioactivity in test samples and sterilized control samples showed a ratio between radioactivity in normal vs. sterilized SW of 1.6 ± 0.2. This showed that 61% of the radioactivity in the test samples was still present in the sterilized controls (**Figure B.4**). In flasks with 10 mL samples sparged, the ratio between radioactivity in normal vs. sterilized SW was increased to 6.1 ± 1.1. In these samples. The radioactivity in the sterilized controls were therefore reduced to 25 % of the activity in the normal SW (**Figure B.4**).

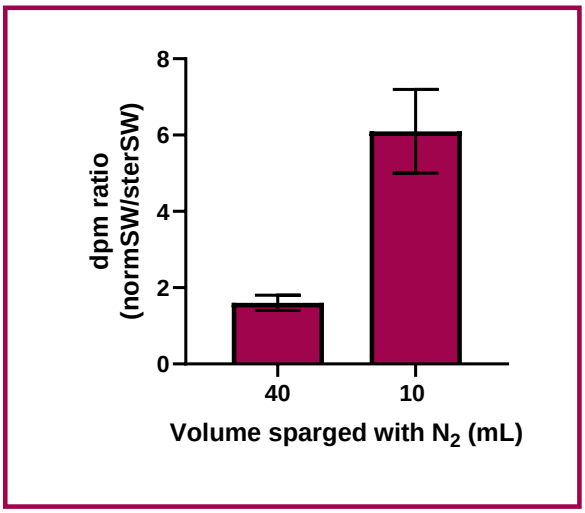

Figure B.4: Ratios between radioactivity (dpm) in normal and sterilized SW when nitrogen sparging was performed on liquid volumes of 40 mL (76 mL headspace) and 10 mL (107 mL headspace).

B.5 Oxidation related to incubation time

Biodegradation rates are normally determined based on successive sampling during an experiment. However, published reports on methane oxidation state that the oxidation follows first-order rate approach, and only one sampling has been used in these reports (e.g. Bussmann et al., 2015; Mau et al., 2013; Pack et al., 2015). This approach was tested in an experiment with successive sampling after 4, 13, 17 and 27 days of incubation at 5°C.

B.5.1 Method

SW in crimp-sealed flasks was pre-adapted with 50 nmol/L HiQ methane for 2 weeks at 5 °C, both test (n=4), sterilized control (n=2) and blank samples (n=1). Test and control samples were the spiked with 50 µL ^{3}H-CH_4 for up to 27 days and sampled after 4, 13, 17 and 27 days. After incubation, liquid was removed from test and control samples, so 10 mL liquid was left in test and control samples. The flasks were then sparged with N_2 gas for 2 hours, and samples of 1 mL mixed with 10 mL Ultima Gold scintillation cocktail (Perkin Elmer) in 20 mL scintillation vials and counted in a LS 6500 multi-purpose scintillation counter (Beckman Coulter). The results were recorded as dpm.

B.5.2 Results

The raw radioactivity data in replicate samples test (T) and sterilized controls (C) SW are shown in **Figure B.5A**. The radioactivity in the sterilized was considerably lower than the normal SW (P=0.0095; unpaired *t*-test), showing that ^{3}H-H_2O had been formed as the result of methane oxidation. The blank values (no ^{3}H-CH_4 applied) showed low background levels of 110-112 dpm. The radioactivity associated with ^{3}H-H_2O formation was then determined by subtracting the radioactivity in the sterilized solutions from the activity in normal SE (see Eq21). For simplicity, we used the average value of the sterilized controls for the subtraction. The results of the subtracted values in test (T) replicates are shown in **Figure B.5B**. The ^{3}H-H_2O radioactivity did not differ significantly between the incubation times (P=0.7385; one-way ANOVA), which indicated that most of the measured oxidation had occurred already after 4 days of incubation. These values were then used for determination of the rate coefficients, as shown in Eq. 22.

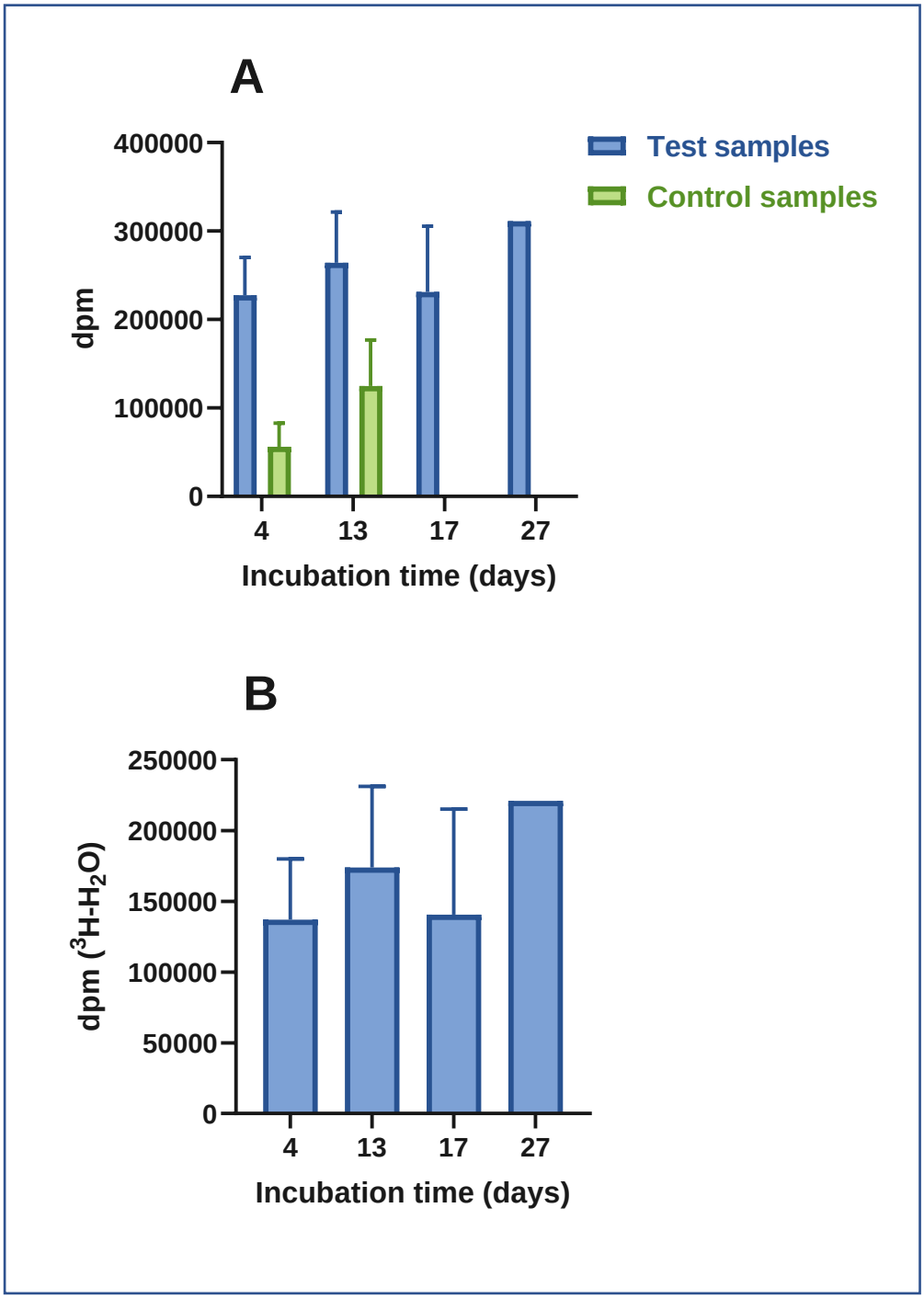

Figure B.5: Radioactivity measured as dpm in N_2-sparged test samples and sterilized control samples spiked with ^{3}H-CH_4 (A), and radioactivity associated with ^{3}H-H_2O formation (B) in test samples after subtracting activity in sterilized controls. The experiment was performed over a period of 27 days at 5 °C after spiking with ^{3}H-CH_4, with sampling after 4, 13 17 and 27 days.

B.6 Conclusions

Testing of different steps in the tritium method resulted in establishment of a method where, purchased ^{3}H-CH_4 was dissolved in 5-6 mL hexane and distributed as stock solutions on 2-mL crimp-sealed GC-glasses which were stored at room temperature to avoid leakages due to temperature changes. Volumes of 50 µL stock solutions were applied to test and control samples, and incubations were performed for 4 days at 5°C.

Sampling was performed by creating a large headspace, leaving 10 mL liquid in the sample. This sample was then sparged with N_2-gas from a custom-made tower for 2 hours to secure significant differences in radioactivity between test and control samples.

Appendix C – Equipment and chemicals needed for field experiments

C.1 Stable isotope method

Equipments and chemicals

- Crimp-sealed serum flasks wit butyl rubber septa
- Parafilm
- Lecture flask with pure $^{13}CH_4$ at low pressure (SigmaAldrich)
- Gas-tight syringe and connections for transfer of $^{13}CH_4$ from lecture flask to samples
- Cannulas to release pressure during spiking with $^{13}CH_4$
- Incubator with temperature control
- Syringes for biocide application (controls) and for termination of oxidation process
- Stock solution of a biocide (e.g. $HgCl_2$; 50 g/L)

Method in brief

Experiments are conducted by filling crimp-sealed serum flasks with water samples.

- Test samples
- Control samples with bioicide to stop biological activity
- Blanks

Test and control samples are spiked with a volume of $^{13}CH_4$ with a gas-tight syringe high enough to measure $d^{13}CO_2$ ratios significantly above the blank values. Parafilm is wrapped around the stoppers to avoid potential leakage though needle punctures. The flasks are incubated at 2-4 days at a selected temperature. The flasks are incubated upside down to avoid gas leakage through the stoppers. After termination of incubation, the test and blank samples are treated with biocide to stop biological activity. Flasks are stored at 4-5°C in the dark until transport to the lab for extraction and IRMS analyses.

C.2 Tritium method

Equipments, chemicals and staff

- Crimp-sealed serum flasks wit butyl rubber septa
- Parafilm
- $^3H\text{-}CH_4$ as gas or dissolves as stock solutions in a solvent like hexane ($^3H\text{-}CH_4$ can be supplied on break-seal ampoules from American Radiolabeled Chemicals).
    - If stock solutions in solvent are prepared, transfer to solvent volume equal to the original gas volume before bringing the solutions onboard.
- Screw-capped tubes to store gas vials or stock solutions of $^3H\text{-}CH_4$ for extra security
- System for secure storage of radiolabelled chemicals
- Fume hood approved for work with radiolabelled chemicals
- Technicians approved to work with radiolabelled chemicals
- Syringes and connections for transfer of $^3H\text{-}CH_4$ to samples
- Cannulas to release pressure during spiking with $^3H\text{-}CH_4$ (if necessary)
- Incubator with temperature control
- Syringes for biocide application (controls) and for termination of oxidation process
- Stock solution of a biocide (e.g. $HgCl_2$ (50 g/L)

Method in brief

Experiments are conducted by filling crimp-sealed serum flasks with water samples.

- Test samples
- Control samples with bioicide to stop biological activity
- Blanks

Test and control samples are spiked with a volume of $^3H\text{-}CH_4$ (e.g. 50 µL per crimp-sealed flask) with equipment relevant for transfer of $^3H\text{-}CH_4$ as gas or as stock solutions. Parafilm is wrapped around the stoppers to avoid potential leakage though needle punctures. The flasks are incubated at 2-4 days at a selected temperature. The flasks are incubated upside down to avoid gas leakage through the stoppers. After termination of incubation, the test and blank samples are treated with biocide to stop biological activity. Flasks are stored at 4-5°C in the dark until transport to the lab for sparging to remove residual 3H-CH4 and for scintillation analyses.